Saccharides as renewable resources for novel functional materials

Dissertation

To attain the doctoral degree (Dr. rer. nat.)

of the Faculty of Forest Sciences and Forest Ecology

Georg-August-Universität Göttingen

Submitted by

Stefanie Rühlicke

born on the 15th September 1990 in Berlin (Germany)

Göttingen, December 2020

1. Referee: **Prof. Dr. Kai Zhang**

Wood Technology and Wood-based Composites, Burckhardt-Institute, Faculty of Forest Sciences and Forest Ecology, Georg-August-University of Göttingen, Germany

2. Referee: **Prof. Dr. Bodo Saake**

Wood Chemistry, Institute of Wood Science, Faculty of Mathematics, Informatica and Natural Sciences, University Hamburg, Germany

Additional examination board members:

Prof. Dr. Carsten Mai

Wood Biology and Wood Products, Burckhardt-Institute, Faculty of Forest Sciences and Forest Ecology, Georg-August-University of Göttingen, Germany

Prof. Dr. Philipp Vana

Macromolecular Chemistry, Institute of Physical Chemistry, Faculty of Chemistry, Georg-August-University Göttingen, Germany

Date of oral examination: 11th November 2020

“Failing to succeed does not mean failing to progress”

-Antichamber

I Acknowledgements

The PhD thesis presented here was carried out from November 2016 to January 2020 under the supervision of Prof. Dr. Kai Zhang at the Faculty of Forest Sciences and Forest Ecology section Wood Technology and Wood-based Composites at the Georg-August-University Göttingen. I would like to extend my sincere gratitude to Prof. Dr. Kai Zhang for providing the exiting topic to me, as well as the liberty to constantly develop myself. The steadily open ear for discussions and care of all kinds as well as for the constant drive to explore my boundaries and to expand them accordingly are also appreciated.

I also would like to express my deepest appreciation to my committee consisting of Prof. Dr. Kai Zhang, from Georg August University for taking the duty as the first supervisor and reviewer, Prof. Dr. Bodo Saake from the University of Hamburg for taking on the role as the second reviewer, Prof. Dr. Carsten Mai and Prof. Dr. Philipp Vana MBA from Georg August University for the inspiring and helpful thesis committee meetings and for being part of my doctoral examination committee. Furthermore, the implementation of the fungi tests would not have been possible without the support and nurturing of Dr. Susanne Bollmus, PD Dr. Christian Brischke, Bernd Bringemeier and Petra Heinze.

I also, would like to thank the German Research Foundation (DFG) with the project number of ZH546/2-1 for the financial support.

Thanks should also go to the administrative and supportive guidance during the PhD studies trough Prof. Dr. Christian Ammer, FOR Dr. Gerhard Büttner and Dr. Inga Mölder.

I would also like to extend my gratitude to the technical employees Cornelia Becke, Gerhard Birke, Bernd Bringemeier, Petra Heinze, Brigitte Junge, Mirko Küppers, Eva Maichner and Dieter Varel, which have always been there when help was needed.

Many thanks go to my colleagues and collaborators from Prof. Dr. Kai Zhang's working group, especially to Pascal Fuchs, Hequin Huang, Saleh Musa, Houjuan Qi, Xiaojie Wang, Yonggui Wang and Hua Zhang, for the entertaining and uplifting hours in the office, for all the advice provided, for the endless but helpful discussions about the work, for the kind and warm exchange of cultural habits and, of course for the nice evenings we spend together philosophising about the world.

I also had great pleasure exchanging expertise and having enjoyable and exhilarating moments with the colleagues from the other sections and would like to give special thanks to Vladimir Biziks, Yagmur Bütün Buschalsky, Andreas Buschalsky, Arne Imken, Brendan Marais, Philip van Niekerk, Maximilian Wentzel and Michaela Zauner.

I would also like to extend my deepest gratitude to my friends Yagmur Bütün Buschalsky, Andreas Buschalsky, Pascal Fuchs, Tim Hollmann, Arne Imken, Robert Krause, Luisa Nobrega, Catharina Riggers, Stefan Vogel and Marcel Wiese for their profound belief in my abilities during times when I was completely lost. I also thank for their unwavering guidance trough tough years and for the innumerable uplifting and encouraging moments at diverse game, chat and dancing nights and at the M'era Luna.

In Addition, I'm extremely grateful to Tim Hollmann, Robert Krause and Stefan Vogel for proofreading my thesis and giving me helpful comments and advice for my work.

Furthermore, I want to thank the people from the sign language practise and my mates from Taekwondo for the balance to the worries of the work.

I gratefully acknowledge the help of Mr. Begemann, Mrs. Göhmann-Ebel and Mrs. Müller.

Last but not least, I would like to give my greatest thanks to my family Bärbel Rühlicke, Gerhard Rühlicke, Sabine Vogel and Stefan Vogel, who have unceasingly helped me on all my ways, who unconditionally supported me in every decision I made and have always accompanied me.

Dankeschön

Thank you very much

谢谢

teşekkür ederim

II Zusammenfassung

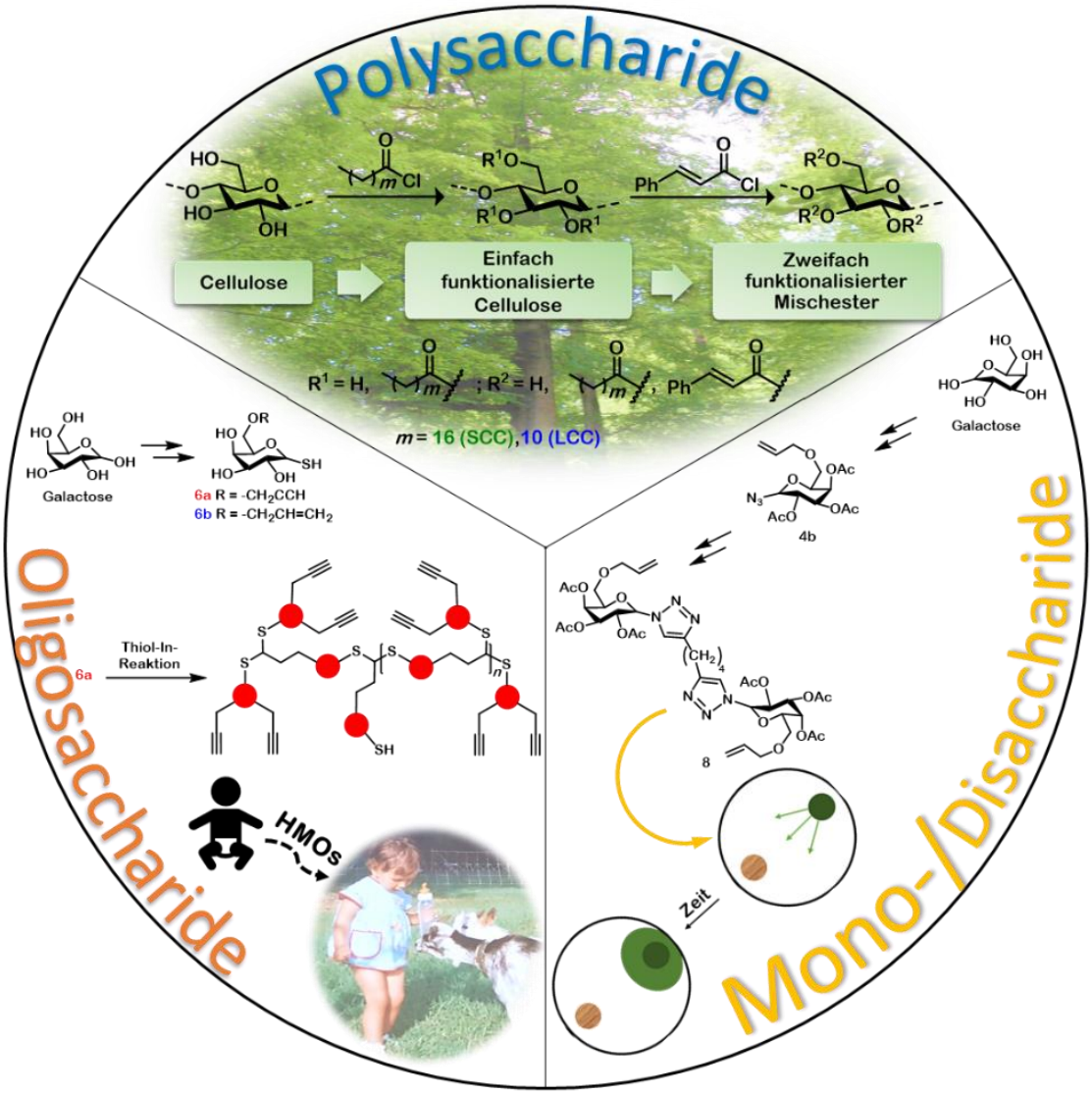

Saccharide, auch bekannt als Kohlenhydrate, sind in der Natur allgegenwärtig und werden schon seit Jahrtausenden von den Menschen genutzt. Dabei sorgt die enorme Variabilität der Saccharide für ein weitreichendes Spektrum der Anwendungsgebiete. Im Allgemeinen können die Saccharide in drei Untergruppen geteilt werden. Zum einen die Gruppe der Mono- bzw. Disaccharide, bei welchen es sich um die sogenannten einfachen Zuckern, meistens Hexosen oder Pentosen, wie z.B. Glucose, oder eine Kombination aus zwei Zuckerbausteinen, wie es bei Lactose der Fall ist, handelt. Sie bilden die Grundsteine für die Biosynthese von Naturstoffen, sowie für die beiden anderen Gruppen, die Oligo-, drei bis zehn Zuckerbausteine, und die Polysaccharide, mit mehr als zehn Bausteinen.

Entsprechend der hohen Variations- und Kombinationsmöglichkeiten von Sacchariden, präsentieren sich auch die Anwendungsmöglichkeiten dieser. Sie reichen von dem einfachen Nutzen als Nahrungsmittel, Energielieferanten, zur Herstellung von Kleidung und Papier bis hin zu den

moderneren komplexeren Nutzen als Ausgangsstoffe für Hydrogele, zur Herstellung transparenter biologisch abbaubarer Verpackungsmaterialien für Lebensmittel, zur Herstellung von flexiblen elektronischen Filmen oder auch für die Herstellung neuer Impfstoffe bzw. neuer Medikamente gegen neurodegenerative Krankheiten wie Alzheimer oder Parkinson.

Des Weiteren dienen die natürlich vorkommenden Saccharide als Inspiration für neuartige Modifizierungen von Sacchariden bzw. mimetische Oligo- und Polysaccharide. Dabei gilt das Augenmerk nicht nur der Herstellung glycosidisch verbundener Monosaccharide, zur synthetischen Herstellung von Oligo- und Polysacchariden, sondern auch dem Aufbau neuer zuckerbasierender Oligomere bzw. Polymere mit nicht glycosidischen Verbindungen, beispielsweise durch eine Click-Verknüpfung über eine Kupfer katalysierte Azid-Alkin-Kupplung, eine Thiol-En-Kupplung oder auch über eine UGI-Reaktion.

In der hier präsentierten Arbeit wurde Cellulose, ein exemplarisches erneuerbares natürliches Polysaccharid, als Ausgangsstoff für eine zweistufige heterogene Veresterung mit einem langkettigen Alkyl-Säurechlorid (Laurinsäurechlorid bzw. Stearinsäurechlorid) in der ersten Stufe und mit Zimtsäurechlorid in der zweiten Stufe, genutzt. Durch diese zweistufige Synthese-Sequenz konnte erfolgreich zwei neuartige Cellulose-Misch-Ester SCC (stearoylated cinnamoylated cellulose ester) und LCC (lauroylated cinnamoylated cellulose ester) dargestellt und vollständig chemisch *via* FTIR, NMR spektroskopisch und über DSC charakterisiert werden. Eine anschließende Prüfung auf besondere materielle Eigenschaften offenbarte die Eigenschaft transparente und flexible Filme zu erzeugen, die unter anderem auf Lösungsmittel und Temperatur ansprechende Eigenschaften zeigen. Des Weiteren weisen die hergestellten Filme selbstheilende Eigenschaften auf.

Neben der Nutzung von Cellulose als Biopolymer, wurde Galactose als natürliches und biologisch interessantes Monosaccharid als Grundmaterial für weitergehende Modifikationen. Galactose konnte in zwei jeweils sechs Stufen umfassenden Synthesen, zum einen mit einer endständigen Alken-Gruppe, sowie einer Marcaptan-Gruppe und zum anderen mit einem endständigen Alkin und ebenfalls einer Mercaptan-Gruppe versehen werden. Da die ungeschützte Mercaptan-Gruppe an Luftsauerstoff zur Dimerisierung neigt, wurden die jeweiligen Vorläufer-Verbindungen einer chemischen Analyse über FTIR und NMR-spektroskopisch charakterisiert. In Anschluss daran wurde eine grundlegende Untersuchung der notwendigen Reaktionsbedingungen für eine erfolgreiche Thiol-En- bzw. Thiol-In-Kupplung, die zu einer Ausbildung Click-verknüpfter linearer bzw. verzweigter Oligosaccharid-Ketten führen soll, durchgeführt.

Neben der bereits beschriebenen Modifikation, wurde Galactose ebenfalls als Ausgangsstoff für eine weitere sechs stufigen Sequenz genutzt, die als angestrebtes Ziel ein Galactose-basierendes Molekül mit einem endständigen Alken- und einer Azid-Funktion hat.

Das angestrebte Ziel konnte mit einer Ausbeute von 32 % über alle sechs Einzelschritte erreicht werden und des Weiteren vollständig FTIR- und NMR-spektroskopisch untersucht werden. Nachfolgend konnte das erhaltene Produkt in einer symmetrischen Kupfer-katalysierten Azid-Alkin-Kupplung mit 1,7-Octadiin in ein zuckerbasiertes symmetrisches Di-Triazol überführt werden. Das symmetrische Triazol wurde in einem Test mit den Pilzstämmen *Coniophora puteana* und *Trametes versicolor* auf potentielle fungizide Eigenschaften überprüft. Außerdem wurden weitere potentielle Modifikationsmöglichkeiten hin zur Ausbildung eines Oligo- bzw. Polysaccharides aufgezeigt.

Bei der hier vorliegenden Arbeit handelt es sich um eine Monographie, die eine bereits veröffentlichte Publikation umfasst. Nach einer allgemeinen Einleitung, gefolgt von der Zielsetzung, werden für jeden Abschnitt, der drei behandelten Themenblöcke, ein Literatur-Überblick des jeweiligen Themenbereichs, sowie eine ausführliche Präsentation der Ergebnisse mit der dazugehöriger Diskussion und einer Zusammenfassung, dargestellt, bevor es zu einer abschließenden allgemeinen Zusammenfassung übergeht. Die Haupt-Themenblöcke sind in den Kapiteln 3 bis 5 zu finden.

III Abstract

Saccharides, also known as carbohydrates, are ubiquitous and have been used by men for millennia. The high variability of the saccharides ensures a wide field of applications. In general, saccharides could be subdivided into three groups. Firstly, the group of mono- or disaccharides, which are the so-called simple sugars, mostly hexoses or pentoses, such as glucose, or a combination of two components as it is the case with lactose. They form the basic building blocks for the biosynthesis of natural compounds. Furthermore, they are the basic building block for the oligosaccharides, which contain three to ten sugar units and the polysaccharides which have more than ten sugar units.

The high variation and combination possibilities of saccharides leads to a broad field of applications. The field contains simple uses as for nourishment, as energy supplier, source for clothes and paper. Besides this, the field also contains more complex uses such as resources for hydrogels, for the production of transparent biologic degradable packaging for food, for the generating of flexible electronical films or for the production of novel vaccines or new drugs for the treatment of neurodegenerative illnesses like Alzheimer disease or the Parkinson disease.

Furthermore, the naturally occurring saccharides serve as inspiration for novel modifications of saccharides or mimetic oligo- and polysaccharides. The focus of the research lies on different aspects. One of those is the production of glycosidic linked monosaccharides for the synthetic production of oligo- and polysaccharides. Another one is the construction of new sugar-based oligomers or polymers with non-glycosidic linkages, for example by click linking like the copper-catalysed azide alkyne coupling, a thiol-ene coupling or *via* a UGI reaction.

In this presented paper, cellulose, as an example for a natural renewable polysaccharide, was used as resource for a two-step containing heterogeneous esterification with a long chain alky acid chloride (stearoylchloride or lauroylchlroride) in the first step and cinnamoylchloride in the second step. Over this two step-synthesis two novel cellulose mix esters SCC (stearoylated cinnamoylated cellulose ester) and LCC (lauroylated cinnamoylated cellulose ester) were successfully generated and have been completely chemically characterised *via* FTIR, NMR spectroscopy and DSC. Afterwards, the products were tested on outstanding material properties. It turned out, that both products were able to form transparent flexible films, which showed solvent and temperature driven properties. Moreover, the films revealed the ability of self-healing.

Alongside the use of cellulose as a biopolymer, galactose as a natural and biological interesting monosaccharide was used for further modifications as a basic material. Galactose was provided in a six-step synthesis on the one hand with an end standing alkene and a thiol group and on the other hand

with an end standing alkyne and a thiol group. Due to the high reactivity of the unprotected thiol groups, the precursor molecules were completely chemically analysed *via* FTIR and NMR spectroscopy. Afterwards, a basic investigation of the necessary reaction conditions for a successful thiol-yne respectively thiol-ene coupling, that lead to click linked linear respectively branched oligosaccharide chains, was examined.

Besides the modifications described, galactose was further used as resource in another six-step reaction with the goal of introducing an alkene and an azide functionalisation. The molecule was synthesised with an overall yield of 32 % and the product was completely examined *via* FTIR and NMR spectroscopy.

Afterwards, the obtained product was converted *via* a symmetrical copper catalysed azide alkyne coupling with 1,7-octadiyne to a symmetrical di triazole. The triazole was tested on antifungal properties with the two different fungi stains *Coniophora puteana* and *Trametes versicolor*. Furthermore, alternative modification possibilities were shown, like a reaction leading to novel oligo- or polysaccharides.

The presented study is a monography, containing one publication. After a general introduction, followed by the objectives, the three main topic blocks, each containing a literature overview of the respective topic area, as well as a detailed presentation of the results with the corresponding discussion and a summary, are presented before moving on to a final general summary.

The main topic blocks can be found in the chapters 3 through 5.

Table of content

1 Introduction

Saccharides are ubiquitous in nature and were used as sources for food, fuel, textiles and also had great impact in the development of cultures for many centuries.[1–5] The name derives from the ancient word ‘saccharon’, which can be translated to sugar.[1,2] Saccharides are also known as carbohydrates, because the empirical formula for the first investigated sugars was $C_n(H_2O)_n$.[1,2] Later investigations lead to the insight, on the one hand, that the idea of carbon connected to water was too simple and, on the other hand, that saccharides could also contain other kinds of atoms like nitrogen or sulphur.[1]

The simplest saccharide is glucose, a monosaccharide, which is also the key building block for natural product biosynthesis.[2,6,7] Saccharides can be divided into three subgroups. The elemental building components are monosaccharides as glucose or galactose.[1] They form the first group of saccharides together with the disaccharides, which contain two elemental sugar units connected over a glycosidic bond.[1,2] One well known representative is lactose.[8] The next group are saccharides containing three to ten sugar monomers, the so called oligosaccharides.[9–11] The last group are the polysaccharides, which contain more than ten sugar units, as for example cellulose or starch.[1,2,12,13]

Since saccharides are renewable and sustainable resources, the general interest in saccharide-based materials and components is growing fast.[5] Due to the great variability of saccharide-based natural materials, they offer a broad field of applications.[1,2,6,7,14] Examples for those applications are aggregation induced emission luminogens[15], nanocarriers for medical applications[16,17], polysaccharide-based food packaging[18] and for the reversible binding of CO_2.[19]

Polysaccharides are ideal for the development of novel functional materials. MITURA *et al*. reported about different biopolymers used for the synthesis of hydrogels, that can be used in cosmetics.[20] Furthermore, polysaccharides could operate as filler materials for pharmaceutics to generate a better handling of the dosage forms of pharmaceutics.[21]

Cellulose is a representative polysaccharide[1,2,12,13] and it is one of the most abundant and divers biopolymers in modern times.[3,4,12,13,22–24,25] The application possibilities of cellulose range from its use as composite or reinforcing agent in nanocomposites[3,4,24], in the biomedical field[3,4,23,24] and printing[1–4,12,13,24] to electronics respectively biosensors.[22,24] This broad variability makes cellulose to a unique resource for the development of novel functional materials.

Alongside the polysaccharides, the monosaccharides and disaccharides as the key elements of oligo- and polysaccharides, also offer a broad field of application.[26–28] In general, mono- and disaccharides show mostly biological, therapeutic and pharmacological properties.[27,29–32] Monosaccharides such as

for example glucose, galactose and disaccharides as e.g. lactose have a significant impact on the mammalian metabolism.[8,27,28,32,33] As mentioned previously, monosaccharides are the elemental building blocks of oligo- and polysaccharides. Therefore many biologically active compounds are based on saccharides.[27,28,34] Important examples are provided by the galacto-oligosaccharides GOS, which are closely connected to the human milk oligosaccharides HMO.[34,35,36,37] The GOSs as well as the HMOs can be found in the human breast milk and are vital for the intestinal development of infants.[36,38]

Together with the discovery of new saccharide based functional materials and biologically active saccharides, the chemical synthesis evolved to simplify and design novel strategies for creating glycomimetics.[17,39]

In order to conserve the resources as far as possible, suitable high yielding synthetic strategies for novel glycomimetics are preferred, as for example the click reactions.[40–42] Established reactions reach from photoinitiated thiol-ene couplings TEC[43], over multicomponent reactions such as the UGI reaction[44] to the well-known copper-catalysed azide-alkyne cycloaddition CuAAC reaction.[45]

Here, in the thesis presented, cellulose was used, as a representative polysaccharide, and galactose, representatively for a monosaccharide, as natural renewable resources for the creation of novel functional materials respectively biologic active compounds.

In the first part of this work, cellulose was modified *via* a heterogeneous esterification in two steps with one long chain acid chloride for the first reaction and cinnamic acid chloride in the second step, in order to prepare two novel materials with outstanding functionalities. This part of this thesis was already published.[46]

The second part deals with the modification of galactose to obtain two potential monomers, containing a double or triple bond and a thiol group, for a TEC and a comparable thiol-yne coupling.

In the last part of this work, the synthesis of a galactose-based monomer with a double bond and an azide group and the following symmetrical CuAAC with 1,7-Octadiyne is discussed. Furthermore, the resulting symmetrical sugar-based di triazole was tested on antifungal properties.

2 Objectives

The main topic of the present work are saccharides, which are a big representative sustainable substance class in nature. Saccharides could be divided into three subgroups. Every chapter of the presented work deal with a different kind of group (Figure 2.1).

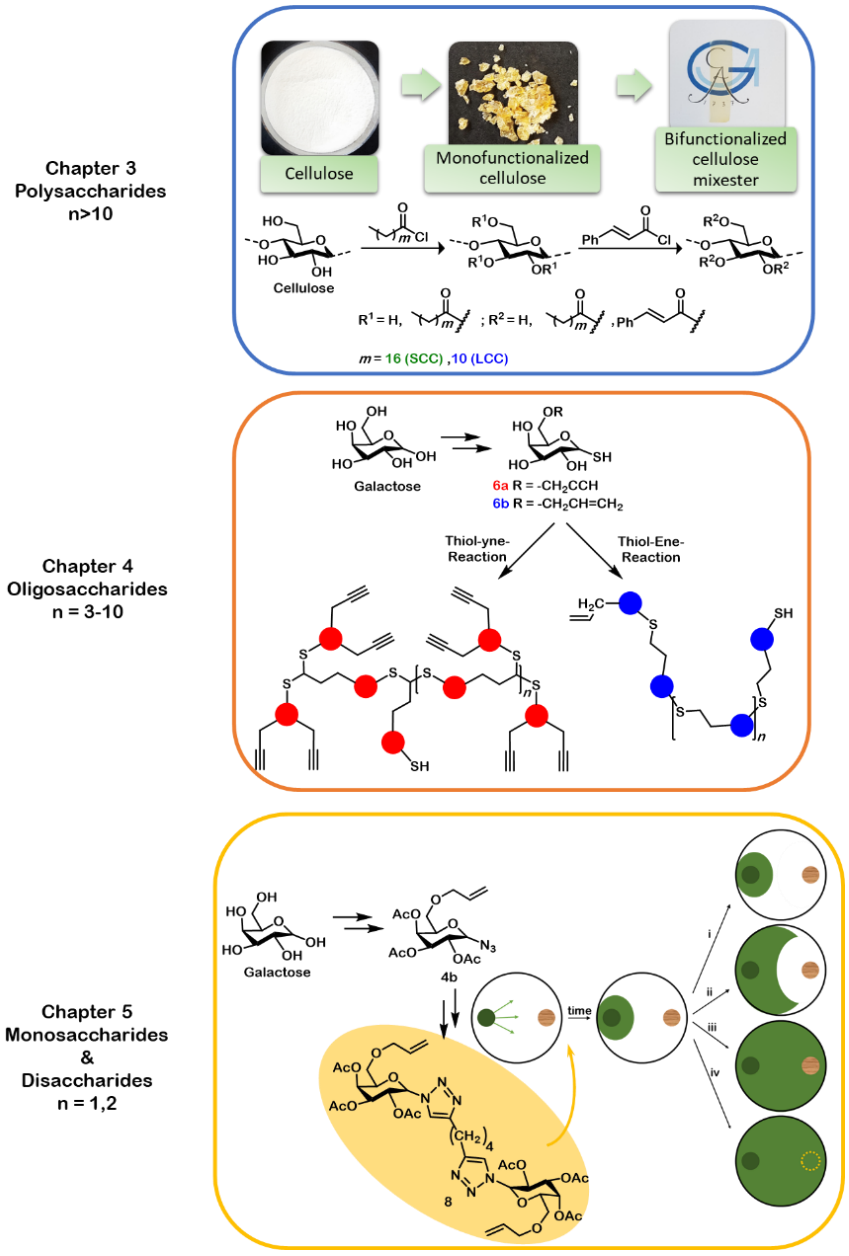

Figure 2.1 Graphical abstract of this work. The main part of this work is subdivided into three chapters. Chapter 3, marked with the **blue** box on the top, deals with the modification of cellulose in order to prepare bifunctionalised cellulose mixesters with outstanding mechanical properties. Chapter 4, marked with the **orange** box on the left, is treating the idea to synthesise branched and linear oligosaccharides over thiol-ene respectively thiol-yne coupling starting from two galactose-based monomers. In chapter 5, marked in **yellow** on the right, a galactose-based symmetrical di triazole is synthesised and tested on potential antifungal properties.

Saccharides containing more than ten sugar units are classified as polysaccharides. Cellulose, as one well known representative of the polysaccharides, is used in chapter 3 as resource for two sequentially heterogeneous esterifications. For this esterifications stearoyl chloride respectively lauroyl chloride is used for the first sequence followed by the second reaction with cinnamoyl chloride. This should lead to bifunctionalised cellulose mixesters (SCC and LCC), which can be used for the formation of multifunctional transparent cellulose films. This part of the thesis has already been published.[46]

The second group of saccharides, are the oligosaccharides containing three to ten sugar units. In chapter 4 it was aimed to prepare oligomers starting from galactose-based monomers. For this, two different monomers with a thiol group each and a triple bond **6a** respectively a double bond **6b** should be synthesized over two six-step synthesis. To get the aimed branched and linear oligomers, the reaction conditions for the thiol-yne respectively thio-ene coupling is basically examined.

The last group are the mono and disaccharides. Within chapter 5, a five-step synthesis of the double bond and azide containing monosaccharide **7** was intended. In a symmetrical CuAAC reaction with 1,7-octadiyne the di triazole **8** was obtained. Starting from the prepared disaccharide, promising antifungal properties have been tested.

3 „Synthesis of novel cellulose mixesters for transparent responsive films with switchable mechanical properties“

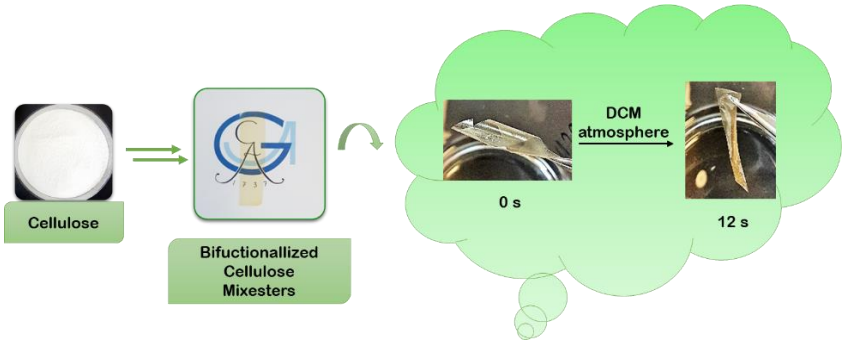

This part of the thesis was already published.[46]

Soft actuators have attracted much attention during the last decades due to their potentially broad applications ranging from sensors to artificial muscles. Until now, most of such soft actuators are still based on synthetic polymers. Herein, a novel group of materials derived from sustainable cellulose as potential starting materials for the preparation of soft actuators was described. To be precise, cellulose mixesters with acyl esters of distinct chain lengths and cinnamic ester were synthesised through a two-step synthesis and used for the preparation of responsive thin film actuators. These cellulose mixesters have degree of substitution ascribed to stearoyl (DS_{St}) of 1.51 or lauroyl groups (DS_{La}) of 1.48 and degree of substitution ascribed to cinnamoyl groups (DS_{Ci}) of 1.34 to 1.35. Furthermore, the influence of the chain lengths of the two different aliphatic esters as well as the switchable crosslinking of cinnamoyl moieties on the materials properties was further shown. Using these cellulose mixesters, transparent thin films with thickness a of 4-15 µm were prepared via facile solvent casting. These films had light-responsive mechanical properties from rigid to elastic after illumination with UV light of distinct wavelengths (254 nm and 310-400 nm). Moreover, the thin films showed shape memory effect and the ability of self-healing.

3.1 Literature overview

Actuators are devices and materials that are able to change their shape or some special properties in response to changes in their environment.[47,48] Those changes differ from relaxation[48] over changes in the crystalline order[49] to changes in the volume[50] and changes in the shape.[51] Since the last century, hard actuators, e.g. metals, metal oxides or bimetal strings, are well known and used in many mechanical systems.[47,52] In recent years, the demand for soft polymeric actuators raised the development of polymer-based actuators.[53] The great advantage of the polymeric actuators is the high variety and huge diversity for tunable material and mechanical properties.[47,54,55] Together with the rapid development of the preparation of actuators using diverse materials, many new applications have been found, such as for soft robotics[55,56], drug delivery systems[50,51,57], micro sensors[58] and artificial muscles.[59,60]

Further great improvement on actuators is the effort to prepare actuators by incorporating renewable[61,62] and sustainable components.[59,63,64] To achieve this goal, various organic and inorganic sustainable materials were integrated into either two-layer or single-layer systems to prepare actuators.[59,65] As typical examples for the use of renewable materials in bilayer systems are graphene/gold bilayer complexes[61], graphite-carbon nanotube hybrid films[62] and actuators made of poly-(vinyl alcohol-*co*-ethylene) nanofibers and cellulose nanocrystals.[66]

Especially, cellulose as a renewable biobased material shows great potential as a resource for sustainable actuators.[67,68] Cellulose-based actuators have already been known for several years and typical examples are the electroactive papers that can be used as sensors or for energy storage.[69] In order to endow cellulose with desired functionalities, chemical modifications are often applied and quite a few pathways for the modification of cellulose have also been developed in the past decades.[64,68,70] Among them, a common and facile method to modify cellulose is the esterification.[71,72]

In this work, a novel group of cellulose mixesters containing two groups as the starting material for film actuators was prepared. Cellulose was modified via two subsequent esterification steps, leading to novel bifunctionalised cellulose mixesters containing diverse functional groups. One type of these diverse functional groups is long alkanoyl groups, such as stearoyl or lauroyl moieties, which are known for their flexibility and their engagement in VAN DER WAALS as well as hydrophobic interactions.[73] The other type of these diverse functional groups is cinnamoyl groups that are known to be able to photodimerize.[74–77] These bifunctionalised cellulose mixesters were characterized with various analytical methods including elemental analysis, FOURIER-transform infrared (FTIR) spectroscopy and nuclear magnetic resonance (NMR) spectroscopy. They were further transformed

into transparent films, which demonstrated multistimuli responsive shape-transition and mechanical properties.

3.2 Results and discussion

3.2.1. Synthesis and characterisation of cellulose mixesters

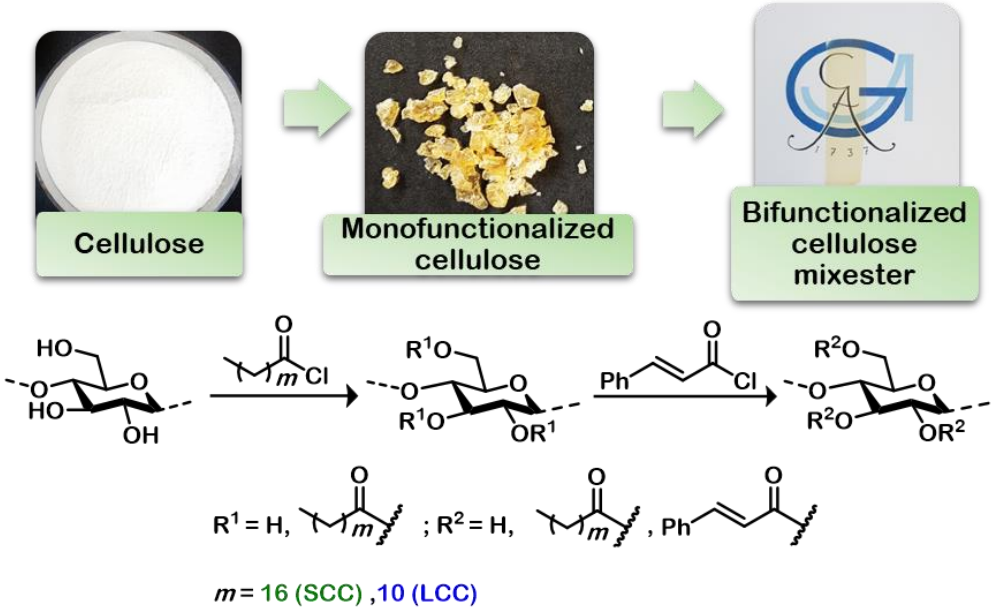

Figure 3.2.1.1. Schematic illustration for the preparation of the bifunctionalised cellulose mixesters, which starts with the first reaction on cellulose using a long chain acid chloride and ends with the second reaction with cinnamoyl chloride.

In this work, monofunctionalized cellulose using stearoyl and lauroyl chloride leading to stearoylated cellulose SC and lauroylated cellulose LC were synthesized (Figure 3.2.1.1). Then, SC and LC were further modified with cinnamic acid chloride under heterogeneous reaction conditions for the second functionalisation. Following along this route, stearoylated cinnamic cellulose mixesters SCC and lauroylated cinnamic cellulose mixesters LCC were synthesised, which have different aliphatic chain lengths. The chemical structures of these mixesters were further systematically characterised via DSC, FTIR and NMR-spectroscopy (Figure 3.2.1.2).

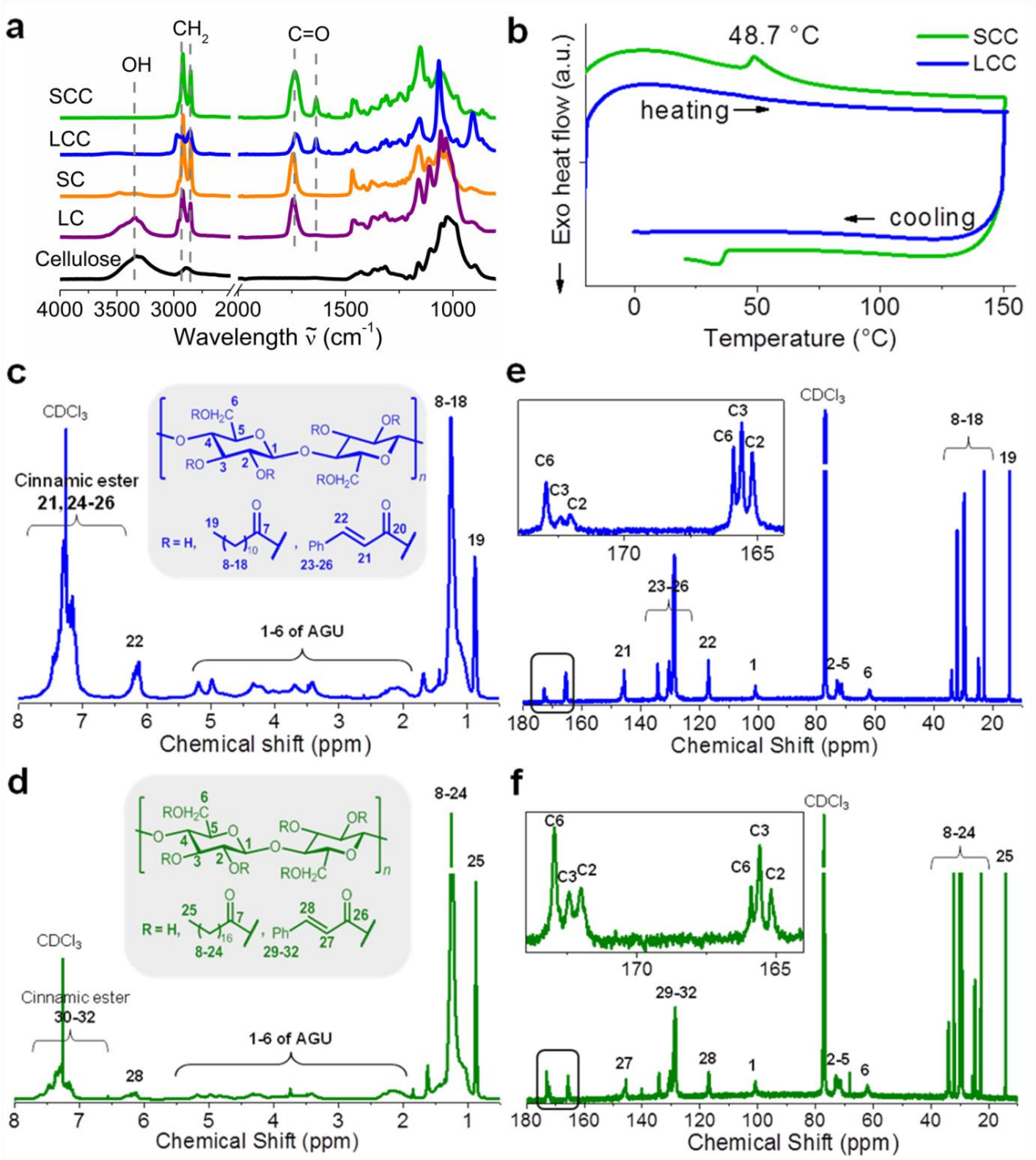

Figure 3.2.1.2. a) FTIR spectra of cellulose and cellulose derivatives. b) Representative DSC curves of the bifunctionalised cellulose derivatives SCC and LCC. ^{1}H-NMR spectrum of c) LCC and d) SCC measured in $CDCl_3$. ^{13}C-NMR spectrum of e) LCC and f) SCC measured in $CDCl_3$.

FTIR spectrum of cellulose shows a significant wide signal at 3350 cm^{-1} attributed to hydroxyl groups and an exceedingly small signal at 2900 cm^{-1} for the sp^3-CH (Figure 3.2.1.2a). In comparison, the signal ascribed to hydroxyl groups in the FTIR spectrum of SC or LC is barely visible and the signal of sp^3-CH increased significantly. Moreover, a new signal emerged at 1700 cm^{-1}, which is derived

from carbonyl groups of the corresponding alkanoyl moieties. Within the FTIR spectrums of the mixesters SCC and LCC, the signal attributed to hydroxyl groups disappeared. In addition, the CH-signal changed slightly compared to the signal in the FTIR spectrums of the SC and LC. A further new carbonyl peak due to the introduction of cinnamoyl moieties appeared next to the first carbonyl signal derived from the long chain alkanoyl moieties.

Figure 3.2.1.2b shows the DSC measurement of SCC and LCC. Both cellulose mixesters showed a wide glass transition state in the temperature range of 5 °C-150 °C. This wide glass transition temperature leads to the expectation of glassy behaviours of materials represented as sufficient flexibility. Furthermore, the DSC measurement shows that SCC could partially crystallize with a crystallisation point at 48.7 °C during the heating process, while it is approximately 15 °C lower during the cooling process. In contrary, LCC did not show any significant crystallisation signal according to the DSC measurement. This is primarily due to the presence of shorter lauroyl chains of LCC in comparison to SCC, which could not crystallize under applied environment compared to the longer stearoyl groups.

Within the ^{1}H-NMR spectrum of LCC (Figure 3.2.1.2c), the terminal methyl group **19** has its signal at 0.80 ppm, while the CH_2 signal **8** to**18** lies around 1.20 ppm. The signals of the carbon atoms **1** to **6** of cellulose backbone are in the range of 2.08-5.27 ppm. The signals ascribed to double bonds **22** are between 6.09 and 6.29 ppm. The second signal of the double bond **21** is in the same range as the aromatic signals of the cinnamic ester **24** to **26** between 7.11-7.46 ppm. Within the ^{1}H-NMR spectrum of SCC (Figure 3.2.1.2d), the signal **25** ascribed to terminal methyl can be found at 0.8 ppm, whereas signal **8** to **24** of the alkyl groups is around 1.26 ppm. The signals for the carbon atoms **1** to **6** of cellulose backbone are between 1.62 and 5.5 ppm. The aromatic signals of the cinnamic ester carbon atoms **30** to **32** are between 7.11 and 7.59 ppm. The signals of the double bonds are at 7.80 ppm for carbon atom **27** and 6.18 ppm for **28**.

Within the ^{13}C-NMR spectrum of LCC, the terminal methyl shows a signal of **19** at 14.2 ppm (Figure 3.2.1.2e). The signals of the remaining alkyl chain **8** to**18** can be found between 22.8 to 32.1 ppm. The signals of carbons atoms **1** to **6** of cellulose backbone are between 62.1 and 100.8 ppm. The double bonds result in two signals at 145.6 ppm for **21** and 116.9 ppm for **22**. The aromatic signals are between 128.4 and 134.2 ppm. As well, two groups of separate signals ascribed to two types of esters containing three peaks for each ester moiety at the cellulose backbone can be observed. Due to the two different groups of ester moieties, two groups containing three signals each are visible. These signals can be found at 165.2, 165.6 and 165.9 ppm for the cinnamoyl moieties and at 171.9, 172.4 and 172.9 ppm for the alkanoyl moieties.[71,73]

Within the ^{13}C-NMR spectrum of SCC, the signal of the terminal CH_3-group **23** can be found at 14.3 ppm (Figure 3.2.1.2f). The signals of the alkyl chain carbon atoms **8** to **24** lie between 22.8 and 34.1 ppm. The carbon signals of the cellulose backbone are visible in the range of 61.9-101.1 ppm, which is typical for carbons **1**-**6** of cellulose. The signals attributed to double bonds **27** and **28** are in the range of 116.9-45.6 ppm. The aromatic signals **29** to **32** lie between 128.4 and 130.8 ppm. Moreover, the ester groups for the cinnamoyl moieties at 165.2, 165.6 and 165.8 ppm and for the alkanoyl moieties at 171.9, 172.4 and 172.9 ppm can be found.

The ^{1}H-NMR spectra of SCC and LCC were further used to determine the DS of the corresponding alkanoyl (DS_{La}/DS_{St}) and cinnamoyl groups (DS_{Ci}). The ratios between the integrals of the signals ascribed to the terminal methyl group and one hydrogen of the double bonds of cinnamoyl groups and the integrals of the signals attributed to the cellulose backbone were used for the calculation (Figure 3.2.1.2c and 3.2.1.2d). Obtained DS were summarized in Table 3.2.1.1.

Table 3.2.1.1. Calculated DS of the corresponding groups in LCC an SCC based on integral ratios of the terminal methyl groups of **19** (LCC) / **25** (SCC) as well as one hydrogen signal of the cinnamoyl double bond of **22** (LCC) / **28** (SCC) to the cellulose backbone signals.

	Integral -CH_3	DS_{St}	DS_{La}	Integral Ph-CH=CH-	DS_{Ci}
LC	--	--	1.48[a]	--	
LCC	4.44	--	1.48	1.34	1.34
SC	--	1.66[a]	--	--	
SCC	4.53	1.51	--	1.35	1.35

[a] These DS were calculated based on the elemental analysis.

Thus, the chemical structures of synthesized cellulose mixesters were clearly characterised by FTIR- and NMR-spectroscopic measurements. Moreover, both cellulose mixesters SCC and LCC had distinct thermal properties according to the DSC measurements.

3.2.2. Preparation and characterization of films using the bifunctionalised mixesters

Both bifunctionalised SCC and LCC were further used for the preparation of transparent responsive film actuators. Films of defined dimensions were fabricated via solvent casting in teflon moulds. 100 mg of the corresponding mixester was dissolved in 10 ml THF and the solution was transferred in a teflon mold with a diameter of 5 cm. The THF was allowed to evaporate at room temperature overnight to produce thin films with a thickness of 4-15 µm. After complete drying, highly transparent films were obtained using both SCC and LCC (Figure 3.2.2.1a). The flexible films produced from LCC and SCC turned out to be slightly yellow.

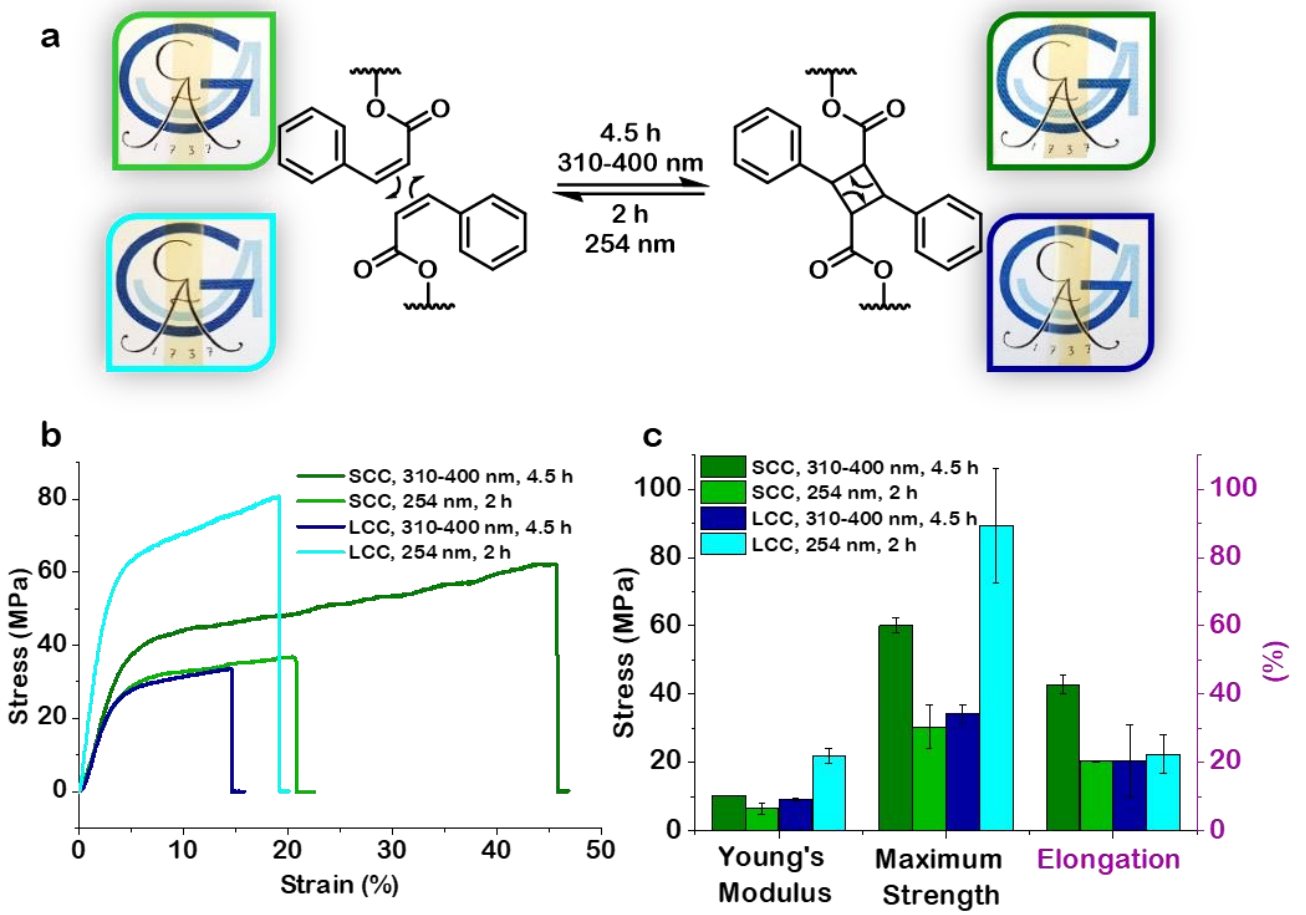

Figure 3.2.2.1. a) Schematic illustration for the photodimerisation and reverse reaction of films fabricated using SCC and LCC as well as the photos of the films. b) Representative tensile test curves. c) Average mechanical parameters of films fabricated using SCC and LCC after diverse treatments with UV light of 310-400 nm for 4.5 h and UV light of 254 nm for 2 h.

As reported previously in several studies, cinnamoyl moieties can undergo a reversible photodimerisation via the exposure to UV light of different wavelengths.[74–77] Using the UV light of 310-400 nm, a [2+2]-cycloaddition of the double bonds within neighboured cinnamoyl moieties occurs after 4.5 h, which can be reversed after the irradiation with UV light of 254 nm for 2 h. After the UV-illumination, the films maintained the high transparency (Figure 3.2.2.1a). In comparison, their mechanical properties were strongly modified (Figure 3.2.2.1b and 3.2.2.1c). The mechanical properties and the effects of the illumination by corresponding UV lights on YOUNG's modulus, maximal strength and elongation of films were determined at a constant temperature of 20 °C and a relative humidity of 60 % (Figure 3.2.2.1b and 3.2.2.1c). The green curves in Figure 3.2.2.1b show the results of the SCC films and the blue curves the results of the LCC films, while the specific results are summarised in Figure 3.2.2.1c.

Using SCC with longer stearoyl side chains, the dimerisation of cinnamoyl moieties led to increased elasticity (45 % elongation) at the beginning of the tensile test. This could be because of the presence of self-assembled semicrystalline structures by the long stearoyl moieties.[73] The dimerisation also elevated maximum strength (~60 MPa stress), whereas the non-crosslinked films were rather rigid (20 % elongation) and fragile (25 MPa stress). In comparison, LCC films containing shorter aliphatic esters showed different mechanical behaviours. After the irradiation with UV light of 310 to 400 nm, the LCC films became stiff with 15 % elongation and the maximum strength dramatically decreased to 25 MPa. In comparison, the decrease of the YOUNG's modulus was marginal, compared to SCC films after equal treatments. After the exposure to the UV irradiation of 254 nm for two hours, the films turned from brittle to tough with a maximal stress of ~90 MPa, but the films were still quite stiff (with only 20 % elongation).

These results clearly showed that the chain length of the introduced alkyl groups as well as the photo-dimeriseable cinnamoyl groups have a great impact on the mechanical properties of obtained films. Moreover, longer stearoyl chains form semicrystalline structures in the obtained films and have a higher steric hindrance than the shorter lauroyl chains.[73] This should lead to fewer dimers of cinnamoyl moieties during the irradiation with UV light of 310-400 nm. In addition, alkyl moieties with these diverse chain lengths could have VAN DER WAALS interactions of distinct extents and thus distinct influence on the mechanical properties. By including these diverse aliphatic moieties, distinct overall elasticity, maximum extensibility and load-bearing capacity of the films are adjustable. Nevertheless, the UV dimerisation of cinnamoyl groups is reversible, so that the mechanical properties of SCC/LCC films can be switched between two states simply by using UV illumination of different wave lengths (Figure 3.2.2.1a).

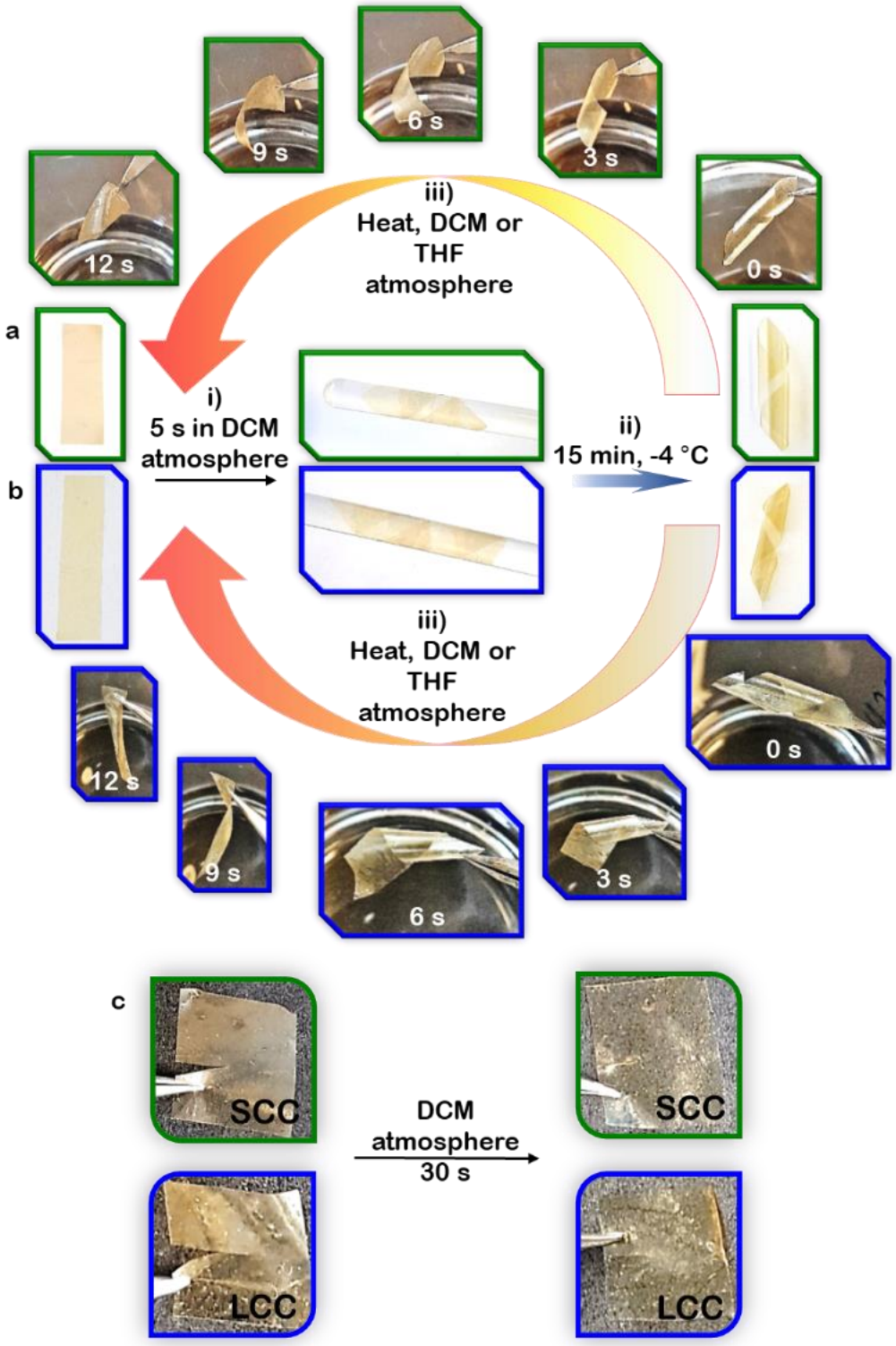

Figure 3.2.2.2. Responsive shape-memory behaviours of a) LCC and b) SCC. i) The films around a glass rod were placed above DCM or THF at room temperature to give a spiral shape. ii) The prefixed films were cooled to -4 °C for 15 minutes to get the stable spiral shape. iii) Exposing the spiral films to DCM or THF atmosphere or heat led to original film shape. c) Self-healing properties of SCC and LCC. When an LCC or SCC sample with a notch was held into a DCM atmosphere for 30 seconds, the film was healed.

Both SCC and LCC films showed the ability of one-way shape memory and self-healing properties (Figure 3.2.2.2). To present the shape memory effect of the films, a sample of each was firstly fixed in a spiral shape via exposure to a THF or DCM atmosphere for a few seconds and further cooling at 4 °C for 15 min (Figure 3.2.2.2a and 3.2.2.2b). Upon exposure to a DCM or THF atmosphere or heat, the films turned back from the spiral shape to their original shape. Apart from the shape memory property, the films exhibited the self-healing character (Figure 3.2.2.2c). To show this property, SCC and LCC films with a size of 1 cm×1 cm (length and width) and a thickness of 4.4-15 µm were cut with a sharp scalpel. After exposing the samples to a DCM atmosphere for 30 seconds, the notches in the films got sealed.

3.3 Conclusion

In total, a novel strategy for the synthesis of bifunctionalised cellulose mixesters and further preparation of responsive film actuators was reported. Bifunctionalised cellulose mixesters were obtained via a two-step heterogeneous reaction. It proceeded with the esterification of cellulose with a long chain aliphatic acid chloride in the first step and cinnamoyl chloride in the second step, leading to SCC and LCC. SCC had a melting point of 48.7 °C, while LCC showed a broad glass transition without a significant melding point. Furthermore, both compounds formed transparent films with tuneable mechanical properties based on the reversible photodimerisation of cinnamoyl moieties. These films showed tuneable elastic deformation ability and plastic deformation properties, which depended on the length of the aliphatic chains and the crosslinking of cinnamoyl moieties. In addition, SCC and LCC films exhibited responsive shape-memory behaviours and self-healing property.

4 "Synthesis of linear and branched sugar polymers *via* thiol-ene / thiol-yne reaction"

Oligosaccharides are abundant in nature. They show a wide spectrum of biological functionalities. Therefore, the synthesis and research on oligosaccharides was increased in the recent years. Together with the synthesis of defined structures, new oligosaccharide mimics were developed. An easy way for preparing those oligosaccharide mimics is provided by the well-known click reactions CuACC and the thiol-ene coupling. Herein, the synthesis of two different monomers as starting material for the green thiol-ene coupling respectively thiol-yne coupling were described. Because of the high reactivity of the prepared monomers, the protected precursor molecules were analysed completely *via* NMR and IR spectroscopy. Using those precursor molecules, highly reactive monomers were obtained, that were able to perform an oligomerisation. In order to optimise the reaction, the properties of the deprotection followed by the oligomerisation were further investigated. To evaluate the success of the reaction mass spectroscopy was used. It turned out, that oxygen had great impact on the reaction. For further research on this reaction, also the use HPLC to get more information about the composition of the resulting reaction mixture was suggested.

4.1 Literature overview

In nature many different substance classes can be found. One important substance class are the saccharides, which can be divided into three subgroups. The first group are the monosaccharides and disaccharides, mainly hexoses, pentoses and combinations of them, like glucose, xylose or respectively saccharose and lactose. The second group are the oligosaccharides. They consist of three to ten carbohydrate monomers and are mostly connected over glycosidic bonds.[9,11,78] The last group are the polysaccharides, such as cellulose and starch, that are build-up of more than ten carbohydrate monomers.

Especially the oligosaccharides display a broad spectrum of different functionalities in biological processes.[10] Examples for these functionalities in biological processes are galacto-oliogosaccharides, human milk oligosaccharides and cyclodextrins.[9] The galacto-olidosaccharides have a prebiotic functionality.[9,11] Human milk oligosaccharides are found in the human breast milk and are vitally important for the growth and development of infants.[79,80] The afore mentioned cyclodextrines have a plethora of different functionalities, like to stabilise emulsions or volatile compounds and they can be used for drug delivery systems[9,81]

Besides the afore mentioned health benefits, oligosaccharides were also found out to have antiviral and antibacterial effects[38,79], they could have positive effects on diabetics[79] and are promising targets for the creation of new vaccines.[82]

Due to this wide spectrum of functionalities, oligosaccharides are desired structures for synthesis. Along with physical methods, like hydrolysis, and chemical methods, as isomerisations and extractions, enzymatic methods could be used for producing oligosaccharides.[9] All kinds of methods for synthesising natural oligosaccharides undergo a steady improvement and are focused in research. In 2010, the group around EBRAHIM *et al*. developed a new reactor system for the enzymatic production of galacto-oligosaccharides from lactose.[37] Since lactose can be found in milk and is a by-product of cheese production, it is a suitable substance for further reactions. XIAO *et al*. gave an overview about further derivation of lactose.[8] Apart from the biological methods, chemical processes such as the synthesis of human milk oligosaccharides can also be mentioned.[83]

Not just natural oligosaccharides are of great interest, also the development of new oligosaccharide mimics is focused by researchers.[84] Although, structures seem to be more simple to reach the synthesis on carbohydrates show some challenges compared to the synthesis of other natural structures, like peptides or nucleotides.[42,85] Due to these challenges click reactions provide an easy way to synthesise novel oligosaccharide or polysaccharide mimics with non-glycosidic linkings.[42,86–90] One

of the most famous methods is the CuAAC reaction.[40,41] Because of its simplicity it found its way into the saccharide chemistry.[90] One example for the usage of this reaction was given by UHRIG *et al.*.[91] This working group used CuAAC to click different oligosaccharide analoges on a given carbohydrate based matrix to prepare novel interesting carbohydrate based oligo and polysaccharides. Another example is the work of HOTHA et al. who used the CuAAC to obtain pseudo oligosaccharides.[88,89] Many more examples for the usage of the well-known CuAAC were published to date.

Apart from this well studied and commonly used reaction, there are more useful click reactions playing important roles in synthetic chemistry.

Another commonly used click reaction is the thiol-ene coupling reaction.[92–94] Compared to the CuACC reaction, it is an environmental friendly reaction. After the CuAAC reaction was mainly used in the synthesis of novel biologically reactive molecules, it was found out, that the copper catalyst in the reaction has a certain cytotoxity.[95] Because of this, using UV light as a catalysator for the reaction turned out to be more suitable for creating materials in high yield without any disturbing residues from the reaction.[92,93,96] Now, many working groups are using the thiol-ene coupling as click reaction in carbohydrate related chemistry.[42,97]

It was reported as a tool for the synthesis of thiodisaccharides[98] and imino disaccharides.[99] The working group of BORBÁS *et al*. for example was investigating the synthesis of thiol linked glycoconjugates by the thiol-ene coupling starting from enoses.[43,100] Another example was given by the working group around KRAMER *et al.* who first used a thiol-ene coupling to prepare glycosylated *L*-cysteine-*N*-carboxyanhydride monomers. Afterwards they used the monomers in a living polymerisation to get glycopolypetides.[101]

Furthermore the thiol-ene coupling also proved its suitability for connecting saccharides to cyclodextrine rings in a simultaneous reaction.[102] Besides the given examples for the usage of the thiol-ene coupling, it was further reported as a suitable reaction for linking carbohydrates to proteins.[103]

In this work two novel galactose-based monosaccharides containing a thiol group were prepared. One of these synthesised monomers contained a double bond, whereas the other monomer had the respective triple bond. The six-step containing synthesis of the monomers was reported. Since the monomers of this kind showed a rather low stability when exposed to air,[94,104,105] the more stable precursor molecules were characterised completely. Up till now, just few examples of click linked oligo- respectively polysaccharide mimics were reported.[90] In order to pave the way for further

research, the conditions for an oligomerisation *via* thiol-ene respectively thiol-yne coupling of the designed monomers were examined.

4.2 Results and discussion

Synthesis and Characterisation

In this work, the two different monomers on base of the galactose monosaccharide were build up firstly (Fig. 4.2.1).

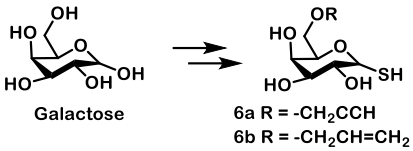

Figure 4.2.1 Planned synthesis of the monomers **6a** and **6b** for the polymerisation *via* thiol-yne /thiol-ene coupling starting from galactose.

Both of those monomers contained a thiol group and a triple bond **6a** or a double bond **6b** and were synthesised in a six-step sequence as shown in Figure 4.2.2. In the first step of the synthesis the hydroxyl groups at the C-1 to C-4 were protected by building up two acetals with acetone. For this reaction a yield of 83 % was achieved. After this step the hydroxyl group at the C-6 of the protected galactose was free for further reactions.

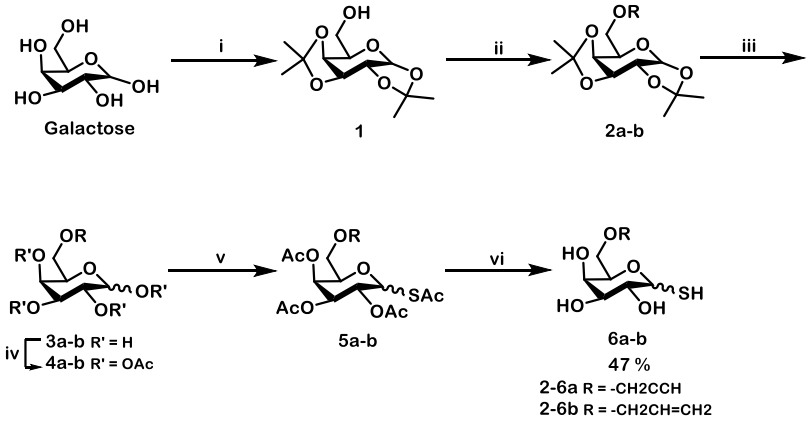

Figure 4.2.2 Multistep synthesis of the desired monomers **6a** and **6b** with an overall yield of 47 % (over six steps) in both cases. i) I_2, Acetone, rt, 20 h; ii) NaH, **a)** propargyl bromide **b)** allyl bromide, *abs.* DMF, 0 °C to rt, 3.5 h; iii) Dowex®, H_2O, 80 °C, overnight; iv) pyridine, Ac_2O, rt, 20 h; v) thio acetic acid, $BF_3 \cdot Et_2O$, DCM, 0 °C to rt, 24 h; vi) NaOMe, *abs.* methanol, rt, 2 h.

The next step was the etherification of the free hydroxyl group with propargyl bromide which leads to **2a** with a yield of 92 % or respectively allyl bromide to get **2b** with a yield of 71 %. The next two steps were the deprotection of the etherified molecules **2a** and **2b** with Dowex® and the following protection with acetic anhydride in pyridine. The deprotection of **2a** and **2b** lead to a mixture of the α and the β anomer of the corresponding carbohydrate **3a** and **3b**. This appearance of the anomers was observed

in all further reaction steps. The new protection gave a yield of 85 % over two steps for **4a** and a yield of 84 % over two steps for **4b**.

After this the acetyl ester at the C-1 of **4a** and **4b** was replaced by a thio acetic ester leading to **5a** with a yield of 72 % and **5b** with a yield of 95 %.

The obtained carbohydrates **5a** and **5b** were used as precursor molecules for the preparation of the desired thiol-yne complex **6a** and the desired thiol-ene complex **6b** by saponification of the acetyl groups. This last step was meant to be quantitative due to being a deprotection reaction.

The overall yield from galactose to the desired monomers **6a** and **6b** was in both cases 47 %.

After the successful synthesis, it was planned to further characterise **6a** and **6b**.

Unfortunately, it turned out, that the thiols **6a** and **6b** were highly reactive, so the monomers dimerised within a short time, when getting in contact with the oxygen from the air (Figure 4.2.3).[94,104,105] This reaction is well known and can be avoided by working under inert gas atmosphere. For the further coupling, it was important to improve the reaction set up. The changes that were taken so far are discussed later, after the characterisation of the exact structure.

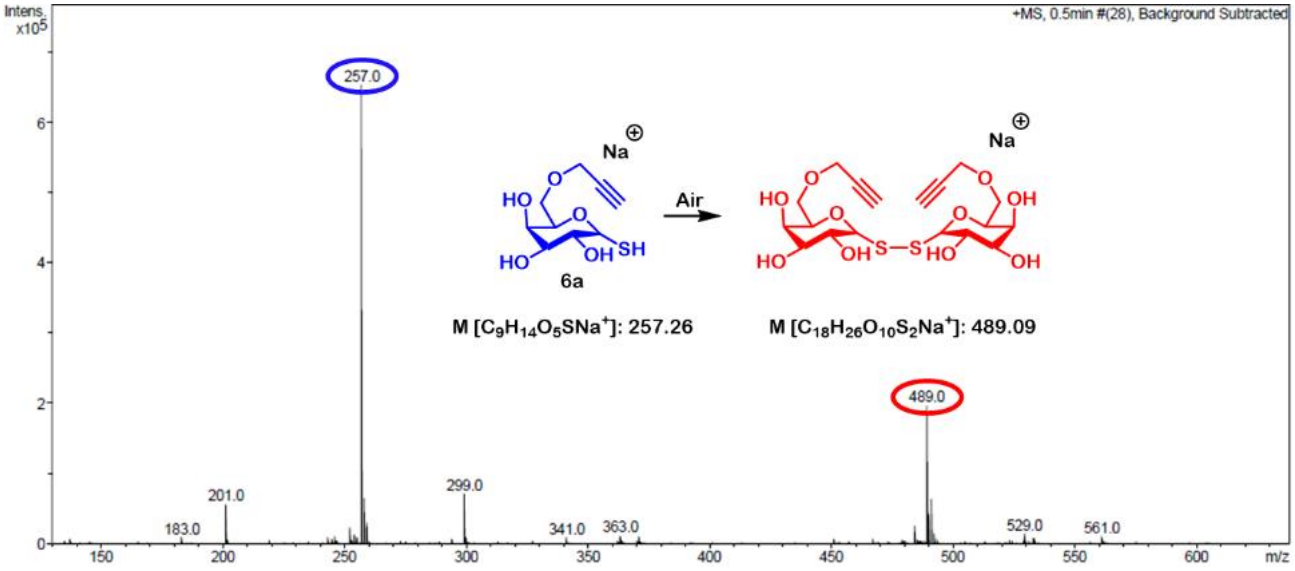

Figure 4.2.3 Mass spectrometric analysis of **6a**. It shows the dimerization of the synthesised monomer.

Because of the instability of the monomers **6a** and **6b**, the precursor molecules **5a** and **5b** were completely chemically characterised for further discussions and for proving the designed structure. Figure 4.2.4 shows the FTIR, one dimensional and two-dimensional NMR measurements of **5a**.

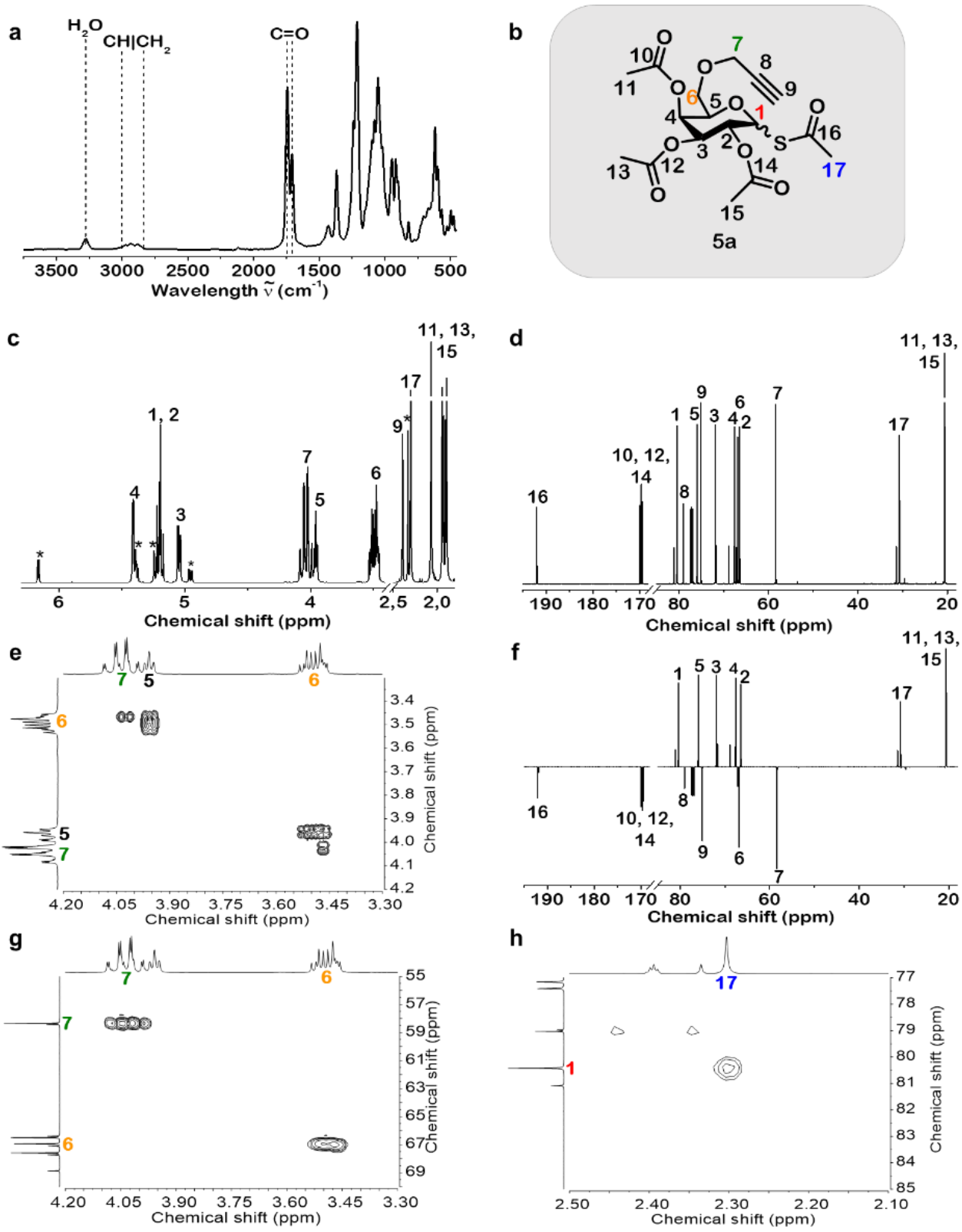

Figure 4.2.4 Chemical analysis of the precursor molecule **5a**. a) FTIR spectrum; b) Molecular structure; c) ^{1}H-NMR in $CDCl_3$; d) ^{13}C-NMR in $CDCl_3$; e) ^{1}H-COSY in $CDCl_3$; f) APT in $CDCl_3$; g) HSQC in $CDCl_3$; h) HMBC in $CDCl_3$.

Figure 4.2.4a shows the FTIR spectrum of the precursor molecule **5a**. In this spectrum different structural properties are visible. There are two different C=O bands visible at 1730 cm^{-1} and 1750 cm^{-1}, which are related to the acetyl esters and to the thio acetic ester, that were formed during the reaction sequence. Furthermore, a weak broad band from 2800 cm^{-1} to 3000 cm^{-1} could be found, that can be ascribed to the aliphatic CH, CH_2 and CH_3 groups of the molecule. Moreover, there is a weak sharp signal at 3250 cm^{-1} indicating some residual water in the sample.

The mass analysis clearly confirms the precursor molecule **5a**. The calculated mass of M $[C_{17}H_{22}O_9NaS]^+$: 425.0877 fits to the found mass of 425.0882.

The ^{1}H- and the ^{13}C-NMR (Figure 4.2.4c and d) point out the mentioned formation of anomers for all derivatives from step iii) on, during the multistep synthesis. In all showed spectra a second pair of signals is observable. The anomers of compound **5a** have a ratio of approximately 1:5.

Within the ^{1}H-NMR of the precursor molecule **5a** (Figure 4.2.4c) the CH_3 groups **11**, **13** and **15** of the according acetat esters have their signals at 1.89 ppm, 1.94 ppm and 2.07 ppm. The thio acetic ester **17** is shifted downfield to 2.30 ppm. The peaks of the introduced propargyl ether can be found at 2.39 ppm for the terminal proton **9** and between 3.96 ppm and 4.11 ppm as a multiplett for the CH_2 group **7**. The signals of the galactose skeleton **1** to **6** are appearing as usual between 3.40 ppm and 5.50 ppm except the signal of the **H-1**. The signal of the main anomer is shifted high field to 5.04 ppm, whereas the other anomer has its **H-1** signal at the more common value of 6.16 ppm.

Within the ^{13}C-NMR spectrum of the precursor molecule **5a** (Figure 4.2.4d) the signals of the methyl groups of the actetic esters **11**, **13** and **15** are at 20.5 ppm and at 20.6 ppm. As seen in the ^{1}H-NMR the methyl group of the thio acetic ester **17** is shifted downfield to 30.8 ppm. The signals of the propargyl ether are at 58.3 ppm for the CH_2 **7**, 75.1 ppm for the CH **9** and at 79.0 ppm for the quaternary C atom **8**. Furthermore, the peaks of the galactose structure **1-6** are like usual between 66.9 ppm and 80.4 ppm. The peaks of the quaternary ester atoms **10**, **12** and **14** are set at 169.4 ppm, 169.7 ppm and 170.0 ppm. As well the quaternary signal of the thio actetic ester **16** is significantly shifted downfield to 192.0 ppm.

Figure 4.2.4f shows the APT of molecule **5a**. The negative signals at 58.3 ppm and at 66.9 ppm can clearly be assigned to the CH_2 groups **7** and **6**. Furthermore, the quaternary C atom **8** of the propargyl ether leads to a negative signal at 79.0 ppm. The negative signals at 169.4 ppm, 169.7 ppm, 170.0 ppm and the significantly downfield shifted signal at 192.1 ppm can be allocated to the oxo esters **10**, **12**, **14**, respectively the thio ester **16** of compound **5a**.

Figure 4.2.4g shows a cut-out of the HSQC in the range of 3.30 ppm to 4.20 ppm for the ^{1}H-NMR spectrum and 55.0 ppm to 70.0 ppm for the corresponding ^{13}C-NMR spectrum. The accorded ^{1}H-NMR spectrum is showed on the top and the accorded ^{13}C-NMR is shown on the left side of the 2D area. It clearly shows two cross peaks. One cross peak is at 66.9 ppm and 3.44 ppm to 3.59 ppm which can be assigned to the CH_2 group **6**, marked in **yellow**, of the galactose skeleton. The other cross peak can be found at 58.3 ppm and 3.96 ppm to 4.11 ppm and can be assigned to the CH_2 group **7**, marked in **green**, of the introduced propargyl side chain.

Figure 4.2.4e shows the ^{1}H-COSY of compound **5a** in the range of 3.30 ppm to 4.20 ppm. The associated ^{1}H-NMR spectrum is showed on the top and on the left side of the 2D spectrum. In the range chosen are the two signals of the both CH_2 groups **6** and **7** and the signal of **H-5** of compound **5a**. The spectrum reveals cross peaks between both CH_2 groups at 3.44 ppm to 3.59 ppm and 3.96 ppm to 4.11ppm and a cross peak between the **H-5** and the CH_2 group **6** at 3.44 ppm to 3.59 ppm and 3.96 ppm. This is a great evidence that the etherification at **C-6** worked out as predicted.

Figure 4.2.4h shows the HMBC of compound **5a** in the range of 2.10 ppm to 2.50 ppm for the ^{1}H-NMR spectrum and 77.0 ppm to 85.0 ppm for the ^{13}C-NMR spectrum. The accorded ^{1}H-NMR spectrum is shown on the top and the accorded ^{13}C-NMR spectrum is shown on the left side of the 2D spectrum. Within this cut-out of the spectrum only one cross peak is visible at 2.30 ppm and 80.4 ppm. The signal at 2.30 ppm is the downshifted methyl group of the thioester, whereas the signal at 80.4 ppm is addressed to the carbon **1**, marked in **red**, of the galactose skeleton. These cross-peak proofs the connection between the sugar skeleton and the successfully introduced thioester. Another evidences of the replacement of the oxo ester at carbon **1** by the thio ester, are the shifted signals of the methylene signal **17**, marked in **blue**, in the ^{1}H-NMR to 2.30 ppm (figure 4.2.4c) and the shifted signals of the methylene carbon **17** to 30.8 ppm and the quaternary atom **16** to 192.0 ppm in the ^{13}C-NMR (figure 4.2.4d).

Figure 4.2.5 shows the FTIR, one dimensional and two dimensional NMR measurements of **5b**.

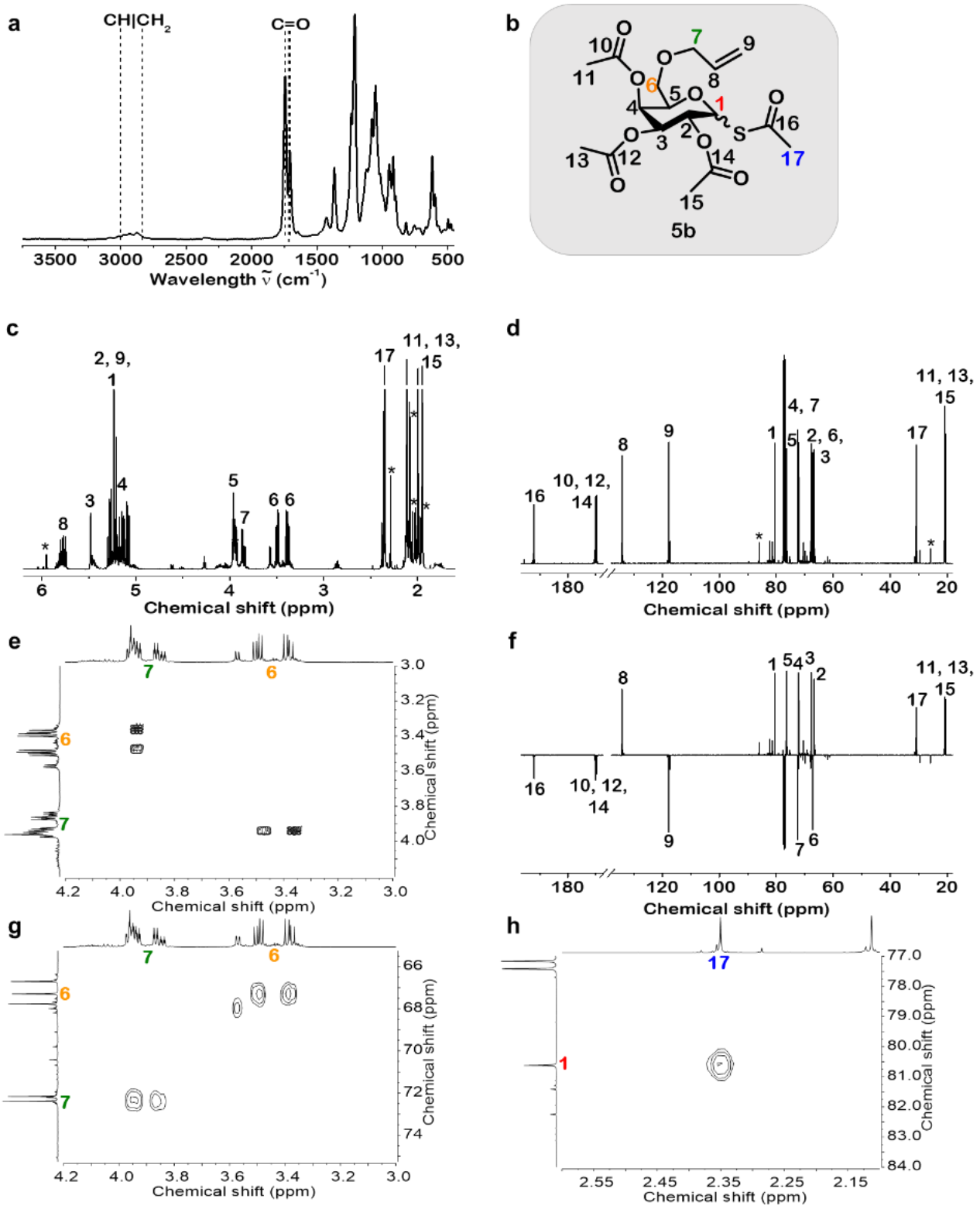

Figure 4.2.5 Chemical analysis of the precursor molecule **5b**. a) FTIR spectrum; b) Molecular structure; c) ^{1}H NMR in $CDCl_3$; d) ^{13}C NMR in $CDCl_3$; e) ^{1}H-COSY in $CDCl_3$; f) APT in $CDCl_3$; g) HSQC in $CDCl_3$; h) HMBC in $CDCl_3$.

Figure 4.2.5a shows the FTIR spectrum of the precursor molecule **5b** in which some different structural properties are visible. First of all, there are two different carbonyl signals at 1730 cm^{-1} and 1745 cm^{-1}. Those are related to the acetic ester and thio acetic esters, which were introduced into the molecule during the synthesis. Also, the wide small signal between 2800 cm^{-1} and 3000 cm^{-1}, which could be referred to the different CH, CH_2 and CH_3 groups in the precursor molecule **5b**.

The mass analysis clearly confirms the precursor molecule **5b**. The calculated mass of M $[C_{17}H_{24}O_9NaS]^+$: 427.1141 fits to the found mass of 427.1033.

The ^{1}H- and the ^{13}C-NMR (Figure 4.2.5c and d) of compound **5b** also show the mentioned formation of anomers with a ratio of 1:6.

Within the ^{1}H-NMR of the precursor molecule **5b** (Figure 4.2.5c) the CH_3 groups of the acetic esters **11**, **13**, **15** and the thio acetic ester **17** have their signals at 1.95 ppm, 1.99 ppm, 2.11 ppm and 2.35 ppm. The peaks of the introduced allyl ether are at 3.85 ppm to 3.95 ppm for the sp^3-CH_2 **7**, from 5.12 ppm to 5.31 ppm for the terminal sp^2-CH_2 group **9** and at 5.78 ppm for the CH group **8**. Besides that, the signals of the galactose backbone could be found at 3.38 ppm and 3.50 ppm for the **H-6**s, at 3.95 ppm for the **H-5**, at 5.09 ppm for **H-4**, from 5.12 ppm to 5.31 ppm for **H-2** and the **H-1** and at 5.48 ppm for **H-3**.

Within the ^{13}C-NMR of compound **5b** (Figure 4.2.5d) the signals of the CH_3 groups **11**, **13**, **15** and **17** of the acetic esters and the thio acetic ester are at 20.7 ppm, 2×20.8 ppm and at 30.9 ppm. The signals of the corresponding allyl ether could be found at 72.4 ppm for the sp^3-CH_2 **7**, at 117.7 ppm for the sp^2-CH_2 **9** and at 134.2 ppm for the CH group **8**. The signals of the galactose structure can be found at 66.7 ppm for the **C-2**, 67.3 ppm for the **C-6**, at 67.8 ppm for the **C-3**, at 72.2 ppm for the **C-4**, at 76.4 ppm for the **C-5** and at 80.6 ppm for the **C-1**. The peaks of the quaternary ester atoms **10**, **12**, **14** and **16** could be found at 169.7 ppm, 169.9 ppm, 170.1 ppm and 192.3 ppm.

Figure 4.2.5f shows the APT of compound **5b**. Here, seven negative signals can be found. Both signals at 67.3 ppm and 72.4 ppm can clearly be assigned to the CH_2 groups **6** and **7**. The next negative signal at 117.7 ppm can be clearly assigned to the terminal sp^2-CH_2 **9**. The last four negative signals at 169.7 ppm, 169.9 ppm, 170.1 ppm and the shifted signal at 192.3 ppm can be allocated to the quaternary carbons of the oxo esters **10**, **12**, **14** respectively to the thio ester **16** of compound **5b**.

Figure 4.2.5g shows a part of the HSQC in the range of 3.00 ppm to 4.20 ppm for the ^{1}H-NMR spectrum and 65.0 ppm to 75.0 ppm for the ^{13}C-NMR. The accorded ^{1}H-NMR spectrum is showed at the top and the accorded ^{13}C-NMR is shown at the left side of the 2D NMR spectrum. The spectrum

shows two cross peaks. One is at 67.3 ppm and 3.38 ppm to 3.50 ppm, which can be assigned to the galactose skeleton CH_2 **6**, marked in **yellow**. The other cross peak is at 72.4 ppm and 3.85 ppm to 3.95 ppm and can clearly be assigned to the CH_2 group of the introduced CH_2 group **7**, marked in **green**, of the allyl rest.

In figure 4.2.5e a cut-out of the ^{1}H-COSY is presented. It ranges from 3.00 ppm to 4.20 ppm. The accorded ^{1}H-NMR spectrum is shown at the top and at the left side of the correlation spectrum. The spectrum has two cross peaks. Both cross peaks are between 3.38 ppm to 3.50 ppm and 3.85 ppm to 3.95 ppm. It shows the coupling between the both CH_2 groups **6** and **7** and proofs the success of the planned etherification.

The last spectrum (figure 4.2.5h) is a cut-out of the HMBC. The cut-out ranges from 2.10 ppm to 2.60 ppm for the ^{1}H-NMR spectrum and from 77.0 ppm to 84.0 ppm for the ^{13}C-NMR spectrum. The accorded ^{1}H-NMR spectrum is shown at the top and the ^{13}C-NMR spectrum is shown on the left side of the 2D spectrum. The spectrum shows only one cross peak at 2.35 ppm and 80.6 ppm. The ^{1}H signal at 2.35 ppm can clearly be assigned to the methyl group of the thio ester **17**, marked in **blue**. The signal at 80.6 ppm is accorded to the galactose carbon **1**, marked in **red**. This cross peak shows the correlation between the galactose skeleton and the thio ester. It proofs the successful exchange of the formally oxo ester to the thioester.

Other evidence is given by the significant downfield shifting of the signals belonging to the thioester. The methyl group **17** is shifted to 1.35 ppm in the ^{1}H-NMR spectrum and to 30.9 ppm in the ^{13}C-NMR spectrum. Furthermore, the quaternary carbon of the thioester is also shifted to 192.3 ppm in the ^{13}C-NMR.

Thus, the chemical structures of both precursor molecules **5a** and **5b** were clearly characterised by FTIR and NMR spectroscopic measurements.

Oligomerisation of the prepared monomers

After the successful synthesis of the precursor molecules **5a** and **5b**, it was planned to remove the acetylic protection to get the monomers **6a** and **6b**. Those monomers should be oligomerized in the further proceeding to synthesise a branched fractal like polymer through a thiol-yne coupling or respectively a linear polymer through a thiol-ene coupling (Figure 4.2.5).

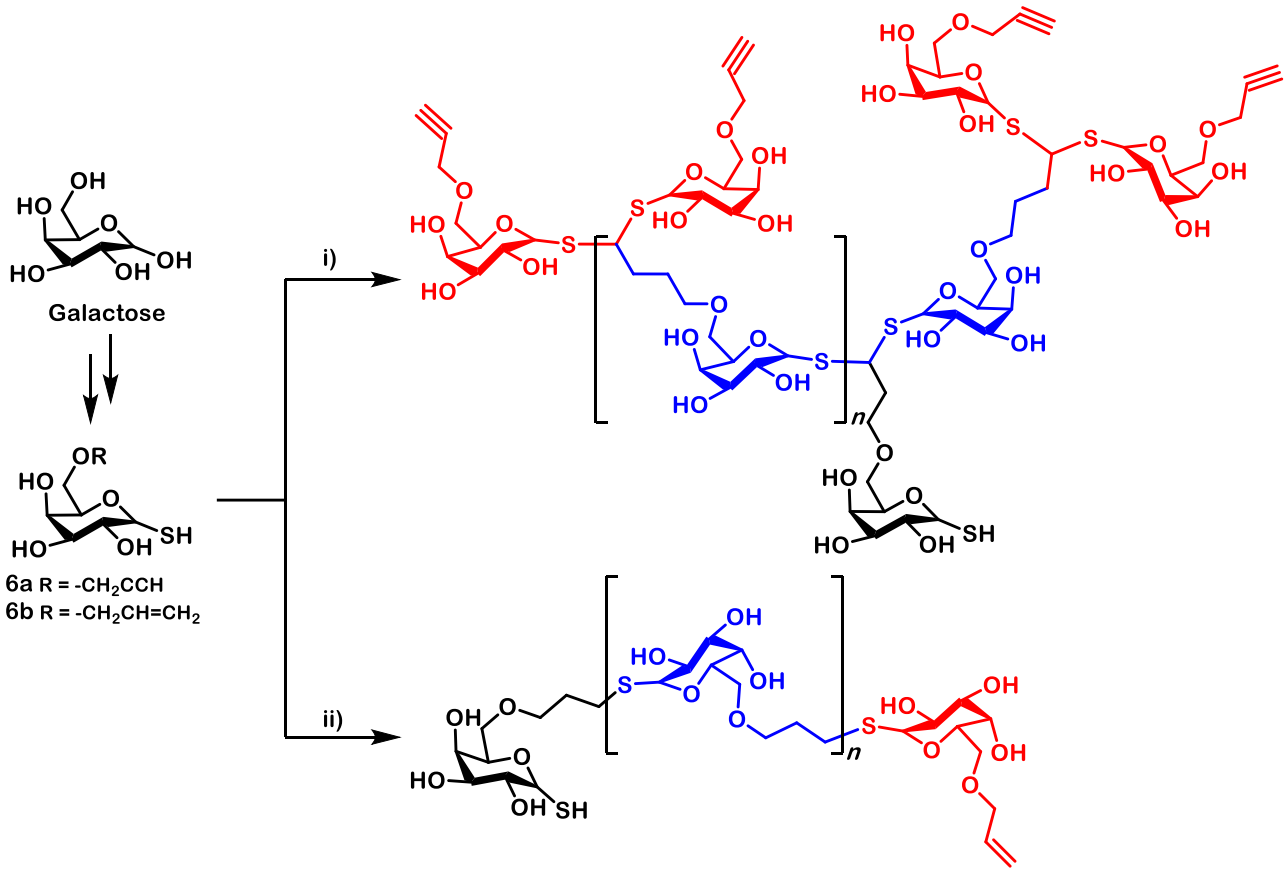

Figure 4.2.5 Planned polymerisation of **6a** and **6b.** i) The polymerisation was carried out *via* thiol-yne coupling creating a branched fractal like polymer. ii) In the second case the polymerisation was carried out by a thiol-ene coupling leading to a linear polymer.

As mentioned above, the monomer **6a** showed an instability according to the exposure to oxygen, which leads directly to a disulphide formation (Figure 4.2.3). To avoid this dimerisation the reaction needed some improvements. Simultaneous to these changes, the oligomerisation was enhanced. The precursor molecule **5a** was taken as representative example for the whole optimisation process. Table 4.2.1 shows all changes made.

Table 4.2.1 Stepwise improvement of the deprotection of **5a** followed by the strived oligomerisation of the monomer **6a**. The resulting solution was analysed via mass spectrometry.

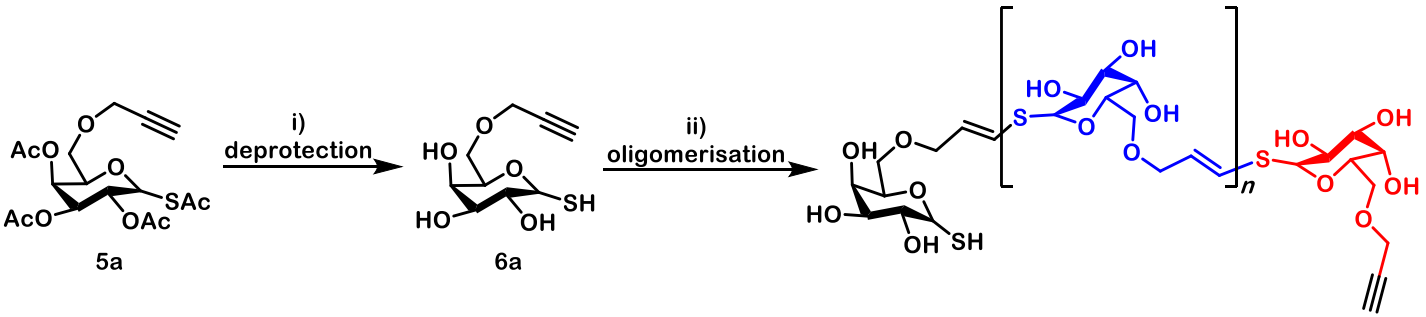

Reaction	i) Deprotection		Treatment of 6a	ii) Oligomerisation		Mass analysis of the resulting product			
	Solvent	Reaction conditions		Reaction conditions	Time	Percentual distribution[e]			Highest observable oligomer
						Monomer	Dimer	Trimer	
1	*abs*. MeOH	NaOMe, rt, 2 h	Dowex®, MeOH, concentrated at air	--	--	69.4	9.9[a] 20.7[b]	--	--
1a			TLC[c] after 2 weeks; Fraction 1	--	--	76.8	8.6[a] 8.6[b]	2.6[a] 3.2[b]	6
1b			TLC[d] after 2 weeks; Fraction 2	--	--	44.8	6.3[a] 40.8[b]	1.9[a] 6.1[b]	6
2	*abs*. MeOH	NaOMe, rt, 2 h, Dowex®[f]	*abs*. MeOH, argon atmosphere	UV, argon atmosphere, rt	24h	not detected	34.7[a] 8.8[b]	27.9[a] 28.6[b]	5
3	*abs*. MeOH[f]	NaOMe, rt, 2 h, Dowex®[f]	*abs*. MeOH[f], argon atmosphere	UV, argon atmosphere, rt	24h	51.2	24.4[a] 20.6[b]	2.7[a] 1.1[b]	3
4	*abs*. MeOH[f]	NaOMe, rt, 2 h, Dowex®[f]	*abs*. MeOH[f], argon atmosphere	DMPA, UV, argon atmosphere, rt	24h	no clear results measurable			

a Thiol-yne connected oligomers.
b Disulphide connected oligomers.
c Column chromatography on silica gel (DCM/MeOH: 9/1; R_f = 0.11).
d Column chromatography on silica gel (DCM/MeOH: 9/1; R_f = 0.04).
e For the percentual distribution, the amount of the monomer of the two different dimer masses and the two different trimer masses were taken as 100 % to get a defined correlation between them.
f Oxygen free. Solvents were degassed *via* lowered pressure and ultra-sonification for 5×3 min. Solids were evacuated for at least 2 h and kept under argon before usage.

In the beginning the precursor molecule **5a** was deprotected with NaOMe in methanol for 2 h at room temperature under air. After this the reaction was stopped by adding methanol washed Dowex®. Subsequently, the Dowex® was filtered off and the methanol removed under reduced pressure. The received product **6a** was analysed through mass spectrometry. This analysis showed clearly the ongoing dimerisation between the deprotected thiol groups. Besides this, also the aimed link between the thiol and the alkyne group was build up. Both dimers could be found in the mass analysis with a ratio of 69.4:9.9:20.7. (monomer:thiol-yne linked:disulphide). The thiol-yne linked dimer shows a m/z of 491.1 whereas the disulphide dimer has a m/z of 489.1. The oxidation of the both thiol groups leads to the loss of two hydrogen atoms in the molecule, which explains the difference in the mass analysis.

The product was stored concentrated at room temperature, while being exposed to air. After two weeks the product showed two different spots on TLC. After the careful separation of those two spots *via* column chromatography on silica gel (DCM/MeOH: 9/1; $R_{f,1} = 0.11$, $R_{f,2} = 0.04$), both fractions were also analysed *via* mass spectrometry. Fraction 1 showed nearly no difference between the amount of the desired thiol-yne linking and the disulphide. In contrast the second fraction showed higher thiol-thiol linked dimers and trimers.

These observations lead to the assumption, that the product **6a** should not be exposed to air. Therefore, in reaction 2 all solids used during the synthesis were degassed for at least 2 h to avoid oxygen in the reaction mixture and the product was kept in *abs.* methanol under argon atmosphere, before getting oligomerised *via* irradiation with 310 nm to 400 nm UV light. The analysis of the results of the mass spectrometry showed a significant increase of the formation of the desired thiol-yne linked products. Also, the monomer **6a** was not detected. This indicates, that the oxygen free reaction leads to the desired thiol-yne linked oligomer and prevents the thiol-thiol linking. For the reaction *abs.* methanol was added to the evacuated highly viscous precursor molecule **5a**. Because of its viscosity, oxygen could probably have remained in the resin like starting material **5a**.

Therefore, in reaction 3 the precursor molecule **5a** was solved in *abs.* methanol and the mixture was degassed *via* sonification under reduced pressure. This resulted in a deterioration of the relative distribution of the thiol-yne linking and the disulphide linking. Also, the highest observable oligomer was a trimer. In comparison the new reaction setting didn't show the expected success. This means evacuating the precursor molecule **5a** before solving it in already degassed *abs.* methanol is more effective, than vice versa.

In order to get a higher degree of polymerisation, in reaction 4 DMPA was added. Unfortunately, the mass spectrometry didn't show any of the expected signals. Neither the signal of the deprotected

monomer **6a** nor any signals of the possible oligomerisations have been visible. This leads to two suppositions. The first one is, that the reaction didn't work as planned. This needs further testing with different amounts of DMPA and different irradiation times. The other possibility is, that a higher oligomer (n>5) was built during the reaction, which is either not soluble or too big for the previous HPLC filtration and can't be measured *via* mass spectroscopy.

For further progression of the oligomerisation, more testing is necessary as well as the repetition of reaction settings leading to unexpected results. The basic examination of the deprotection followed by the oligomerisation provided the following information. The first one is, that the reaction needs to be free from oxygen. Also, the optimisation showed the need to evacuate all solids for at least 2 h first, as well as to degas the *abs*. methanol, before solving the precursor molecule **5a** in *abs.* methanol, in order to reduce possible oxygen in the reaction. For this reason, longer evacuation periods should be tested. In order to avoid any possible source of oxygen potential error sources should be identified and corrected. One potential error source could be the usage of gas bags for the irradiation in the UV chamber. It was observed, that the gas bag used slowly deflated over time, which indicates a leaking and therefore a potential exposure to air. One possible solution to this problem is the use of a gas bag of a higher quality. Also, instead of using the UV chamber, a UV probe could be a practicable solution. By using a UV probe the reaction setup needs to be considered due to safety reasons. Another possibility to reduce possible oxygen in the reaction is the usage of a glove box, instead of the SCHLENK-technic. Another part of the optimisation is the influence of the irradiation time with UV light.

Another great challenge, in the attempt to oligomerise the monomer **6a**, is the analysis of the formed products. As mentioned above, the mass spectrometry was mainly used to evaluate the success of the corresponding reaction. But this analysis just shows two types of information. First of all, it gives the relative amounts of the prepared dimers and trimers. The second information provided by the mass analysis, is, if there is any disulphide formation in the molecule. In this study presented, these disulphide formations only occurred once in a molecule. Once two molecules linked between the thiol groups, only terminal alkyne groups are left for further polymerisation. This leads to many different possibilities of oligomers obtained during the reaction.

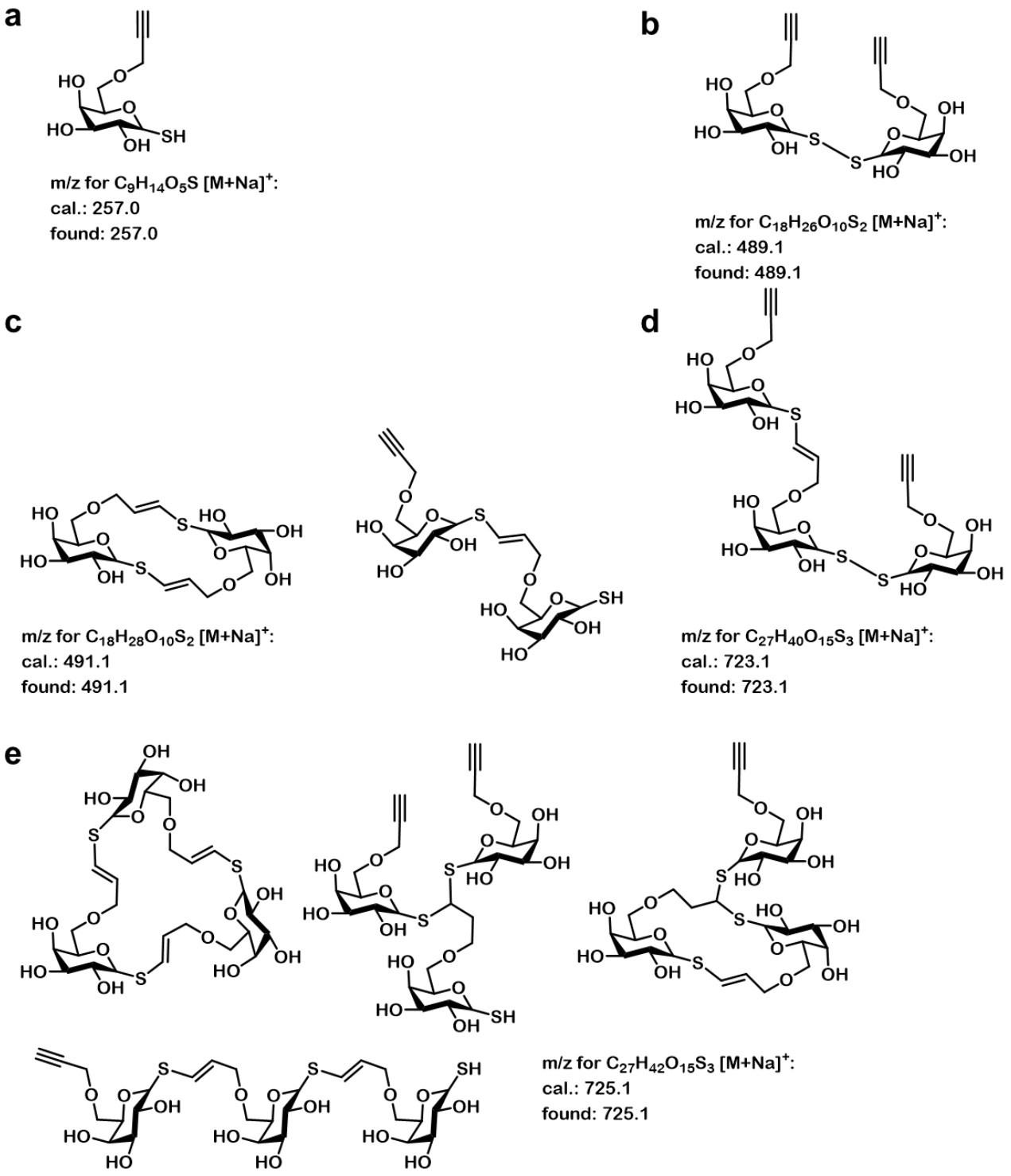

Figure 4.2.7 Selection of calculated and found peaks of the measured mass analysis. a) monomer **6a**; b) disulphide dimer; c) thiol-alkyne linked dimers; d) thiol-thiol linked trimer; e) thiol-alkyne linked trimers.

Figure 4.2.7 shows a selection of possible dimers and trimers formed during the reaction. For the disulphide dimers and trimers is just one possibility. Thinking about possible tetramers it changes to three options, since there are three possible positions for a new molecule to react (see Figure 4.2.7d). The thiol-alkyne linked molecules could be sorted into three categories. The first one are the linear

polymers. The second are the cyclic compounds. And the last one are branched ones mixed with one of the first categories. The compounds of the last category should not occur often, since UV controlled polymerisation between thiols and alkynes mostly lead to linear products.[106]

This clearly demonstrates the disadvantage of the mass analysis. Although, it shows the amounts of dimers and trimers and gives information about the links between the monomers, it can't give any information of what overall structure the resulted oligomers have.

So, it is very important to find a good way, to separate the resulting oligomers and analyse them. One possible solution to this problem could be the use of an HPLC. With this it should be feasible to separate the mixture of oligomers into defined fractions, which can be further evaluated. Compared to the mass analysis, which only gives quantitative results, the HPLC in combination with further analysis could potentially lead to a deeper understanding of the formed products.

Apart from changing the analysis of the resulting oligomers, the reaction itself needs some rethinking.

The goal was to synthesise a thiol alkyne linked oligomer. To achieve this target other initial conditions should be considered. One potential starting point could be to initial put of a suitable starting material in order to slowly add the monomer to keep the concentration as low as possible to avoid the disulphide formation and to attain a steady and controlled oligomerisation. One starting material could be one of the previously synthesised galactose ethers **2a**, **3a** or **4a**. The disulphide itself could be another suitable starting material, since there are just two end standing alkyne functionalisations to react with. Taking the disulphide as a starting material would also mean ether to change the previously aimed oligomer or to add another reaction after the oligomerisation to cleave the disulphide bond.[107]

Lastly, other possible reactions for a oligomerisation trough thiol-yne coupling respectively TEC should be tested as reported in literature.[43,106]

4.3 Conclusion

In total, two novel literature unknown precursor molecules **5a** and **5b** were synthesised *via* a five-step containing sequence. Both molecules were able to be deprotected quantitatively to give two important monomers **6a** and **6b** with a yield of 47 % over all six reaction steps. Those molecules contained a thiol group and an alkyne group for the molecule **6a** and a thiol group and an alkene group for the molecule **6b**. Because of this both molecules could be used for the respective thiol-yne coupling or thiol-ene coupling.

Since the obtained monomers **6a** and **6b** showed low stability when exposed to air, the precursor molecules **5a** and **5b** were completely chemically characterised representatively for the deprotected monomers **6a** and **6b**.

The planned deprotection of the precursor molecules, followed by the oligomerisation of those, was basically examined. It was found, that oxygen has a great effect in the reaction and suggested to keep the whole process under inert gas in further projects. Furthermore, it is necessary to further improve the degree of polymerisation by using different reported catalysts or different reaction conditions.

For the analysis of the prepared oligomers mass spectrometry was mainly used. It turned out, that this just gives quantitative information about the success of an oligomerisation. To get some more information about the exact composition of formed oligomers during the reaction the usage of HPLC based measurements is highly suggested for future work on this project.

5 "Symmetrical sugar-based triazole with fungicidal effect"

For many decades people have been using the healing components of nature, like different herbs, roots or fruits. Researcher all over the world set themselves the goal to examine the responsible compounds inside the plants giving them the pharmacological and bioactive properties. Those revealed substances served as inspiration for new synthetical bioactive mimics in various modern areas of application, like medicine or agriculture. In this work sugar based natural compounds and natural triazoles as model for a novel synthetic structure with possible antifungal properties were used. A symmetrical galactose based di triazole was successfully synthesised over a six-step route. After the complete characterisation *via* NMR-spectroscopy and FTIR-spectroscopy, the obtained structure was tested on antifungal properties. Since the triazole didn't show the desired properties against *Coniophora puteana* and *Trametes versicolor*, further possible applications were described and more testing on other fungi or even herbs was suggested.

5.1 Literature overview

Herbs and other plants are known for the treatment of medical issues for many centuries.[108] Due to this, researcher all over the world tried to examine the key compounds in nature, that have these positive effects on human health.[6,7,109,110] In 1935 the first penicillins and sulfonamides were used for the treatment of bacterial infections.[109,110] Since then, many different substance classes with pharmacological properties were found, which inspired researcher for new several promising structures in medical chemistry.[109,110,111]

One well known source for natural products with pharmacological traits is ginseng.[112] It was shown that the ginsenoide Rg1 in ginseng has many positive effects like anticancerogenic, antiallergenic, antidiabetic properties.[112,113] Even more examples from nature are cinnamic acid and garlic. The working group around DINIZ *et al*. reported about the antidepressant potential of cinnamic acid, whereas CHOO *et al*. showed the antimicrobial properties of allicin, which could be found in garlic.[114] Also, marine plants have a broad spectrum of pharmacologically interesting compounds, as the review from HUANG *et al*. demonstrates.[115] Here, several natural compounds for PARKINSON'S disease treatment with many different chemical structures are reported. The far-reaching application possibilities for natural substances also include other neurodegenerative diseases like the ALZHEIMER disease, the HUNTINGTON disease, multiple sclerosis and amyotrophic lateral sclerosis.[116]

Besides the pharmacological properties, some natural products, like for example eugenol, have antifungal traits.[117] HEDENSTRÖM *et al*. found three different compounds in spruce inhibiting the growth of certain fungi.[118] In addition citrus extracts and volatiles were observed to have antifungal effects and are discussed as potential natural fungicides.[119] On top of that, star anise also contains compounds with antifungal activity.[120]

On closer inspection such natural products, some defined chemical structural classes are revealed. One of these distinct classes is the group of carbohydrates. In 2018 KIM *et al*. found novel compounds with antifungal activity.[30] Some of these novel compounds were glycosides. Also, ESPOSITO *et al.* found glycosides in the waste of chestnuts showing potential antifungal properties.[121] Next to the glycosides, certain saponins were isolated and positively tested as fungicides.[29]

Apart from the analysis of potentially effective natural substances, some representatives form the basis for further modifications.[122] One possibility is the use of the already discussed CuAAC reaction in order to synthesise 1,2,3-triazoles.[123]

The structural motive of the 1,2,3-triazole is another interesting key structure, which is often connected to bioactive properties.[124] 1,2,3-triazoles show among others potential antifungal[125], antidiabetic[126] and antituberculosis traits.[124,127]

Saccharides are commonly known as renewable and for their biodegradability. Because of the recent investigations of their antifungal potential, they are ideal for the use as natural fungicides. Combined with the structural motive of the 1,2,3-triazoles, which also displayed great bioactive properties, and are easy to synthesise. They lead to novel biological compounds with fungicidal activity as reported by the working group around HU *et al.*.[128]

This work also aimed at the combination of a sugar skeleton with the structural motive of the 1,2,3-triazole to prepare a novel structure with potentially antifungal properties. Here, galactose was used as basic structural motive. In a six-step containing synthesis a galactose based symmetrical 1,2,3-triazole was obtained. The resulting triazole was chemically analysed *via* NMR-spectroscopy and FTIR-spectroscopy and tested on antifungal properties against the fungi stains *Coniophora puteana* and *Trametes versicolor*.

5.2 Results and discussion

Synthesis and Characterisation

In this work, the symmetric sugar based di triazole **8** was synthesised, starting from galactose over the allyl ether galactose **4a** (Fig. 5.2.1).

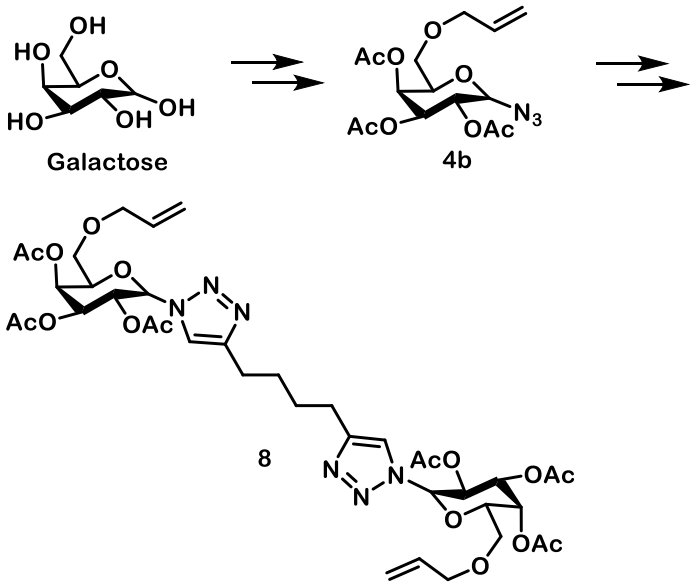

Figure 5.2.1 Planned synthesis of the symmetrical sugar based triazole **8**.

Figure 5.2.2 Shows the two-step synthesis of the symmetrical triazole **8** starting from compound **4b**. The starting molecule **4b** was synthesised over a four-step route, which is shown in chapter 4.2. The next step was converting the ester at C-1 to an azide group followed by a CuAAC reaction with a symmetrical diyne as it is shown in figure 5.2.2.

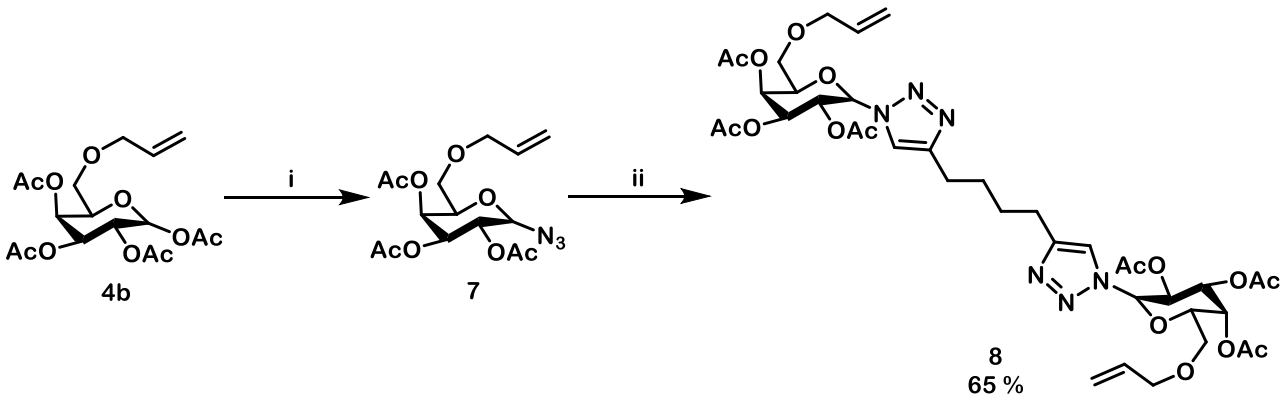

Figure 5.2.2 Stepwise synthesis of the symmetrical sugar based triazole **8** starting from the protected allyl ether **4b** with a yield of 65 % over two steps. i) $TMSN_3$, $SnCl_4$, DCM, 0 °C to rt, 3 h; ii) 1,7-octadiyne, $CuSO_4$, Na ascorbate, $^tBuOH : H_2O$ = 1:1, rt, 12 h.

The first reaction step was carried out by using azido(trimethyl)silane together with tin(IV) chloride as a catalyst. The yield of this step was 82 %. In the final step the biofunctionalised molecule **7** was

clicked *via* a CuAAC reaction with 1,7-octadiyne. A yield of 79 % was achieved in this reaction, which leads to a yield of 65 % over the last two steps. The yield over all six-step was 32 %. After completing the synthesis, the produced symmetrical triazole **8** was completely characterised. The measured FTIR and NMR spectra are summarised in Figure 5.2.3.

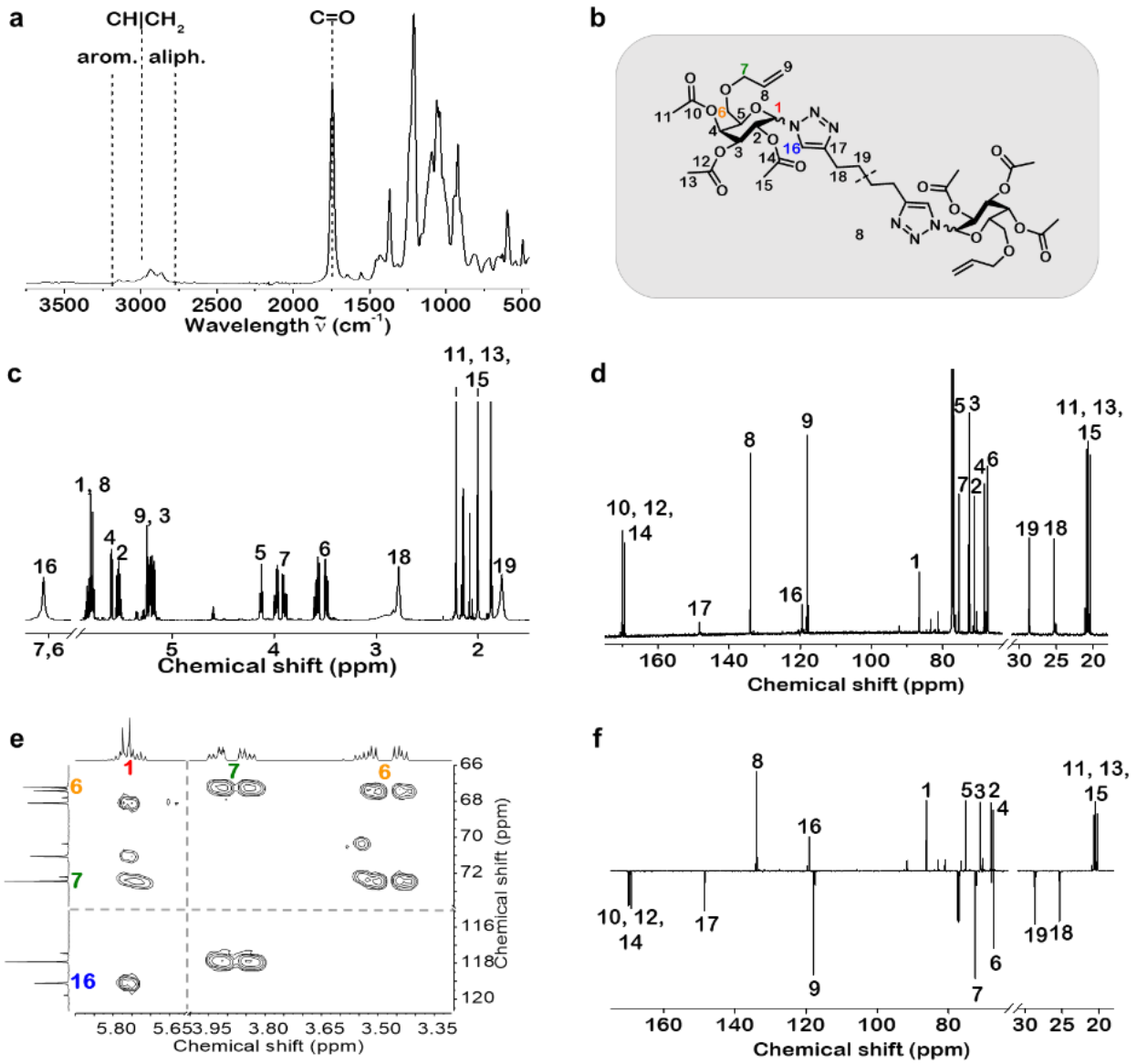

Figure 5.2.3 Chemical analysis of the desired symmetrical sugar based triazole. a) FTIR spectrum; b) chemical structure; c) ^{1}H-NMR spectrum; d) ^{13}C-NMR; e) HMBC; f) APT of the triazole **8** measured in $CDCl_3$.

Figure 5.2.3a shows the FTIR of the symmetrical triazole **8**. In the spectrum are weak bands in the range of the aromatic C-H oscillation visible at 3145 and 3092 cm^{-1}. Also, aliphatic C-H vibration band can be found at 2991, 2949 and 2870 cm^{-1}. At 1748 cm^{-1} is the band from the C=O groups.

The chemical structure of the synthesised symmetrical di triazole is shown in figure 5.2.3b. Here, all the atoms have been numbered to assign them to the individual signals in the NMRs. Since the molecule is symmetrical, there is just one half needed to be numbered.

Within the ^{1}H-NMR spectrum of the symmetrical triazole **8** (Figure 5.2.3c) the signals of the methyl groups are at 1.80-1.83 ppm, 1.95 ppm and 2.16 ppm. The both CH_2-Signals **18** and **19** coming from the octa di yne could be found at 1.67-1.72 and 2.67-2.74 ppm. The signals of the galactose backbone can be found at 3.42-3.46 and 3.50-3.54 ppm for the H-6, at 4.10 ppm for the H-5, at 5.10-5.22 ppm for the H-3, at 5.46-5.52 ppm for the H-2 at 5.54 ppm for the H-4 and at 5.71-5.80 ppm for the H-1. The signals for the allyl ether are at 3.82-3.96 ppm for the sp^3-CH_2 **7**, at 5.10-5.22 ppm for the sp^2-CH_2 **9** and at 5.71-5.80 for the CH **8**. Finally, the aromatic signal of the triazole **16** can be found at 7.54 ppm.

Within the ^{13}C-NMR spectrum of the symmetrical triazole **8** (Figure 5.2.3d) the signals of the methyl groups **11**, **13** and **15** can be found at 20.3, 20.6 and 20.7 ppm. The signals of the CH_2 groups of the former octa di yne **18** and **19** can be found at 25.3 and 28.6 ppm. The signals of the galactose backbone are found at 67.2 ppm for the C-6, at 67.4 ppm for the C-4, at 68.1 ppm for the C-2, at 71.1 ppm for the C-3, at 75.2 ppm for the C-5 and at 86.2 ppm for the C-1. The signals of the allylic part could be found at 72.4 ppm for the sp^3-CH_2 **7**, at 117.9 ppm for the sp^2-CH_2 **9** and at 133.9 ppm for the CH signal of **8**. The signals of the reacted triple bond are now an aromatic CH **16** at 119.1 ppm and a quaternary aromatic signal at 148.5 ppm. The signals of the quaternary C=O **10**, **12** and **14** are at 169.1, 169.8 and 170.0 ppm.

Figure 5.2.3 shows the APT of the triazole **8**. In this APT are in total eight negative signals. The first two are at 25.3 ppm and 28.6 ppm and can be assigned to the symmetrical CH_2 groups **18** and **19** of the alkyl chain of the formally 1,7-octadiyne. The next both negative signals are at 67.2 ppm and 72.4 ppm which can be assigned to the both of the CH_2 groups **6** and **7**. The sp^2-CH_2 group **9** has its negative signal at 117.9 ppm. The quaternary aromatic signal **17** formed during the click reaction reveals in a negative signal at 148.5 ppm. The final negative signals that can be found are at 169.1 ppm, 169.8 ppm and 170.0 ppm. They clearly can be assigned to the quaternary carbons of the protection groups **10**, **12** and **14**.

In figure 5.2.3e parts of the HMBC of compound **8** is shown. The cut-out ranges from 3.35 ppm to 4.00 ppm followed by a small interruption of axes starting at 5.60 ppm again till 5.90 ppm for the ^{1}H-NMR spectrum. The accorded spectrum is shown with the same axis interruption is shown on the top of the 2D area. The correlating ^{13}C-NMR spectrum is having also an interruption and ranges from 66.0 ppm to 74.0 ppm, in the first part and from 115 ppm to 120.5 ppm in the second part. This part shown of the HMBC, has several different cross peaks. Within the ^{1}H-NMR spectrum at the top are three signals. The signal of the CH_2 group of the galactose skeleton **6** at 3.42 ppm to 3.54 ppm, marked in **yellow**, shows a cross peak with the carbon **7** at 72.4 ppm, marked in **green**. Furthermore, a cross peak between the carbon of the CH_2 group of the galactose **6** and the hydrogens of the CH_2 group **7** is visible. This is proof for the successful etherification and the existing connection between galactose and the allyl rest. The last part of the ^{1}H-NMR spectrum shows the hydrogen signal of **H-1**, marked in **red**. Since the **H-1** and the signal of the sp^2-H **8** are overlapping a cross peak with the carbon **7** is visible. More important is the cross peak between the **H-1** to the aromatic carbon signal of **16**, marked in **blue**. This is proof for the success of the planned click reaction.

In summary, the complete characterisation of the symmetrical sugar based di triazole **8** through the FTIR, mass spectrometry, one dimensional as well as two-dimensional NMR spectroscopy on the one hand proofs the success of the aspired six step synthesis and on the other hand confirms the aimed structure of the galactose based ditriazole **8**.

Fungi test

The synthesised symmetrical sugar based di triazole **8** was further examined. Since triazoles are commonly known to have promising pharmacological properties, the symmetrical triazole **8** should be tested on antifungal properties.[124–127]

The test was inspired by the work of MILITZ *et al*.[129] Thin slices of beechwood with a diameter of 10 mm and a thickness of 2.5 mm were used. These slices were dried carefully and weighted. After that the slices were put into prepared solutions of the triazole **8** in methanol at different concentrations. In total six different concentrations, two high concentrations of 10 % and 3 %, two medium concentrations of 1 % and 0.5 % and two low concentrations of 0.1 % and 0.01 % were prepared. Additionally, five slices have been taken as a reference, which were impregnated in pure methanol and another five slices, which were not impregnated at all. For impregnation five wood slices for each concentration and each fungus were used and put into small beakers together with the prepared solutions. The seven beakers were positioned into a desiccator. With the help of an adjustable vacuum pump, the pressure inside the desiccator was set to 400 mbar for 30 min. After this procedure the impregnated beechwood slices were taken out of the solutions and dried again carefully. Table 5.2.1 shows the development of the mass of the beechwood slices during the treatment.

Table 5.2.1 Development of the mass from the beech samples after the first drying to the second drying. The samples were put into a solution of set concentrations and put into the desiccator for 30 min at 400 mbar. After this the samples were taken out of the solution and dried carefully before being weight again.

Concentration of the solution [%]	Mass development after treatment [%]
10	6.45
3	1.44
1	0.14
0.5	-0.43
0.1	-0.64
0.01	-0.37
0	-0.35
--	0.08

The impregnation of the wood samples shows, that methanol had an influence on the composition of the wood. By treating the wood with methanol some small components of the wood got removed, which explains the loss of mass. The table also indicates that adding small amounts of the symmetrical

triazole **8** leads to an increased loss of small wood components. For higher concentrations mass was gained, which leads to the assumption, that the impregnation with compound **8** worked out.

After the treatment, the wood slices were left two weeks in a standard climatised room (20 °C, 65 % r.h.) before sterilisation in the autoclave. Afterwards, a malt agar was prepared for the petri dishes with a diameter of 9 cm and filled into them. The dishes were allowed to cool down overnight.

Subsequently, the dishes were arranged for the fungi test. For this one wood slice was put on the right side of the petri dish, whereas a fungi sample with 1 cm diameter was put on the opposite site of the dish. In total two different fungi were used. The first one was the fungus *Coniophora puteana* (CP) and the second one was the fungus *Trametes versicolor* (TV).

Now the fungi and the impregnated wood slices were positioned, the test should have the procedure as shown in Figure 5.2.4.

After the placement of the fungi and the wood slices the petri dishes were closed carefully with para film and kept in a standard climatised room (22 °C, 65 % r.h.).

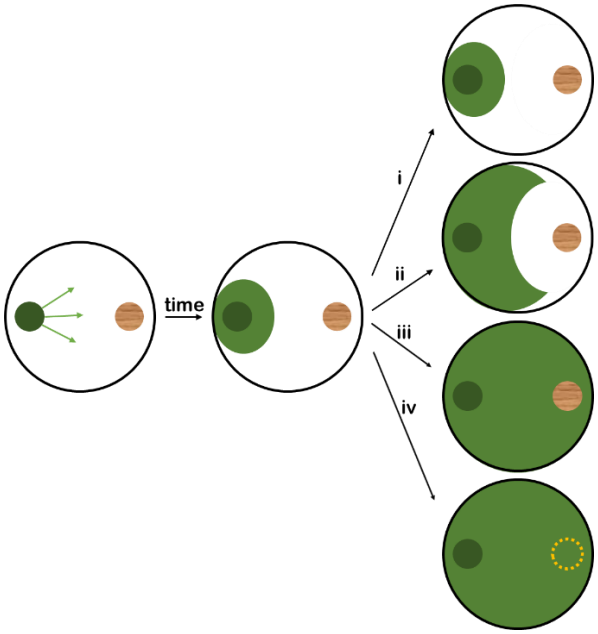

Figure 5.2.4 Structure and functionality of the prepared fungi test. The fungi with a diameter of approximately 1 cm, here marked in dark green, was put on the left side of a petri dish filled with malt agar. On the right side, the impregnated wood sample with a diameter of 1 cm and 2.5 mm thickness was placed. After some time (usually after 2-3 days) the fungus started to grow in every direction, as shown in the middle dish. Now, there are four possible scenarios, that could have happened: i) The fungus stops to grow or is just on the left side growing, in order to escape the impregnated wood sample; ii) the fungus keeps on growing, but a cycle around the wood sample is formed; iii) The fungus covers the complete malt agar, besides the wood sample; iv) the fungus is not effected at all form the impregnated wood sample and grows over it.

The fungus started to grow as expected in a symmetrical cycle around the initial fungus sample. After that initial growing, there would be four possible ways of the further progress of this test. The first is the best-case scenario (Figure 5.2.4i). In this case the fungus stops growing at all. The second case (Figure 5.2.4ii) is, that the fungus keeps on growing till a certain point. It stops growing in a defined cycle around the impregnated sample. This scenario indicates, that the triazole **8** would go out of the wood slice into the malt agar and build up an antifungal area around the sample.

The third case (Figure 5.2.4iii) is the most probable. Here, the fungus would grow till the wood slice and then stop growing, so the sample would not be affected at all from the fungus.

The last case (Figure 5.2.4iv) is also the worst one. Herein, the impregnated wood doesn't have an antifungal effect and the fungus grows all over the beechwood.

The Results of the fungi test are visualised in Figure 5.2.5.

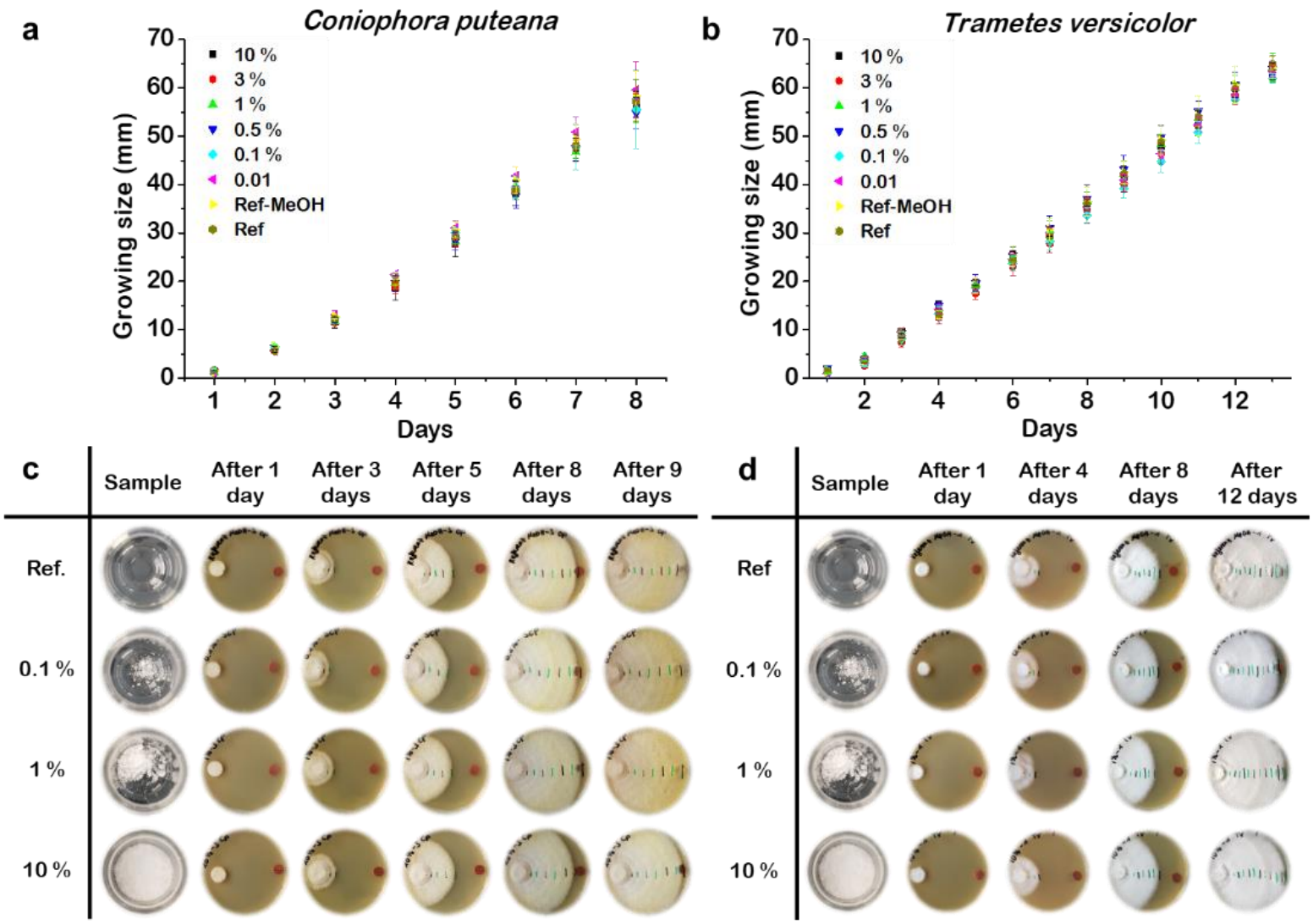

Figure 5.2.5 Results of the fungi tests. a) Average growing rate of the fungi *Coniophora puteana*,, b) Growing rate of the fungi *Trametes versicolor*, c) Pictures of the fungi growth of *Coniophora puteana* over time for the different treated beech slices; d) Pictures of the fungi growth of *Trametes versicolor* over time for the different treated beechwood slices.

Figure 5.2.5a shows the average growing rate of the fungi *Coniophora puteana* at the different concentrations. The graph shows clearly the fungi was growing steadily 9 to 10 mm per day. The different concentrations used during the treatment did not have any effect on the average growing rate of the fungi. Also, the use of methanol in the impregnation process did not have any negative effect on the growth of the fungi.

The Figures 5.2.5c shows some pictures of the fungi growth of *Coniophora puteana* over the time for the reference, one high concentration, one medium concentration and a low concentration. It is shown from the beginning after the first day till the end of the test after nine days. The pictures clearly show the steady growth of the fungi over the time. The pictures also prove, that the used concentration during the treatment didn't have any effect. After the ninth day the wood slices are completely covered by *Coniophora puteana*.

The average growing rate of the fungi *Trametes versicolor* (Figure 5.2.5b) was approximately 5 to 6 mm per day. As well, the used concentrations during the impregnation process did not have any effect on the average growing rate. Furthermore, the applied methanol did not influence the test in a negative way.

Figure 5.2.5d shows some pictures from the fungi test with *Trametes versicolor* over the time. Herein, the same concentrations were taken as for the other fungi to have a better comparability. Since the fungi *Trametes versicolor* is growing more slowly than *Coniophora puteana* the time interval during the pictures is bigger. The pictures shown, point out, that the different concentration didn't have any effect on the growth of the fungi. Furthermore, the wood slices were overgrown after 12 days.

The synthesised galactose based di triazole **8** didn't show any antifungal properties for both fungi tested. One reason for this could have been the impregnation process. Although Table 5.2.1 displays an increase of the weight for the concentrations of more than 1 %, but it also shows a great weight loss for the concentrations of less than 1 %. Also, concentrations of less than 1 % have had a greater weight loss than the reference, which was impregnated with *abs*. methanol. All in all, the impregnation process needs to be optimised and changed accordingly to make sure compound **8** is able to permeate itself into the porous structure of the beechwood. Since the fungi test on those small beechwood slices is pretty uncommon, it should be considered to change to bigger wood samples or to more common comparable tests with defined settings. Another opportunity could be to repeat the test with impregnated thin papers or to add compound **8** into the prepared malt agar.

Besides the fungi test setup, it should be considered that the synthesised di triazole **8** does not have any effect on the fungi tested. Because of this, compound **8** should be tested on other potential fungus strains.

In summary, the designed sugar based symmetrical di triazole **8** didn't show any antifungal effect for both fungi tested. To make sure the symmetrical di triazole **8** doesn't have any effect on both fungi, further testing is necessary. One additional test could be to perform the test with pieces of paper, that got impregnated with the di triazole **8**, instead of the used beechwood. Another possibility would be to introduce the molecule **8** into the malt agar and observe, if the fungi are able to grow in such an environment. Also, other fungi could be used for further testing.

Furthermore, other commonly used tests for investigating on antifungal properties should be considered to be used.

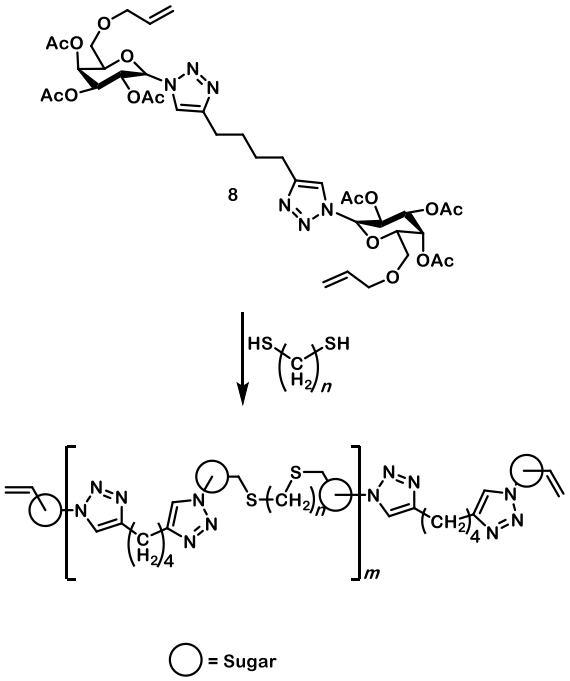

Figure 5.2.6 Possible further reaction with a symmetrical dithiol compound to generate a long chain polymer.

Besides the focused examination of the potential antifungal properties, additional modifications respectively reactions could be made on the symmetrical triazole **8**. As the molecule has double bonds at each end, it offers the opportunity for a second symmetrical reaction. On the one hand the ends could be treated separately or a symmetrical molecule could be used to generate cyclic compounds or to generate long chain polymeric structures. A suitable reaction would be the in chapter 4 discussed thiol-ene coupling with a symmetrical thiol as shown in Figure 5.2.6.

5.3 Conclusion

In total a symmetrical sugar based di triazole **8** was synthesised successfully over a two-step modification of structure **4b** with a yield of 65 %. The overall yield of the six-step synthesis starting from galactose is 32 %. Furthermore, the structure of the synthesised molecule **8** was chemically characterised over NMR- and FTIR-spectroscopy.

After the complete analysis the generated symmetrical di triazole **8** was tested on possible antifungal properties. For this test beechwood slices (diameter: 1 cm, thickness: ~2.5 mm) were impregnated with different concentrated solutions of molecule **8** in methanol. For the examination *Coniophora puteana* and *Trametes versicolor* were used. Unfortunately, the symmetrical triazole **8** didn't show any antifungal properties.

Besides the potential on antifungal properties, the synthesised symmetrical sugar-based molecule has a high potential for further modification. One opportunity is offered by the thiol-ene reaction with a symmetrical dithiol to construct a symmetrical long chain polymer.

6 Conclusion and outlook

The work was subdivided into three parts (Figure 6.1). In the following section all obtained results of the three chapter 3 to 5 are summarised.

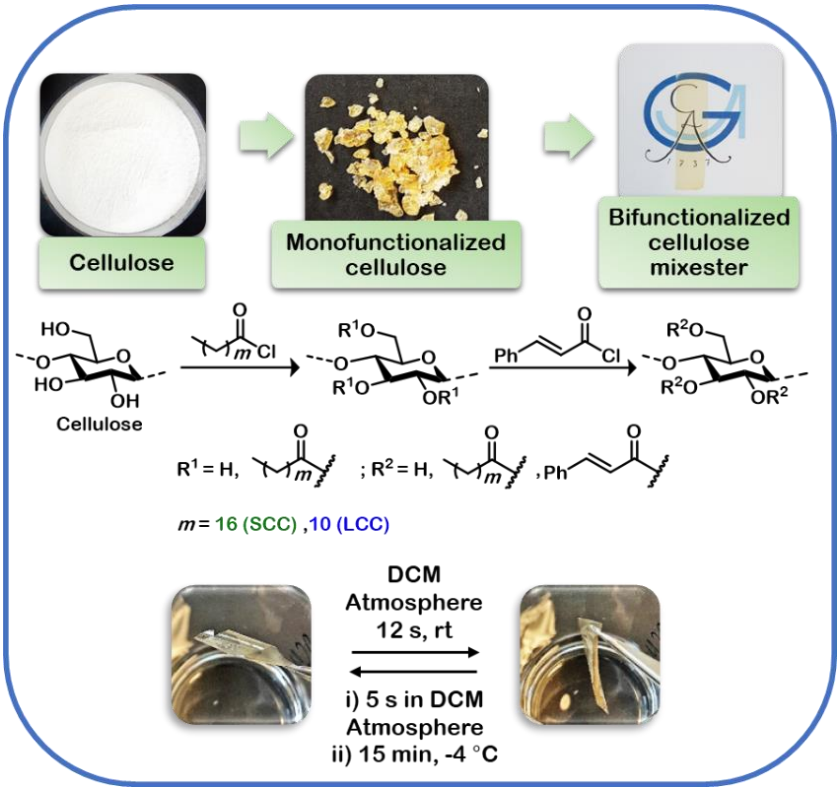

Figure 6.1 Schematic illustration for the preparation of the bifunctional cellulose mixesters, which starts with the first reaction on cellulose using long chain acid chlorides, as stearoylchloride and lauroylchloride, and ends with the second reaction with cinnamoyl chloride and the demonstration of the shape memory behaviour.

In Section 3 of the work presented here, Cellulose was used as a renewable natural resource for two heterogenic consecutive esterifications with a long chain chloride acid in the first step and cinnamoyl chloride in the second step (Figure 6.2). In total, two novel bifunctional cellulose mixesters were synthesised. SCC and LCC. Both compounds were completely chemically characterised *via* NMR and FTIR spectroscopy. DSC measurements revealed the melting point of SCC at 48.7 °C. LCC didn't show a melting point, but a wide glass transition. In addition, both compounds were able to form transparent films with switchable mechanical properties due to the integrated cinnamoyl moieties. Those films showed tuneable elastic deformation properties and plastic deformation abilities, which are conditionally on the introduced aliphatic chains and the crosslinked cinnamoyl groups. Furthermore, the prepared films displayed responsive shape memory behaviours and self-healing property.

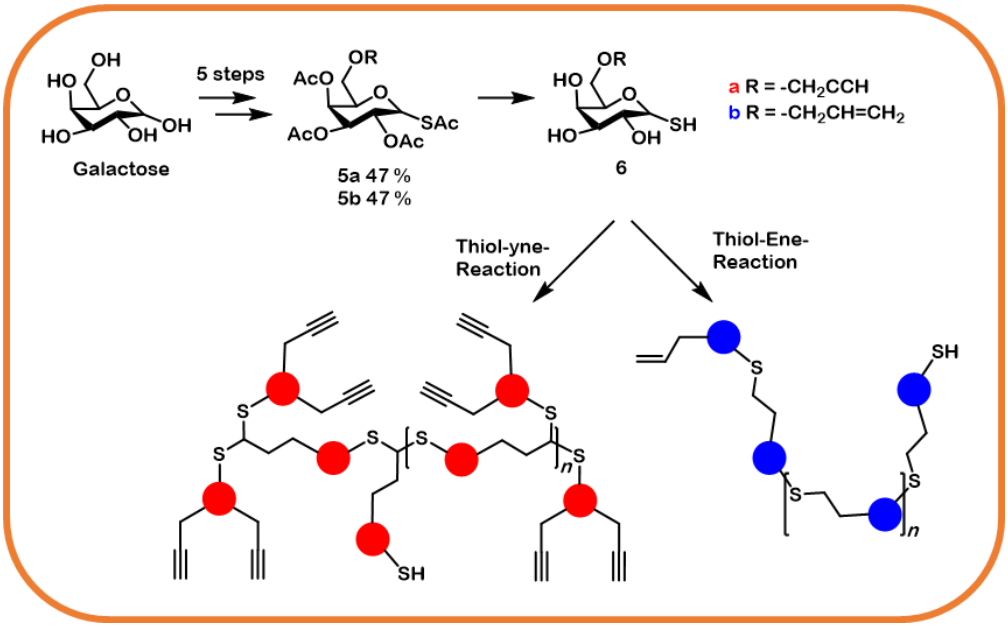

Figure 6.2 Schematic illustration for the preparation of the desired branched and linear oligosaccharides starting from prepared galactose monomers in a thiol-yne respectively tiol-ene coupling.

In chapter 4, it was aimed to synthesise two novel galactose-based molecules containing a thiol group and a triple bond respectively a double bond. Due to their high reactivity, the corresponding precursor molecules were successfully synthesised in two five-step sequence with an overall yield of 47 % each. The precursor molecules **5a** and **5b** were completely chemically analysed with NMR and FTIR spectroscopy. Afterwards, the reaction conditions for the deprotection followed by the UV controlled polymerisation was basically investigated. For the evaluation of the success of the performed reaction, mass analysis was used. Unfortunately, mass analysis is not suitable at detecting different formations of oligomers with similar mass. For this purpose, it was suggested to take HPLC measurements for further analysis of the reaction mixture, which gives more information about the detailed composition of products after the reaction.

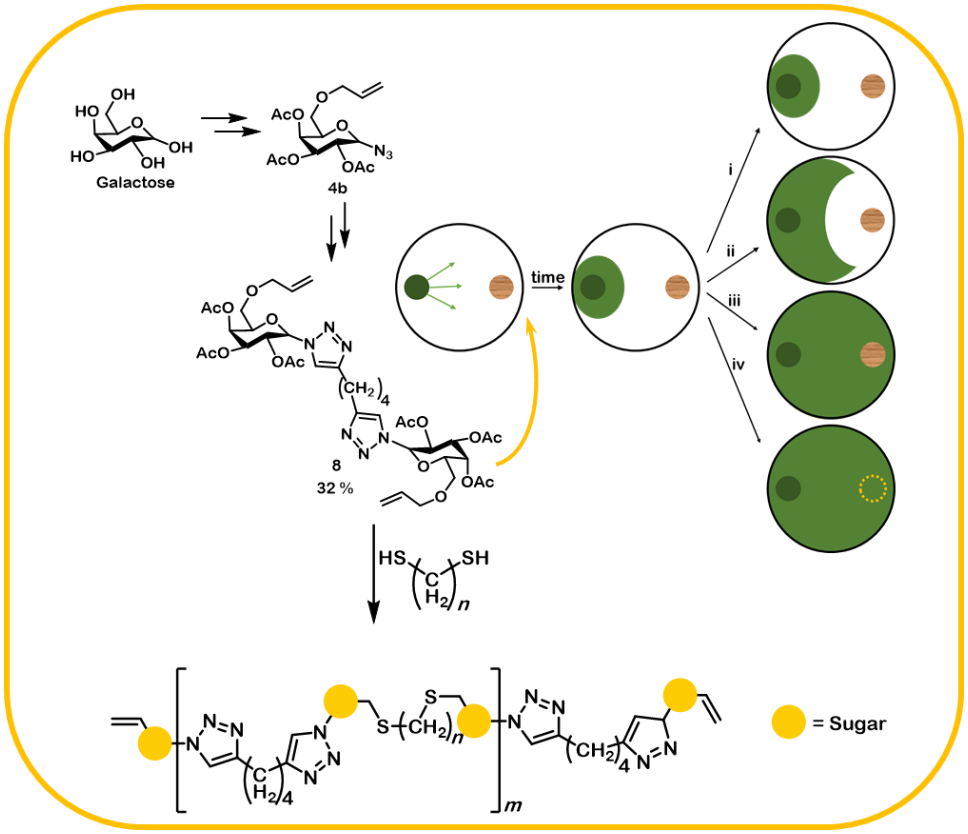

Figure 6.3 Schematic illustration for the preparation of the aimed symmetrical galactose based di triazole, the conducted fungi test and possible further reaction plans.

Section 6 was concerned with the synthesis of an adequate monosaccharide containing a double bond and an azide group **4b**. This monosaccharide was used for a symmetrical CuAAC reaction with 1,7-octadiyne to synthesise the symmetrical galactose based di triazole **8** with an overall yield of 32 % over a five-step sequence. Furthermore, the obtained di triazole was tested on anti-fungal properties against *Coniophora puteana* and *Trametes versicolor*, but it didn't show any effect. For further modification, the designed di triazole **8** has two terminal double bond functionalities, that are able to perform different reactions. One possible modification is a symmetrical thiol-ene coupling with a symmetrical long chain di thiol to synthesise a novel sugar-based oligomer or even a polymer.

In total, novel functional stimuli responsive materials with outstanding mechanical properties were synthesised. Furthermore, different sugar-based monosaccharides were designed, examined different reaction conditions to set the foundation for further polymerisation and tested on potential biological characteristics.

7 Experimental section

7.1 General procedures

7.1.1 Abbreviations

abs.	Absolute
arom.	Aromatic
Ac_2O	Acetic anhydrate
AGU	Anhydro glucose unit
APT	Attached proton test
ATR	Attenuated total reflection
$CDCl_3$	Deuterated Chloroform
COSY	Correlation spectroscopy
CuAAC	Copper catalyzed azide-alkyne cycloaddition
CP	*Coniophora puteana*
d	Doublet
DCM	Dichloromethane
deform.	Deformation
DMF	Dimethylformamide
DMPA	2,2-Dimethoxy-2-phenylacetophenone
DS	Degree of substitution
DSC	Differential scanning calorimetry
DS_{Ci}	Degree of substitution ascribed to cinnamoyl groups
DS_{La}	Degree of substitution ascribed to lauroyl groups
DS_{St}	Degree of substitution ascribed to stearoyl groups
ESI	Electrospray ionisation

EtOAc	Ethylacetat
FTIR	Fourier-transform infrared spectroscopy
GOS	Galactose oligosaccharide
^{1}H-COSY	^{1}H correlation spectroscopy
HMBC	Heteronuclear multiple bond correlation
HMO	Human milk oligosaccharide
HPLC	High performance liquid chromatography
HRMS	High resolution mass spectroscopy
HSQC	Heteronuclear single quantum coherence spectroscopy
J	*J*-coupling or indirect dipole- dipole coupling
LC	Lauroylated cellulose
LCC	Lauroylated and cinnamoylated cellulose esters
M	Molecular weight
m	Multiplet
MCC	Microcrystalline cellulose
MeOH	Methanol
MS	Mass spectroscopy
NMR	Nuclear magnetic resonance
PE	Petroleum ether (40/60)
ppm	Parts per million
Ph	Phenyl
q	Quintet
R_f	Retardation factor
r.h.	Relative humidity

rpm	Rounds per minute
rt	Room temperature
s	Singlet
SC	Stearoylated cellulose
SCC	Stearoylated and cinnamoylated cellulose esters
t	Triplet
TEC	Thiol-ene coupling
THF	Tetrahydrofurane
TLC	Thin layer chromatography
TOF	Time of flight
TV	*Trametes versicolor*
UV	Ultra violet

7.1.2 Materials

Chemicals

Microcrystalline cellulose (MCC) with a granule size of 50 µm, stearoyl chloride (90 %), lauroyl chloride, allyl bromide (99 %), thio acetic acid (96 %), boron trifluoride diethyl etherate, sodium methoxide, iodine, azido tri methyl silane (95 %), sodium hydride (60 wt.% dispersion in mineral oil) and tri ethyl amine (99.5 %) were bought from Sigma-Aldrich (Steinheim, Germany). Cinnamoyl chloride (98 %) was bought from Merck (Darmstadt, Germany). Pyridine (99 %), ethanol (technical grade), dichloromethane (99.9 %), tetrahydrofuran (technical grade), dimethylformamide (technical grade), sodium hydrogen carbonate (97 %), sodium sulphate (99 %), Dowex® (50 WX2 200-400 mesh), ethyl acetate (99.5 %), galactose (99 %), acetone (technical grade), *n*-hexane, tin (IV) chloride, sodium chloride (99 %), *tert*- butyl alcohol, 1,7 octa diyne (98.5 %), sodium ascorbate and methanol (99.8 %) were bought from Th. Geyer Ingredients GmbH (Renningen, Germany). Petroleum ether 40/60 was bought from VWR (Darmstadt, Germany). Propargyl bromide was bought from Alfa aesar. Other chemicals are all of analytical grade. All chemicals were used as received.

Wood samples (diameter 1.0 cm, thickness ~2.5 mm) were obtained from untreated European beech (*Fagus sylvatica L.*) rods of 1.0 cm diameter.

For the fungi test two different fungus strains were tested. *Coniophora puteana* DSM 3085 and *Trametes versicolor* DSM 3086 were obtained from Deutsche Sammlung von Mikroorganismen und Zellkulturen GmbH from the Leibniz-Institut.

Inert gas

The inert gas argon (5.0) bought from Air liquid (Düsseldorf, Germany) was used for synthesis carried out in a protective atmosphere. Experiments under argon were carried out in previously triple-heated apparatus.

Solvents

Dried solvents were used for the individual experiments, which were carried out in an inert gas atmosphere. Those solvents are titled with the index *abs*.. The solvents used were dried by various methods:

- Methanol was refluxed over magnesia for three hours, fractionally distilled and then stored over molecular sieve 3 Å under an Ar atmosphere.

- Dimethylformamide was mixed with toluene and water, fractionally distilled and then stored in the cold over molecular sieve 3 Å under an Ar atmosphere and exclusion of light.

The water used is deionized water (DI), which is provided decentral by the university.

7.1.3 Characterisation

Elemental analysis

The contents of carbon and hydrogen were determined with an Elemental Analyzer 4.1 vario EL III (Elementar, Germany). The DSs of SC and LC were calculated according to the reference.[130]

FTIR spectroscopy

FTIR spectra were recorded at room temperature using a Bruker Alpha spectrometer equipped with a versatile high throughput ZnSe ATR crystal. All samples were measured in the range of 400 to 4000 cm^{-1} with accumulated 24 scans.

Mass spectrometry

ESI mass spectrometry was performed on a maXis from Bruker Daltonik with a TOF analyser and on a micrOTOF from Bruker Daltonik with a TOF mass spectrometer.

MALDI mass spectrometry was performed on an Autoflex Speed from Bruker Daltonik with a TOF detector in reflection mode.

NMR spectroscopy

^{1}H- and ^{13}C-NMR spectroscopy were recorded with a Bruker Avance III 500 spectrometer in $CDCl_3$ solution. Chemical shifts were referenced to the $CDCl_3$ signals at 7.26 (^{1}H-NMR) and 77.16 ppm (^{13}C-NMR).[131] Signal assignments were supported by two-dimensional NMR correlation spectroscopic measurements (COSY).

Thermal analysis

The thermal properties were determined *via* differential scanning calorimetry (DSC) on a DCS200 F3 Maia (Netzsch Germany). The measurements were carried out with a heat flow of 10 K/min between -20 and 150 °C.

Tensile tests

The tensile tests were performed on a Z3 microtensile test machine from Grip-Engineering Thümler GmbH at a constant temperature of 20 °C and relative humidity of 60 %. The measurements were implemented with an extension rate of 3 mm/min with a 15 mm gauge length. Before the measurement, the films were cut in a rectangle form (with a dimension of 45 mm in length and 10 mm in width).

Thin layer chromatography

The thin layer chromatograms are prepared on DC- aluminum foil with fluorescence indicator (silica gel 60 UV_{254}) from VWR. The R_f-values, as well as the solvents used are given for each compound. The respective compound was stained via an iodine chamber.

Column chromatography

For the column chromatographical separation silica gel (60-200 µm) from VWR was used. The used solvents and mixing ratios are given in each experiment.

7.2 General preparations

7.2.1 Synthesis of novel cellulose mixesters for transparent responsive films

General procedure A

The synthesis of monofunctionalised cellulose esters are carried out as reported before [72]. Dried MCC (6.0 mmol, 1.0 equivalent) is suspended in pyridine (30 ml). Stearoyl or lauroyl chloride (15 mmol, 2.5 equivalents per anhydro glucose unit, AGU) is added drop by drop at 100 °C. After stirring at 100 °C for 1 h, the solution is poured into 200 ml ethanol. The precipitate is separated by centrifugation (20 min at 12 000 rpm at 4 °C). Subsequently, the product is dispersed in dichloromethane (75 ml) and precipitated in ethanol (300 ml). After collecting the precipitate from the liquid by using centrifugation (20 min at 12 000 rpm at 4 °C), the solid is washed with ethanol for several times. After that, the solid is dispersed in THF (150 ml) under stirring and the suspension is centrifuged (20 min at 12 000 rpm at 4 °C) to separate the products from the solution. The solid residue is washed for three times and finally dried for further use.

General procedure B

Obtained SC or LC (1.0 equivalent) is suspended in pyridine (30 ml). Then, the mixture is heated to 100 °C and cinnamoyl chloride (5.0 equivalent) is added drop by drop. After stirring at 100 °C for 5 h, the dark mixture is poured in 150 ml ethanol. The precipitate is separated by filtration. After that, the solid product is dissolved in THF and precipitated again in ethanol. The purified product is dissolved in THF and centrifuged (30 min at 14 000 rpm at 4 °C) to remove impurities before precipitation in ethanol. After the precipitation in ethanol, collected precipitate is washed with ethanol for multiple times. Finally, the solvent is removed on the rotary evaporator under reduced pressure.

Fabrication of films

Each mixester is dissolved in THF at a concentration of 10 mg/ml. 10 ml of the solution is then transferred into a round Teflon petri dish with a diameter of 5 cm. Then, THF is allowed to evaporate overnight at ambient surroundings.

7.2.2 Synthesis of different sugar monomers for polymerisation *via* thiol-ene / thiol-yne coupling

General procedure C

The synthesis of the protected ethers are carried out as reported.[132]

1,2:3,4-Di-*O*-isopropylidene-*α*-D-galactopyranose (**1**) (1.0 equivalent) is dissolved in anhydrous DMF (5 ml per mmol) and cooled to 0 °C. Sodium hydride (1.8 equivalents) is added carefully and the mixture is stirred for 30 min. Afterwards propargyl bromide (**a**, 1.8 equivalents) or allyl bromide (**b**, 1.2 equivalents) is added and the mixture is allowed to warm up to room temperature. After stirring for 3 more hours the reaction is carefully quenched with methanol. The reaction mixture is extracted with DCM (3×5 ml per mmol). The combined organic layers are washed with an aqueous sodium hydrogen carbonate solution (2×5 ml per mmol) and DI water (2×5 ml per mmol) and dried with anhydrous $NaSO_4$. The solvent is removed at the rotary evaporator under reduced pressure and the crude residue was purified by column chromatography on silica gel to gain the products 1,2:3,4-di-*O*-isopropylidene-6-*O*-(2.propynyl)-α-D-galatopyranose (**2a**) or 1,2:3,4-di-*O*-isopropylidene-6-*O*-(2.alloynyl)-α-D-galatopyranose (**2b**).

General procedure D

The synthesis of the deprotected galactose ethers were carried out as reported.[133]

1,2:3,4-Di-*O*-isopropylidene-6-*O*-(2.propynyl)-α-D-galatopyranose (**2a**) or 1,2:3,4-di-*O*-isopropylidene-6-*O*-(2.alloynyl)-α-D-galatopyranose (**2b**) (1.0 equivalent) is emulsified in water (11 ml per mmol). Dowex® is added (350 to 360 mg per mmol) and the mixture is heated up to 80 °C. The reaction is stirred overnight at this temperature. After cooling down the reaction is filtrated to remove the Dowex®. The water is removed under reduced pressure. The gained product 6-*O*-prop-2-yn-1-yl-D-galactopyranose (**3a**) or 6-*O*-allo-2-yn-1-yl-D-galactopyranose (**3b**) is used without any further purification.

General procedure E

The acetylation of the galactose ethers are carried out as reported.[87]

The colourless oil 6-*O*-prop-2-yn-1-yl-D-galactopyranose (**3a)** or 6-*O*-allo-2-yn-1-yl-D-galactopyranose (**3b**) is dissolved in pyridine (a, 31 equivalents b, 37 equivalents) and ethyl acetate (a, 31 equivalents b, 37 equivalents) is added carefully. The reaction mixture is stirred over 24 hours at room temperature. Afterwards the reaction is quenched with water (10 ml per mmol). The mixture is extracted with DCM (3×5 ml per mmol). The combined organic layers are dried over anhydrous $NaSO_4$. The solvent is removed under reduced pressure and the crude residue is purified by column chromatography on silica gel to gain the products (2*S*,3*R*,4*S*,5*S*,6*R*)-6-((prop-2-yn-1-yloxy)methyl)tetrahydro-2*H*-pyran-2,3,4,5-tetrayl tetraacetate (**4a**) or (2*S*,3*R*,4*S*,5*S*,6*R*)-6-((allyloxy)methyl)tetrahydro-2*H*-pyran-2,3,4,5-tetrayl tetraacetate (**4b**).

General procedure F

The reaction is carried out as reported.[134]

To the colourless oil (2*S*,3*R*,4*S*,5*S*,6*R*)-6-((prop-2-yn-1-yloxy)methyl)tetrahydro-2*H*-pyran-2,3,4,5-tetrayl tetraacetate (**4a**) or (2*S*,3*R*,4*S*,5*S*,6*R*)-6-((allyloxy)methyl)tetrahydro-2*H*-pyran-2,3,4,5-tetrayl tetraacetate (**4b**) is dissolved in *abs.* DCM (5.5 ml per mmol) and cooled to 0 °C. Thioacetic acid (4.75 equivalents) and boron trifluoride diethyl etherate (7 equivalents) are added carefully. The mixture is allowed to warm up to room temperature again and is stirred for 24 hours. Afterwards the reaction is quenched with cold water (5 to 10 ml per mmol). The mixture is extracted with DCM (3×5 ml per mmol) and the combined organic layers are washed with an aqueous sodium hydrogen carbonate solution (2×5 ml per mmol) and brine (2×5 ml per mmol).

The organic layer is dried over anhydrous $NaSO_4$. The solvent is removed under reduced pressure and the crude residue is purified by column chromatography on silica gel to gain the desired products (2*S*,3*R*,4*S*,5*S*,6*R*)-2-(acetylthio)-6-((prop-2-yn-1-yloxy)methyl)tetrahydro-2*H*-pyran-3,4,5-triyl triacetate (**5a**) or (2*S*,3*R*,4*S*,5*S*,6*R*)-2-(acetylthio)-6-((allyloxy)methyl)-tetrahydro-2*H*-pyran-3,4,5-triyl triacetate (**5b**).

General procedure G

The reaction was carried out as reported.[134]

The colourless oil (2*S*,3*R*,4*S*,5*S*,6*R*)-2-(acetylthio)-6-((prop-2-yn-1-yloxy)methyl)tetrahydro-2*H*-pyran-3,4,5-triyl triacetate (**5a**) or (2*S*,3*R*,4*S*,5*S*,6*R*)-2-(acetylthio)-6-((allyloxy)methyl)tetrahydro-2*H*-pyran-3,4,5-triyl triacetate (**5b**) is dissolved in anhydrous methanol (7.5 ml per mmol). The mixture is degassed under reduced pressure in an ultrasonic bath (5×3min). Afterwards degassed sodium methoxide (3 equivalents) is added and the reactions is stirred for 2 hours at room temperature. Degassed Dowex® (1 g per mmol) is added to the mixture to stop the reaction. The solid part is removed *via* filtration and the liquid phase was kept under argon gas to prevent further reactions. The liquid phase contained the desired monomer (2*S*,3*R*,4*S*,5*R*,6*R*)-2-mercapto-6-((prop-2-yn-1-yloxy)methyl)tetrahydro-2*H*-pyran-3,4,5-triol (**6a**) or (2*R*,3*R*,4*S*,5*R*,6*S*)-2-((allyloxy)methyl)-6-mercaptotetrahydro-2*H*-pyran-3,4,5-triol (**6b**) which were used without further purification.

Impregnation of the beechwood slices

Thin slices of beechwood with a diameter of 10 mm and a thickness of 2.5 mm were used. These slices were dried carefully. Afterwards, the slices were put into prepared solutions of the di triazole **8** in methanol at six different concentrations, two high concentrations of 10 % and 3 %, two medium concentrations of 1 % and 0.5 % and two low concentrations of 0.1 % and 0.01 %. For every concentration five slices of beechwood were taken. Additionally, five slices have been taken as a reference, which were impregnated in pure methanol and another five slices, which were not impregnated at all. For the impregnation process five slices for every concentration and each fungus were used and put into small beakers together with the prepared solutions. All seven beakers were positioned into a desiccator. With the help of an adjustable vacuum pump, the pressure inside the desiccator was set to 400 mbar for 30 min. After this procedure, the impregnated beechwood slices were taken out of the solutions and dried again carefully. Afterwards, the wood slices were kept in a standard climatised room (20 °C, 65 % r.h.) for two weeks.

Fungi test

For the preparation of the growth medium 32 g Malt and 20 g Agar were mixed with 770 ml ultrapure water. The mixture was sterilised in an autoclave for 20 min at 121 °C (withdrawal temperature: 90 °C). The sterilised mixture was poured into petri dishes of 9 cm diameter and cooled overnight. After this, the dishes were arranged for the fungi test. For this, one wood slice was put on the right side of the petri dish with a distance of 1 cm from the edge and the fungi sample was put on the opposite side of the dish, also with a distance of 1 cm from the edge. In total two different fungus strains were tested. The first one was *Coniphora puteana (CP)* and the other one was *Trametes versicolor (TV)*. After the placement of the fungi and the wood slices the petri dishes were closed carefully with para film and kept in a standard climatised room (22 °C, 65 % r.h.). The growth of the fungi was controlled daily.

7.3 Preparation of the targeted molecules

7.3.1 Synthesis of novel cellulose mixesters for transparent responsive films

Monofunctionalisation for the synthesis of stearoylated cellulose **SC**

Following the general procedure A, MCC (1.0 g, 6 mmol) and stearoyl chloride (5.1 ml, 15 mmol) were used for SC. The desired product was obtained as brown solid. Yield: 1.334 g. DS_{St} = 1.66 according to elemental analysis.—

FTIR (ATR) in cm^{-1}: $\tilde{\nu}$ = 3479, 3352 (O-H), 2954, 2914, 2854 (C-H), 1748 (C=O), 1460, 1415, 1377 (CH_2-deform.), 1060 (C-O).—

Monofunctionalisation for the synthesis of lauroylated cellulose **LC**

Following the general procedure A**,** cellulose (1.0 g, 6 mmol) and lauroyl chloride (3.5 ml, 15 mmol) were used for LC. The desired product was prepared as brown solid. Yield: 367 mg. DS_{La} = 1.48 according to elemental analysis.—

FTIR (ATR) in cm^{-1}: $\tilde{\nu}$ = 3477, 3341 (O-H), 2956, 2923, 2851 (C-H), 1744 (C=O), 1462, 1418, 1375 (CH_2-deform.), 1060 (C-O).—

Bifunctionalisation as stearoylated and cinnamoylated cellulose esters **SCC**

Following the general procedure B, SC (1.1 g, 1.8 mmol, DS: 1.66) and cinnamoyl chloride (1.7 ml, 12.1 mmol) were used for SCC. The desired product was synthesised as light brown solid. Yield: 1.245 g, DS_{St} = 1.51 and DS_{Ci} = 1.35.—

FTIR (ATR) in cm^{-1}: $\tilde{\nu}$ = 2925, 2851 (C-H), 1735, 1634 (C=O), 1581 (C=C), 1498, 1467, 1453, 1375 (C-H).—

^{1}H-NMR (500.2 MHz, $CDCl_3$) in ppm: 0.88 [t, 4.44 H, ^{3}J = 6.8 Hz, C$\underline{H}_3$], 1.19-1.32 [m, 29.6 H, -(C$\underline{H}_2$)$_{16}$-] 1.93-2.37 [m, 2 H, CH-C$\underline{H}_2$-OOC], 3.22-5.34 [5 H of AGUs], 6.01-6.39 [m, 1 H, CH=C$\underline{H}$], 7.06-7.66 [m, 7 H, C$\underline{H}_{arom.}$, C$\underline{H}$=CH].—

^{13}C-NMR (125.8 MHz, $CDCl_3$) in ppm: 14.2 [$\underline{C}H_3$], 24.9, 29.4, 29.5, 29.8, 29.9, 32.0 [-($\underline{C}H_2$)$_{16}$-], 34.0 [$\underline{C}H_2$-OOC], 62.0, 68.1, 71.4, 72.6, 73.0 [C of AGUs], 100.8 [$\underline{C}$H=CH-Ph], 116.9 [CH=$\underline{C}$H-Ph], 128.3, 128.4, 128.7, 128.8, 129.0, 130.3, 134.1, 145.6 [$\underline{C}_{q,\ arom.}$, $\underline{C}H_{arom.}$], 165.1, 165.6, 165.9 [$\underline{C}$=O], 172.0, 172.4, 172.9 [$\underline{C}$=O].—

Bifunctionalisation as lauroylated and cinnamoylated cellulose esters **LCC**

Following the general procedure B, LC (733 mg, 1.7 mmol, DS: 1.48) and cinnamoyl chloride (1.8 ml, 12.9 mmol) were used for LCC. The desired product was obtained as light brown solid. Yield: 970 mg, DS_{La} = 1.48 and DS_{Ci} = 1.34.—

FTIR (ATR) in cm^{-1}: $\tilde{\nu}$ = 3066, 3035 (=C-H), 2925, 2854 (C-H), 1721, 1634 (C=O), 1578 (C=C), 1496, 1451, 1415, 1377 (C-H), 1067, 1045 (C-O).—

^{1}H-NMR (500.2 MHz, $CDCl_3$) in ppm: 0.84-0.90 [m, 3 H, C$\underline{H}_3$], 0.99-1.35 [m, 15 H, -(C$\underline{H}_2$)$_{10}$-], 1.87-2.46 [m, 2 H, C$\underline{H}_2$-OOC], 3.27-5.33 [m, 5 H of AGUs], 6.06-6.35 [m, 1 H, CH=C$\underline{H}$], 7.06-7.54 [m, 7 H, C$\underline{H}_{arom.,}$ C$\underline{H}$=CH].—

^{13}C-NMR (125.8 MHz, $CDCl_3$) in ppm: 14.2, 22.8, 24.7, 24.9, 29.3, 29.5, 29.6, 29.7, 29.8, 32.1, [-($\underline{C}H_2$)$_{10}$-], 62.1, 71.5, 72.2, 72.6, 73.1, 100.8 [AGU], 116.9 [$\underline{C}$H=CH-Ph], 116.9, 128.4, 128.5, 128.7, 129.0, 130.2, 130.3, 134.0, 134.2 [$\underline{C}_{q, arom.}$, $\underline{C}H_{arom.}$], 145.6, 146.3 [CH=$\underline{C}$H-Ph], 165.2, 165.6, 165.9 [$\underline{C}$=O], 171.9, 172.4, 172.9 [$\underline{C}$=O].—

7.3.2 Synthesis of different sugar monomers for polymerisation *via* thiol-ene / thiol-yne reaction

1,2:3,4-di-O-isopropylidene-α-D-galactopyranose (**1**)

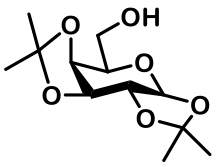

The synthesis of the sugar is carried out as reported.[87]

Galactose (27.8 mmol, 1.0 eq) was suspended in acetone (250 ml) and iodine (5.9 mmol, 0.2 eq) was added. The mixture was stirred for 20 hours at room temperature. The reaction was quenched with a sat. aqueous solution of $Na_2S_2O_3$. Acetone was removed under reduced pressure (rotary evaporator) and the residue was extracted with DCM. The combined organic layers were washed with DI water, dried over anhydrous $NaSO_4$, filtered and the solvent was removed (rotary evaporator). The crude mixture was purified by column chromatography on silica gel (*n*-hexane/EtOAc, 3:1; R_f = 0.24). The Product **1** was obtained as a slightly yellow oil (6.0 g, 83 %).—

FTIR (ATR) in cm^{-1}: $\tilde{\nu}$ = 3450 (O-H), 2980, 2930 (C-H), 1466 (C-H), 1390 (O-H), 1066 (C-O).—

^{1}H-NMR (500.2 MHz, $CDCl_3$) in ppm: 1.32, 1.44, 1.52 [3×s, 12 H, 4×CH_3], 3.67–3.76 [m, 1 H, H-5], 3.80–3.87 [m, 2 H, H-6, H-6'], 4.26 [dd, *J* = 7.9 Hz, 1.5 Hz, 1 H, H-4], 4.32 [dd, *J* = 5.0 Hz, 2.4 Hz, 1 H, H-2], 4.60 [dd, *J* = 7.9 Hz, 2.4 Hz, 1 H, H-3], 5.55 [d, *J* = 5.0 Hz, 1 H, H-1].—

NMR data were in accord with the literature.[87]

^{13}C-NMR (125.8 MHz, $CDCl_3$) in ppm: 24.8, 26.2, 26.3 [4×$\underline{C}H_3$], 62.6 [C-6], 68.3 [C-5], 70.9 [C-2], 71.0 [C-3], 71.8 [C-4], 96.6 [C-1], 108.9, 109.6 [C_q].—

1,2:3,4-di-O-isopropylidene-6-O-(2.propynyl)-α-D-galatopyranose (**2a**)

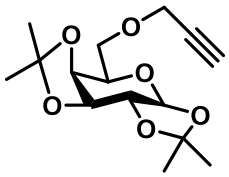

Following the general procedure C, 1,2:3,4-di-*O*-isopropylidene-α-D-galactopyranose (**1**) (5.13 g, 19.7 mmol), sodium hydride (847 mg, 35.8 mmol) and propargyl bromide (2.7 ml, 35.8 mmol) were used for 1,2:3,4-di-*O*-isopropylidene-6-*O*-(2.propynyl)-α-D-galatopyranose (**2a**). The crude residue was purified by column chromatography on silica gel (*n*-hexane/EtOAc; 4/1; R_f = 0.4). The desired product was obtained as colourless solid (5.40 g, 92%).—

M = 298.14 g/mol, $C_{15}H_{22}O_6$

FTIR (ATR) in cm^{-1}: $\tilde{\nu}$ = 3266 (C≡C-H), 2995, 2940, 2900 (C-H), 2115 (C≡C), 1450, 1390 (C-H), 1066 (C-O).—

^{1}H-NMR (500.2 MHz, $CDCl_3$) in ppm: 1.33, 1.34, 1.45, 1.54 [4×s, 12 H, 4×CH_3], 2.43 [t, *J* = 2.4 Hz, 1 H, C_q≡CH], 3.67 [dd, *J* = 10.1 Hz, 7.1 Hz, 1 H, H-6], 3.77 [dd, *J* = 10.1 Hz, 5.3 Hz, 1 H, H-6'], 4.00 [ddd, *J* = 7.1 Hz, 5.2 Hz, 1.9 Hz, 1 H, H-5], 4.17-4.27 [m, 3 H, H-4, C*H*$_2$C≡CH], 4.32 [dd, *J* = 5.1 Hz, 2.4 Hz, 1 H, H-2], 4.61 [dd, *J* = 7.9 Hz, 2.4 Hz, 1 H, H-3], 5.54 [d, *J* = 5.0 Hz, 1 H, H-1].—

NMR data were in accord with the literature.[87]

^{13}C-NMR (125.8 MHz, $CDCl_3$) in ppm: 24.6, 25.1, 26.1, 26.2 [4×CH_3], 58.7 [$\underline{C}H_2C$≡CH], 66.9 [C-5], 68.9 [C-6], 70.6 [C-2], 70.8 [C-3], 71.3 [C-4], 74.7 [C_q≡$\underline{C}$H], 79.8 [$\underline{C_q}$≡CH], 96.5 [C-1], 108.8, 109.5 [2×$C_q(CH_3)_2$].—

1,2:3,4-di-O-isopropylidene-6-O-(2.alloynyl)-α-D-galatopyranose (**2b**)

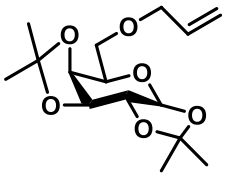

Following the general procedure C, 1,2:3,4-di-*O*-isopropylidene-α-D-galactopyranose (**1**) (5.95 g, 22.8 mmol), sodium hydride (1.03 g, 39.0 mmol) and allyl bromide (2.4 ml, 26.0 mmol) were used for 1,2:3,4-di-*O*-isopropylidene-6-*O*-(2.alloynyl)-α-D-galatopyranose (**2b**). The crude residue was purified by column chromatography on silica gel (PE (40/60)/EtOAc; 8/1; R_f = 0.27). The desired product was obtained as colourless oil (4.86 g, 71%).—

M = 300.16 g/mol, $C_{15}H_{24}O_6$

FTIR (ATR) in cm^{-1}: $\tilde{\nu}$ = 2990, 2936(C-H), 1648 (C=C), 1456, 1390 (C-H), 1207, 1080 (C-O), 999 (C=C).—

^{1}H-NMR (500.2 MHz, $CDCl_3$) in ppm: 1.30, 1.32, 1.42, 1.52 [4×s, 12 H, 4×CH_3], 3.56 [dd, *J* = 10.1 Hz, 6.7 Hz, 1 H, H-6], 3.63 [dd, *J* = 10.1 Hz, 5.8 Hz, 1 H, H-6'], 3.95 [tdd, *J* = 5.8 Hz, 1.9 Hz, 0.5 Hz, 1 H, H-4], 3.98-4.06 [m, 2 H, C*H*$_2$CH=CH_2], 4.24 [dd, *J* = 7.9 Hz, 1.9 Hz, 1 H, H-5], 4.28 [dd, *J* = 5.0 Hz, 2.4 Hz, 1 H, H-2], 4.58 [dd, *J* = 7.9 Hz, 2.4 Hz, 1 H, H-3], 5.13-5.16, 5.23-5.28 [m, 2H, CH_2CH=C*H*$_2$], 5.51 [d, *J* = 5.1 Hz, 1 H, H-1], 5.89 [ddt, *J* = 17.2 Hz, 10.4 Hz, 5.6 Hz, 1 H, CH_2C*H*=CH_2].—

NMR data were in accord with the literature.[135]

^{13}C-NMR (125.8 MHz, $CDCl_3$) in ppm: 24.5, 25.0, 26.1 26.2 [4×CH_3], 66.9 [C-4], 68.9 [C-6], 70.6 [C-2], 70.7 [C-3], 71.3 [C-5], 72.4 [$\underline{C}H_2CH=CH_2$], 96.4 [C-1], 108.3, 109.3 [2×C_q], 117.1 [$CH_2CH=\underline{C}H_2$], 134.9 [$CH_2\underline{C}H=CH_2$].—

6-O-prop-2-yn-1-yl-D-galactopyranose (**3a**)

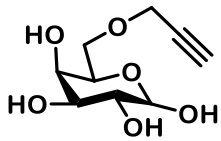

Following the general procedure D, 1,2:3,4-di-*O*-isopropylidene-6-*O*-(2.propynyl)-α-D-galatopyranose (**2a**) (5.60 g, 18.8 mmol) and Dowex® (6.77 g) and water (206.8 ml) were used for 6-*O*-Prop-2-yn-1-yl-D-galactopyranose (**3a**).The crude product was obtained as slightly yellowish oil.—

M = 218.08 g/mol, $C_9H_{14}O_6$

6-O-allo-2-yn-1-yl-D-galactopyranose (**3b**)

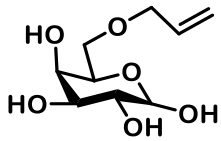

Following the general procedure D, 1,2:3,4-Di-*O*-isopropylidene-6-*O*-(2.alloynyl)-α-D-galatopyranose (**2b**) (4.61 g, 18.8 mmol) and Dowex® (5.35 g), water (158.4 ml) were used for 6-*O*-allo-2-yn-1-yl-D-galactopyranose (**3b**).The crude product was obtained as slightly yellowish oil.—

M = 220.09 g/mol, $C_9H_{16}O_6$

(2S,3R,4S,5S,6R)-6-((prop-2-yn-1-yloxy)methyl)tetrahydro-2H-pyran-2,3,4,5-tetrayl tetraacetate (**4a**)

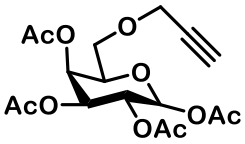

Following the general procedure E, 6-*O*-prop-2-yn-1-yl-D-galactopyranose (**3a**) (4.10 g, 18.8 mmol), pyridine (47.0 ml, 582 mmol) and ethyl acetate (55.0 ml, 582 mmol) was used for (2*S*,3*R*,4*S*,5*S*,6*R*)-6-((prop-2-yn-1-yloxy)methyl)tetrahydro-2*H*-pyran-2,3,4,5-tetrayl tetraacetate (**4a**). The crude residue was purified by column chromatography on silica gel (*n*-hexane/EtOAc; 3/1; R_f = 0.19). The desired product was obtained as colourless oil (6.17 g, 85% over two steps).—

M = 386.12 g/mol, $C_{17}H_{22}O_{10}$

FTIR (ATR) in cm^{-1}: $\tilde{\nu}$ = 3273 (C≡C-H), 2950.2935 (C-H), 2113 (C≡C), 1740 (C=O), 1438 (C-H), 1205, 1063 (C-O).—

The pure product is a mixture of two anomers in a ratio of 3:2. Due to this it is not possible to assign a main isomer.

^{1}H-NMR (500.2 MHz, $CDCl_3$) in ppm: 1.99, 2.00, 2.01, 2.04, 2.11, 2.15, 2×2.16 [8×CH_3], 2.43 [dt, *J* = 4.7 Hz, 2.4 Hz, 1 H, H-5], 3.57 [d, *J* = 6.2 Hz, 2 H, 2×H-7], 3.59-3.64 [m, 2 H, 2×H-7‘], 4.00 [ddd, *J* = 6.7 Hz, 6.0 Hz, 1.2 Hz, 1 H, H-9], 4.11 [t, *J* = 2.2 Hz, 2 H, 2×H-6], 4.14 [dd, *J* = 4.0 Hz, 2.4 Hz, 2 H, 2×H-6‘], 4.30 [tdd, *J* = 6.2 Hz, 1.4 Hz, 0.6 Hz, 1 H, H-9], 5.08 [dd, *J* = 10.4 Hz, 3.4 Hz, 2 H, 2×H-3], 5.29-5.35 [m, 3 H, 2×H-2, H-5], 5.47 [dd, *J* = 3.4 Hz, 1.1 Hz, 1 H, H-4], 5.51-5.57 [m, 1H, H-4], 5.70 [d, *J* = 8.3 Hz, 1 H, H-1], 6.38 [dd, *J* = 1.3 Hz, 0.7 Hz, 1 H, H-1].—

NMR data were in accord with the literature.[87]

^{13}C-NMR (125.8 MHz, $CDCl_3$) in ppm: 2×20.7, 4×20.8, 21.0, 21,1 [×CH_3], 58.7, 58.8 [2×C-6], 66.7 [C-5], 67.0 [C-7], 67.4 [C-2], 67.5 [C-7], 67.6 [C-2], 68.1,68.2 [2×C-4], 70.2 [C-9], 71.1 [C-3], 72.9 [C-9], 2×75.3 [C-3, C-5], 2×79.1 [2×C-8], 90.0, 92.4 [2×C-1], 169.1, 169.2, 169.6, 2×170.1, 3×170.2 [8×-$\underline{C}OOCH_3$].—

MS (ESI^+,TOF): m/z (%) = 409.1 $[MNa]^+$ (100).—

HRMS (ESI^+,TOF): calculated for $[C_{17}H_{22}O_{10}Na]^+$: 409.1105, found: 409.1108.—

(2S,3R,4S,5S,6R)-6-((allyloxy)methyl)tetrahydro-2H-pyran-2,3,4,5-tetrayl tetraacetate (**4b**)

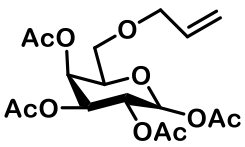

Following the general procedure E, 6-*O*-allo-2-yn-1-yl-D-galactopyranose (**3b)** (3.17 g, 18.8 mmol), pyridine (43.0 ml, 532 mmol) and ethyl acetate (50.0 ml, 532 mmol) was used for (2*S*,3*R*,4*S*,5*S*,6*R*)-6-((allyloxy)methyl)tetrahydro-2*H*-pyran-2,3,4,5-tetrayl tetraacetate (**4b**). The crude residue was purified by column chromatography on silica gel (PE (40/60)/EtOAc; 2/1; R_f = 0.14). The desired product was obtained as colourless oil (4.69 g, 84%).—

M = 388.14 g/mol, $C_{17}H_{24}O_6$

FTIR (ATR) in cm^{-1}: $\tilde{\nu}$ = 2990, 2940, 2870 (C-H), 1750 (C=O), 1650 (C=C), 1439 (C-H), 1205, 1058 (C-O), 940 (C=C).—

The pure product is a mixture of two anomers in a ratio of 3:2.

Major anomer:

^{1}H-NMR (500.2 MHz, $CDCl_3$) in ppm: 1.93, 1.98, 2.05, 2.10 [4×s, 12 H, 4×CH_3], 3.35-3.45 [m, 1 H, H-6], 3.49 [dd, *J* = 9.8 Hz, 5.9 Hz, 1 H, H-6'], 3.84 [dddt, *J* = 12.8 Hz, 5.8 Hz, 3.6 Hz, 1.4 Hz, 1 H, C*H*$_2$CH=CH_2], 3.93 [dddd, *J* = 11.5 Hz, 5.6 Hz, 2.8 Hz, 1.4 Hz, 2 H, C*H*$_2$CH=CH_2, H-4], 5.04 [dd, *J* = 10.4 Hz, 3.4 Hz, 1 H, H-5], 5.12 [dddt, *J* = 10.4 Hz, 4.0 Hz, 1.7 Hz, 1.2 Hz, 1 H, CH_2CH=C*H*$_2$], 5.14-5.20 [m, 1 H, CH_2CH=C*H*$_2$], 5.26-5.28 [m, 1 H, H-2], 5.43 [dd, *J* = 3.4 Hz, 1.1 Hz, 1 H, H-3], 5.65 [d, *J* = 8.3 Hz, 1 H, H-1], 5.76 [dddd, *J* = 17.2 Hz, 10.4 Hz, 2×5.7 Hz, 1 H, CH_2C*H*=CH_2].—

^{13}C-NMR (125.8 MHz, $CDCl_3$) in ppm: 20.5, 2×20.6, 20.8 [4×CH_3], 67.1 [C-6], 67.3 [C-3], 68.0 [C-2], 71.0 [C-5], 72.3 [$\underline{C}H_2$CH=CH_2], 72.9 [C-4], 92.2 [C-1], 117.7 [CH_2CH=$\underline{C}H_2$], 134.0 [$CH_2\underline{C}$H=CH_2], 168.9, 169.4, 169.9, 170.0 [$\underline{C}OOCH_3$].—

Minor anomer:

^{1}H-NMR (500.2 MHz, $CDCl_3$) in ppm: 1.94, 1.95, 2×2.09 [4×s, 12 H, 4×CH_3], 3.35-3.45 [m, 2 H, H-6], 3.80-3.88 [m, 3 H, H-5, C*H*$_2$CH=CH_2], 4.23 [ddt, *J* = 6.6 Hz, 6.1 Hz, 1.1 Hz, 1 H, H-4], 5.12 [dddt, *J* = 10.4 Hz, 4.0 Hz, 1.7 Hz, 1.2 Hz, 1 H, CH_2CH=C*H*$_2$], 5.14-5.20 [m, 1 H, CH_2CH=C*H*$_2$], 5.26-5.28 [m, 1 H, H-2], 5.49 [dd, *J* = 2.5 Hz, 1.4 Hz, 1 H, H-3], 5.76 [dddt, *J* = 17.2 Hz, 10.4 Hz, 2×5.7 Hz, 1 H, CH_2C*H*=CH_2], 6.31 [d, *J* = 2.5, 1 H, H-1].—

^{13}C-NMR (125.8 MHz, $CDCl_3$) in ppm: 20.5, 2×20.6, 20.9 [4×CH_3], 66.6 [C-2], 67.5 [C-3], 67.6 [C-6], 68.1 [C-5], 70.1 [C-4], 72.4 [$\underline{C}H_2$CH=CH_2], 89.8 [C-1], 117.7 [CH_2CH=$\underline{C}H_2$], 134.0 [$CH_2\underline{C}$H=CH_2], 169.0, 169.9, 2×170.0 [$\underline{C}OOCH_3$].—

(2S,3R,4S,5S,6R)-2-(acetylthio)-6-((prop-2-yn-1-yloxy)methyl)tetrahydro-2H-pyran-3,4,5-triyl triacetate (**5a**)

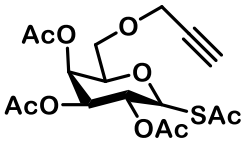

Following the general procedure F, (2*S*,3*R*,4*S*,5*S*,6*R*)-6-((prop-2-yn-1-yloxy)methyl)tetrahydro-2*H*-pyran-2,3,4,5-tetrayl tetraacetate (**4a**) (2.21 g, 5.7 mmol), thioacetic acid (1.9 ml, 27.2 mmol) and boron trifluoride diethyl etherate (4.9 ml, 39.9 mmol) was used for (2S,3R,4S,5S,6R)-2-(acetylthio)-6-((prop-2-yn-1-yloxy)methyl)tetrahydro-2*H*-pyran-3,4,5-triyl triacetate (**5a**). The crude residue was purified by column chromatography on silica gel (*n*-hexane/EtOAc; 2/1; R_f = 0.15). The desired product was obtained as colourless oil (1.65 g, 72%).—

M = 402.10 g/mol, $C_{17}H_{22}O_9S$

FTIR (ATR) in cm^{-1}: $\tilde{\nu}$ = 3282(C≡C-H), 2978, 2943, 2882 (C-H), 2112 (C≡C), 1747, 1701(C=O), 1440 (C-H), 1253, 1207, 1063 (C-O).—

The pure product is a mixture of two anomers in a ratio of 1:5. The signals of the minor anomer can't be assigned to the respective positions of the molecule.

Major anomer:

^{1}H-NMR (500.2 MHz, $CDCl_3$) in ppm: 1.89, 1.94, 2.07, 2.30 [4×s, 12 H, 4×CH_3], 2.39 [t, *J* = 2.4 Hz, 1 H, $CH_2C{\equiv}CH$], 3.44-3.59 [m, 2 H, C-6], 3.96 [td, *J* = 6.3 Hz, 1.2 Hz, 1 H, H-5], 3.96-4.11 [m, 2 H, $CH_2C{\equiv}CH$], 5.04 [dd, *J* = 9.2 Hz, 3.4 Hz, 1 H, H-3], 5.16-5.25 [m, 2 H, H-1, H-2], 5.41 [dd, *J* = 3.4 Hz, 1.1 Hz, 1 H, H-4].—

^{13}C-NMR (125.8 MHz, $CDCl_3$) in ppm: 20.5, 2×20.6, 30.8 [4×CH_3], 58.3 [$\underline{C}H_2C{\equiv}CH$], 66.5 [C-2], 66.9 [C-6], 67.6 [C-4], 71.9 [C-3], 75.1 [$CH_2C{\equiv}\underline{C}H$], 76.0 [C-5], 79.0 [$CH_2\underline{C}{\equiv}CH$], 80.4 [C-1], 169.4, 169.7, 170.0 [3×$\underline{C}OOCH_3$], 192.1 [$\underline{C}OSCH_3$].—

MS (ESI^+,TOF): m/z (%) = 425.1 $[MNa]^+$ (100).—

HRMS (ESI^+,TOF): calculated for $[C_{17}H_{22}O_9NaS]^+$: 425.0877, found: 425.0882.—

(2S,3R,4S,5S,6R)-2-(acetylthio)-6-((allyloxy)methyl)tetrahydro-2H-pyran-3,4,5-triyl triacetate (**5b**)

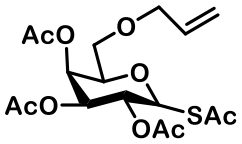

Following the general procedure F, (2*S*,3*R*,4*S*,5*S*,6*R*)-6-((allyloxy)methyl)tetrahydro-2*H*-pyran-2,3,4,5-tetrayl tetraacetate (**4b**) (5.00 g, 12.4 mmol), thioacetic acid (4.3 ml, 58.8 mmol) and boron trifluoride diethyl etherate (11.2 ml, 86.8 mmol) were used for (2*S*,3*R*,4*S*,5*S*,6*R*)-2-(acetylthio)-6-((allyloxy)methyl)tetrahydro-2*H*-pyran-3,4,5-triyl triacetate (**5b**). The crude residue was purified by column chromatography on silica gel (PE (40/60)/EtOAc; 3/1; R_f = 0.12). The desired product was obtained as colourless oil (4.76 g, 95%).—

M = 402.10 g/mol, $C_{17}H_{24}O_9S$

FTIR (ATR) in cm^{-1}: $\tilde{\nu}$ = 2968, 2943, 2872 (C-H), 1750, 1703 (C=O), 1433 (C-H), 1242, 1210, 1057 (C-O).—

The pure product is a mixture of two anomers in a ratio of 1:6. The signals of the minor anomer can't be assigned to the respective positions of the molecule.

Major anomer:

^{1}H-NMR (500.2 MHz, $CDCl_3$) in ppm: 1.95, 1.99, 2.11, 2.35 [4×s, 12 H, 4×CH_3], 3.38 [dd, *J* = 9.9 Hz, 7.0 Hz, 1 H, H-6], 3.50 [dd, *J* = 9.8 Hz, 5.8 Hz, 1 H, H-6'], 3.85 [ddt, *J* = 12.8 Hz, 5.9 Hz, 1.4 Hz, 1 H, C*H*$_2$CH=CH_2], 3.91-3.99 [m, 2 H, H-5, C*H*$_2$CH=CH_2], 5.09 [dd, *J* = 9.6 Hz, 3.4 Hz, 1 H, H-4], 5.12-5.31 [m, 4 H, H-1, H-2, CH_2CH=C*H*$_2$], 5.48 [dd, *J* = 3.4 Hz, 1.2 Hz, 1 H, H-3], 5.78 [ddt, *J* = 17.3 Hz, 10.4 Hz, 5.7 Hz, 1 H, CH_2C*H*=CH_2].—

^{13}C-NMR (125.8 MHz, $CDCl_3$) in ppm: 20.7, 20.8, 20.8, 30.9 [4×CH_3], 66.7 [C-2], 67.3 [C-6], 67.8 [C-3], 72.4 [C-4], 72.4 [$\underline{C}H_2CH=CH_2$], 76.4 [C-5], 80.6 [C-1], 117.7 [$CH_2CH=\underline{C}H_2$], 134.2 [$CH_2\underline{C}H=CH_2$], 169.7, 169.9, 170.1 [3×$\underline{C}OOCH_3$], 192.3 [$\underline{C}OSCH_3$].—

MS (ESI^+,TOF): m/z (%) = 427.1 $[MNa]^+$ (100).—

HRMS (ESI^+,TOF): calculated for $[C_{17}H_{24}O_9NaS]^+$: 427.1033, found: 427.1036.—

(2S,3R,4S,5R,6R)-2-mercapto-6-((prop-2-yn-1-yloxy)methyl)tetrahydro-2H-pyran-3,4,5-triol (**6a**)

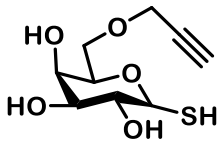

Following the general procedure G, (2*S*,3*R*,4*S*,5*S*,6*R*)-2-(acetylthio)-6-((prop-2-yn-1-yloxy)methyl)tetrahydro-2H-pyran-3,4,5-triyl triacetate (**5a**) 804 mg, 2.00 mmol), sodium methoxide (165 mg, 6.00 mmol) methanol (15 ml) and Dowex® (2.00 g) were used for (2*S*,3*R*,4*S*,5*R*,6*R*)-2-mercapto-6-((prop-2-yn-1-yloxy)methyl)tetrahydro-2*H*-pyran-3,4,5-triol (**6a**).—

M = 234.06 g/mol, $C_9H_{14}O_5S$

MS (ESI^+,TOF): m/z (%) = 257.0 $[MNa]^+$ (100).—

HRMS (ESI^+,TOF): calculated for $[C_{17}H_{14}O_9NaS]^+$: 257.0454, found: 257.0452.—

(2R,3R,4S,5R,6S)-2-((allyloxy)methyl)-6-mercaptotetrahydro-2H-pyran-3,4,5-triol (**6b**)

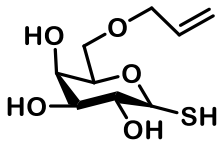

Following the general procedure G, (2*S*,3*R*,4*S*,5*S*,6*R*)-2-(acetylthio)-6-((allyloxy)methyl)tetrahydro-2*H*-pyran-3,4,5-triyl triacetate (**5b**) 808 mg, 2.00 mmol), sodium methoxide (165 mg, 6.00 mmol) methanol (15 ml) and Dowex® (2.00 g) were used for (2*R*,3*R*,4*S*,5*R*,6*S*)-2-((allyloxy)methyl)-6-mercaptotetrahydro-2*H*-pyran-3,4,5-triol (**6b**).—

M = 236.07 g/mol, $C_9H_{16}O_5S$

MS (ESI^+,TOF): m/z (%) = 495.1 $[M_2Na]^+$ (43).—

HRMS (ESI^+,TOF): calculated for $[C_{18}H_{32}O_{10}NaS_2]^+$: 495.1329, found: 495.1273.—

7.3.3 Synthesis of symmetrical sugar based triazoles

(2R,3S,4S,5R,6R)-2-((allyloxy)methyl)-6-azidotetrahydro-2H-pyran-3,4,5-triyl triacetate (**7**)

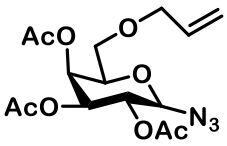

The synthesis of the sugar was carried out as reported.[136]

(2*S*,3*R*,4*S*,5*S*,6*R*)-6-((Allyloxy)methyl)tetrahydro-2*H*-pyran-2,3,4,5-tetrayl tetraacetate (**4b**) (2.50 g, 6.5 mmol) was dissolved in anhydrous DCM (35 ml) and cooled to 0 °C. Afterwards azido trimethyl silane (1.02 ml, 7.7 mmol) and tin (IV) chloride (0.38 ml, 3.25 mmol) were added carefully. The mixture was allowed to warm up to room temperature and was stirred for 3 hours. By adding triethyl amine (2 ml) the reaction was quenched. Then the mixture was extracted with DCM (3×50 ml). The combined organic layers were washed with saturated sodium hydrogen carbonate solution (3×50 ml) and brine (1×50 ml). The organic part was dried over $NaSO_4$ and the solvent was removed under reduced pressure at the rotary evaporator. The crude residue was purified by column chromatography on silica gel (*n*-hexane/EtOAc; 2/1; $R_f = 0.21$). The desired product (2*R*,3*S*,4*S*,5*R*,6*R*)-2-((allyloxy)methyl)-6-azidotetrahydro-2*H*-pyran-3,4,5-triyl triacetate (**7**) was obtained as colourless oil (1.98 g, 82%).—

M = 371.35 g/mol, $C_{15}H_{21}N_3O_8$

FTIR (ATR) in cm^{-1}: $\tilde{\nu}$ = 2940, 2890 (C-H), 2117 (N_3), 1748 (C=O), 1433 (C-H), 1208, 1055 (C-O), 926, 750 (C=C).—

^{1}H-NMR (500.2 MHz, $CDCl_3$) in ppm: 1.98, 2.08, 2.15 [3×s, 9 H, 3×CH_3], 3.48 [dd, *J* = 10.0 Hz, 6.1 Hz, 1 H, H-6], 3.57 [dd, *J* = 10.0 Hz, 6.3 Hz, 1 H, H-6'], 3.90-3.95 [m, 2 H, H-3, C*H*$_2$CH=CH$_2$]4.01 [dddd, *J* = 12.8 Hz, 5.6 Hz, 1.6 Hz, 1.2 Hz, 1 H, C*H*$_2$CH=CH$_2$], 4.60 [d, *J* = 8.7 Hz, 1 H, H-1], 5.03 [dd, *J* = 10.3 Hz, 3.4 Hz, 1 H, H-4], 5.15 [ddd, *J* = 10.3 Hz, 8.7 Hz, 0.4 Hz, 1 H, H-2], 5.17-5.27 [m, 2 H, CH$_2$CH=C*H*$_2$], 5.46 [ddd, *J* = 3.4 Hz, 1.2 Hz, 0.4 Hz, 1 H, H-5], 5.83 [ddt, *J* = 17.2 Hz, 10.4 Hz, 5.7 Hz, 1 H, CH$_2$C*H*=CH$_2$].—

^{13}C-NMR (125.8 MHz, $CDCl_3$) in ppm: 20.7, 2×20.8 [3×CH_3], 2×67.6 [C-5, C-6], 68.4 [C-2], 71.0 [C-4], 72.6 [$\underline{C}H_2CH=CH_2$], 74.6 [C-3], 88.5 [C-1], 118.0 [$CH_2CH=\underline{C}H_2$], 134.1 [$CH_2\underline{C}H=CH_2$], 169.6, 170.1, 170.2 [3×$\underline{C}OOCH_3$].—

(2S,3R,4R,5S)-2-((allyloxy)methyl)-6-(4-(4-(1-((2R,3R,4S,5S,6R)-3,4,5-triacetoxy-6-((allyloxy)methyl)tetrahydro-2H-pyran-2-yl)-1H-1,2,3-triazol-4-yl)butyl)-1H-1,2,3-triazol-1-yl)tetrahydro-2H-pyran-3,4,5-triyl triacetate (**8**)

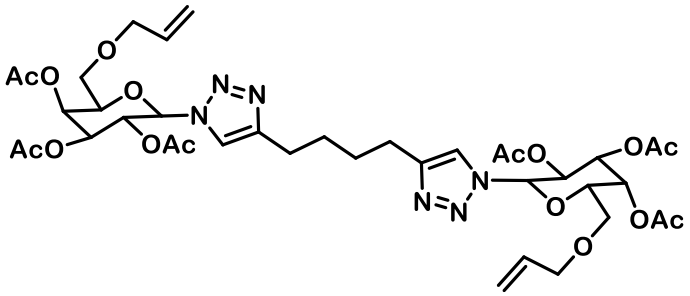

The synthesis of the sugar is carried out as reported.[136]

(2*R*,3*S*,4*S*,5*R*,6*R*)-2-((Allyloxy)methyl)-6-azidotetrahydro-2H-pyran-3,4,5-triyl triacetate (**7**) (742 mg, 2.0 mmol) was dissolved in a mixture of water and tert butyl alcohol (1:1; 15 ml in total). 1,7 octadiyne (0.13 ml, 1 mmol), copper sulfate (1.59 mg, 0.01 mmol) and sodium ascorbate (19 mg, 0.1 mmol) were added. The mixture was stirred for 12 h at room temperature and the progress was controlled *via* TLC. When the reaction turned green new sodium ascorbate was added. The mixture was extracted with DCM (3×50 ml). The combined organic layers were washed with water (3×50 ml) and brine (1×50 ml). The organic part is dried over $NaSO_4$ and the solvent was removed under reduced pressure at the rotary evaporator. The crude residue was purified by column chromatography on silica gel (EtOAc; $R_f = 0.81$). The desired product (2*S*,3*R*,4*R*,5*S*)-2-((allyloxy)methyl)-6-(4-(4-(1-((2*R*,3*R*,4*S*,5*S*,6*R*)-3,4,5-triacetoxy-6-((allyloxy)methyl)tetrahydro-2*H*-pyran-2-yl)-1*H*-1,2,3-triazol-4-yl)butyl)-1*H*-1,2,3-triazol-1-yl)tetrahydro-2*H*-pyran-3,4,5-triyl triacetate (**8**) was obtained as colourless oil (670 mg, 79%).—

M = 848.34 g/mol, $C_{38}H_{52}N_6O_{16}$

FTIR (ATR) in cm^{-1}: $\tilde{\nu}$ = 3145, 3092 (C_{arom}-H), 2991, 2949, 2870 (C-H), 1748 (C=O), 1648 (C=N), 1568 (C=C_{cyclic}), 1442 (C-H), 1370 (C-N), 1206,1076 (C-O), 915 (C=C).—

^{1}H-NMR (500.2 MHz, $CDCl_3$) in ppm: 1.67-1.72 [m, 4 H, 2×$C_{q,arom}$-CH_2-CH_2],1.80-1.83 [m, 6 H, 2×CH_3], 1.95, 2.16 [2×s, 12 H, 4×CH_3], 2.67-2.74 [m, 4 H, 2×$C_{q,arom}$-CH_2-CH_2], 3.42-3.46 [m, 2 H, 2×H-6], 3.50-3.54 [m, 2 H, 2×H-6'], 3.82-3.96 [m, 4 H, CH_2CH=CH_2], 4.10 [td, *J* = 6.3 Hz, 1.2 Hz, 2 H, 2×H-5], 5.10-5.22 [m, 6 H, 2×H-3, CH_2CH=CH_2], 5.46-5.52 [m, 2 H, 2×H-2], 5.54 [dd, *J* = 3.4 Hz, 1.2 Hz, 2 H, 2×H-4], 5.71-5.80 [m, 4 H, 2×H-1, 2×CH_2C*H*=CH_2], 7.54 [s, 2 H, C_{arom}H].—

^{13}C-NMR (125.8 MHz, $CDCl_3$) in ppm: 20.3, 20.6, 20.7 [6×CH_3], 25.3 [2×$C_{q,arom}$-$\underline{C}H_2$-CH_2], 28.6 [2×$C_{q,arom}$-CH_2-$\underline{C}H_2$], 67.2 [2×C-6], 67.4 [2×C-4], 68.1 [2×C-2], 71.1 [2×C-3], 72.4 [2×$\underline{C}H_2$CH=CH_2],

75.2 [2×C-5], 86.2 [2×C-1], 117.9 [2×$CH_2\underline{C}H=CH_2$], 119.1 [2×$C_{arom}H$], 133.9 [2×$CH_2\underline{C}H=CH_2$], 148.5 [2×$C_{q,arom}$], 169.1, 169.8, 170.0 [6×$\underline{C}OOCH_3$].—

MS (ESI^+,TOF): m/z (%) = 871.3 $[MNa]^+$ (100).—

HRMS (ESI^+,TOF): calculated for $[C_{38}H_{52}N_6O_{16}Na]^+$: 871.3332, found: 871.3334.—

8 Attachment

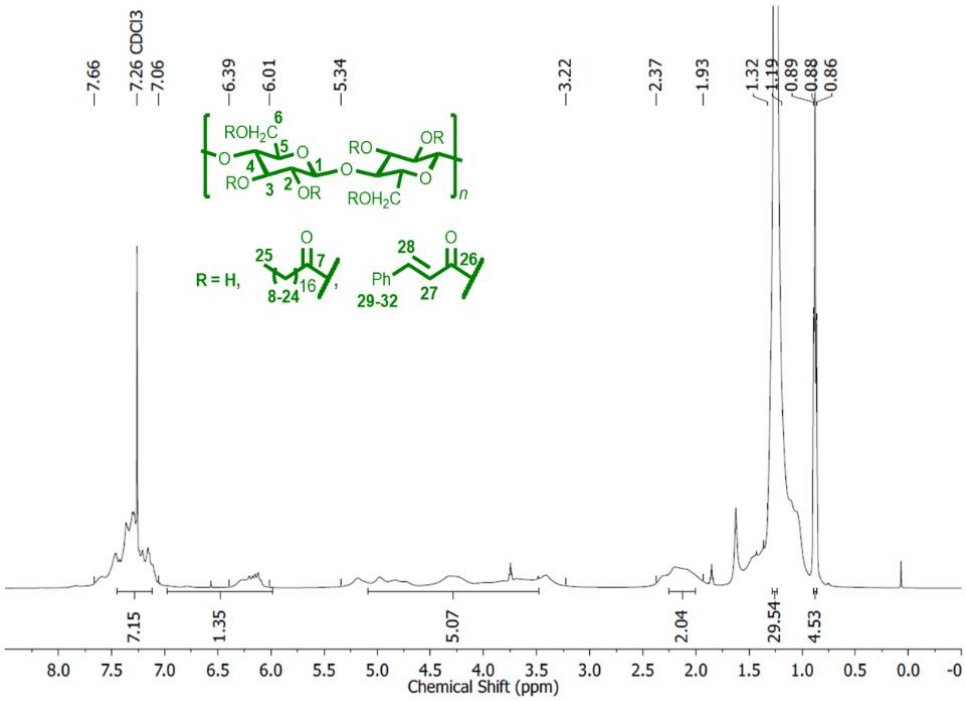

Figure 8.1 ^{1}H-NMR spectrum (500.2 MHz) of SCC measured in $CDCl_3$.

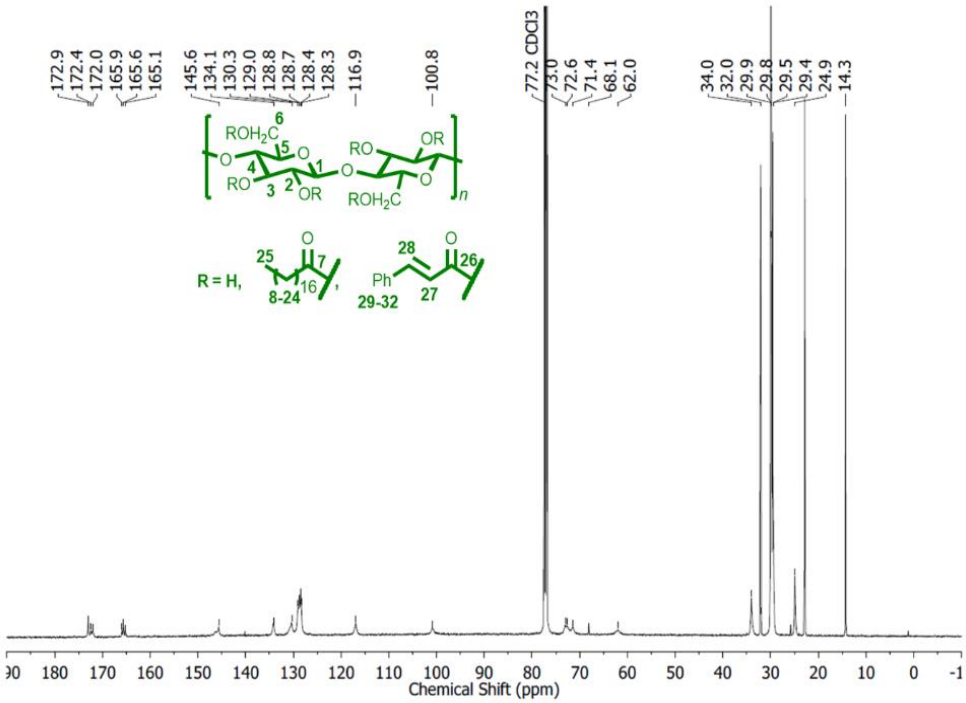

Figure 8.2 ^{13}C-NMR spectrum (125.8 MHz) of SCC measured in $CDCl_3$.

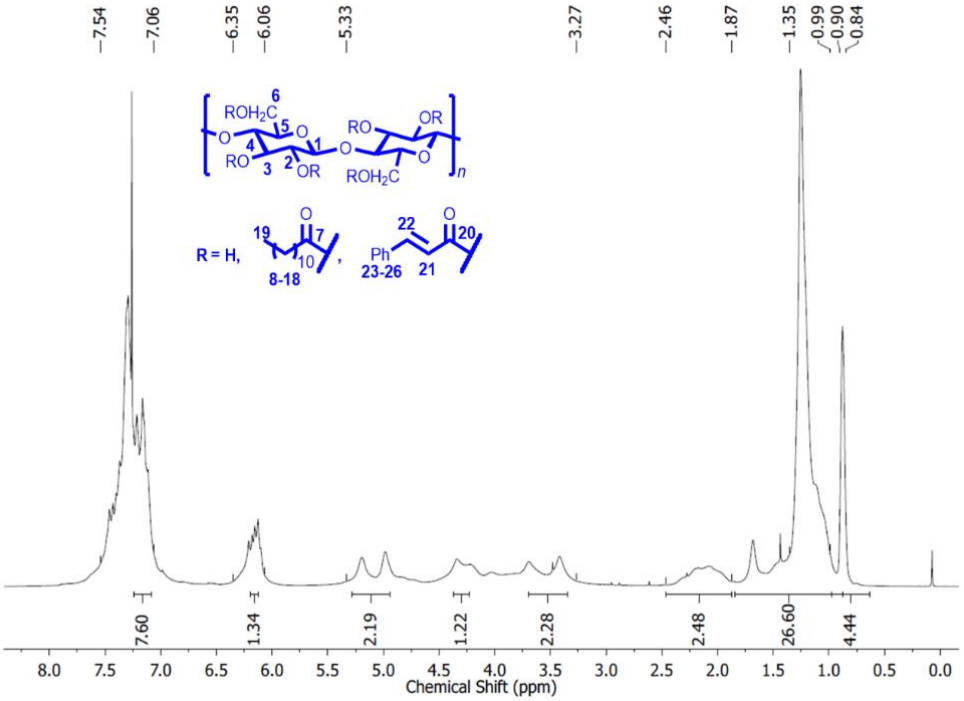

Figure 8.3 ^{1}H-NMR spectrum (500.2 MHz) of LCC measured in $CDCl_3$.

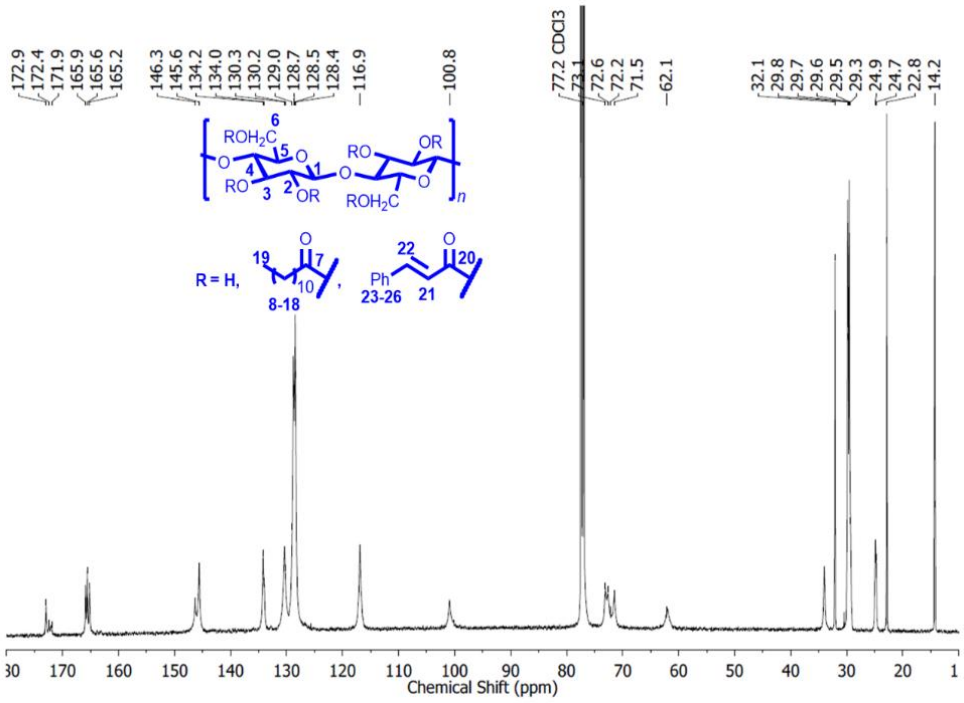

Figure 8.4 ^{13}C-NMR spectrum (125.8 MHz) of LCC measured in $CDCl_3$.

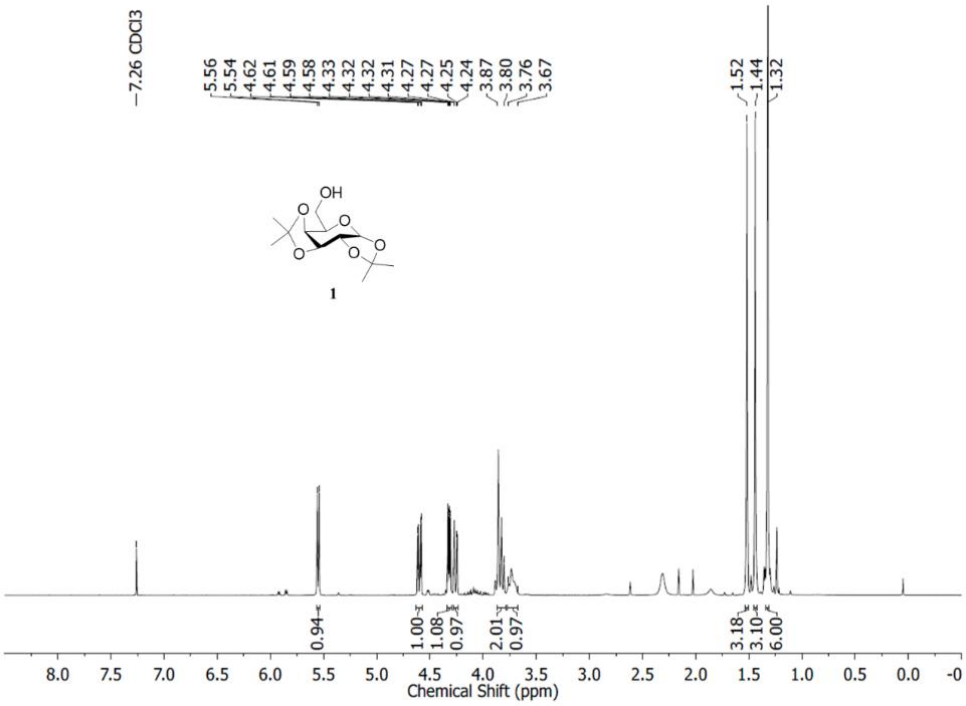

Figure 8.5 ^{1}H-NMR spectrum (500.2 MHz) of **1** measured in $CDCl_3$.

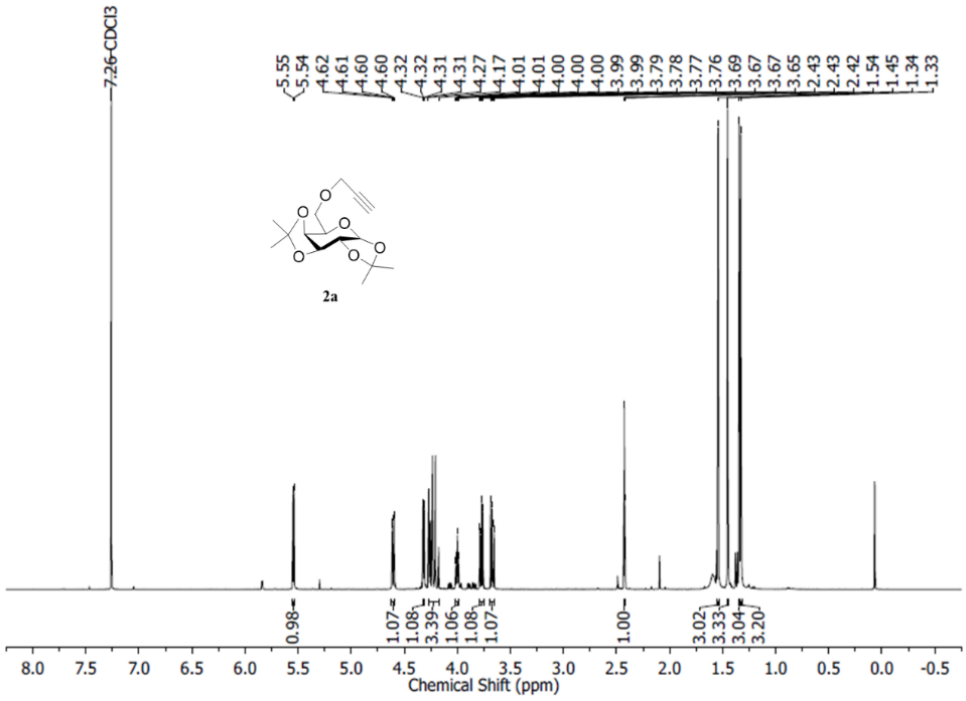

Figure 8.6 ^{1}H-NMR spectrum (500.2 MHz) of **2a** measured in $CDCl_3$.

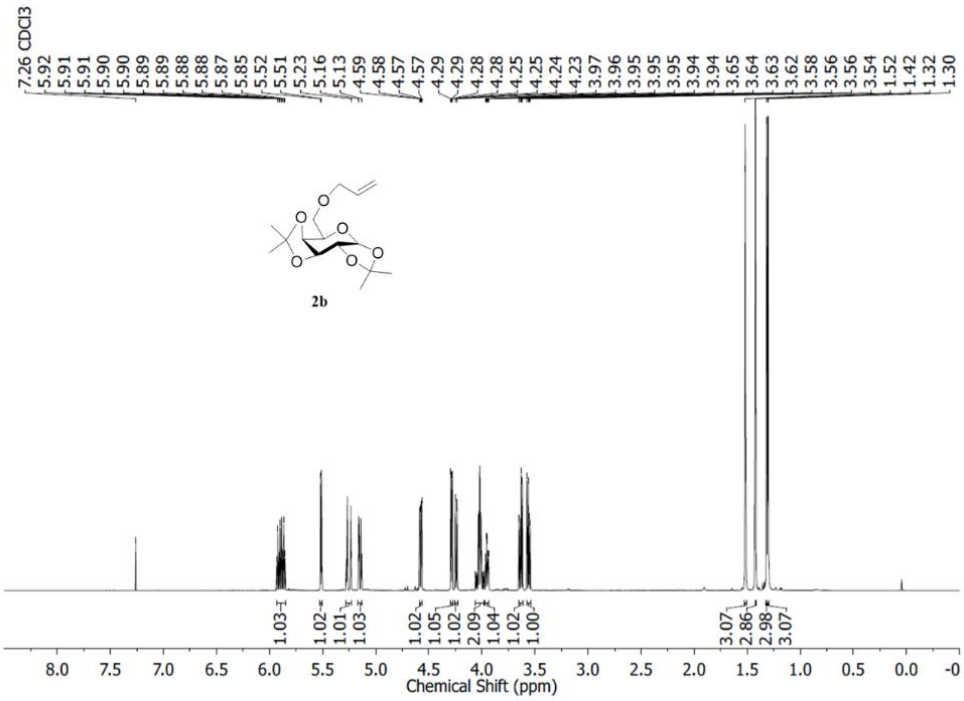

Figure 8.7 ^{1}H-NMR spectrum (500.2 MHz) of **2b** measured in $CDCl_3$.

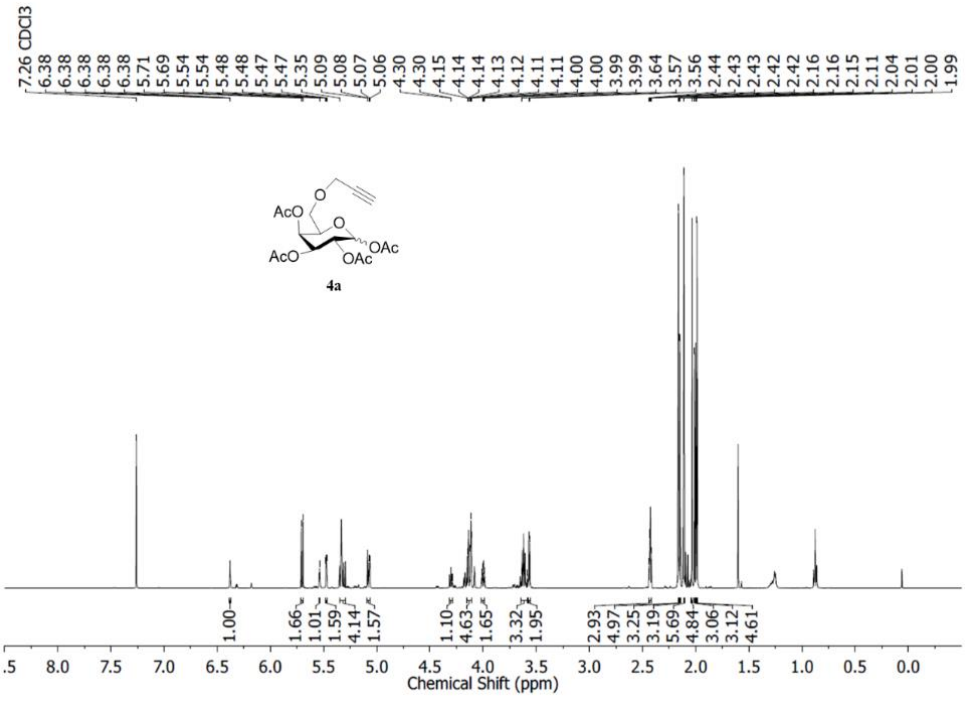

Figure 8.8 ^{1}H-NMR spectrum (500.2 MHz) of **4a** measured in $CDCl_3$.

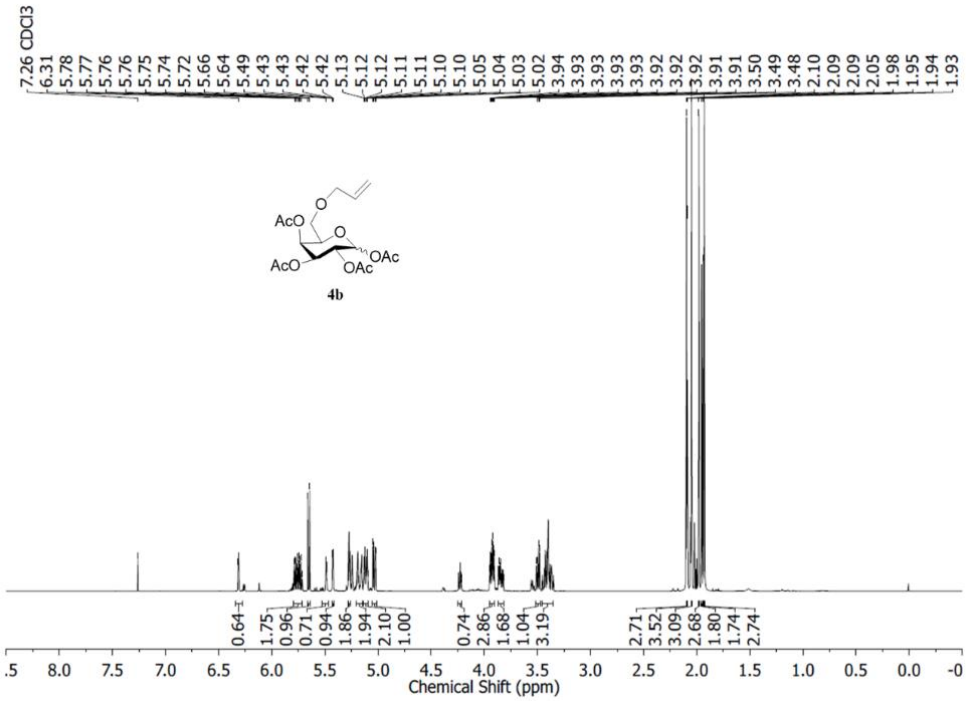

Figure 8.9 ^{1}H-NMR spectrum (500.2 MHz) of **4b** measured in $CDCl_3$.

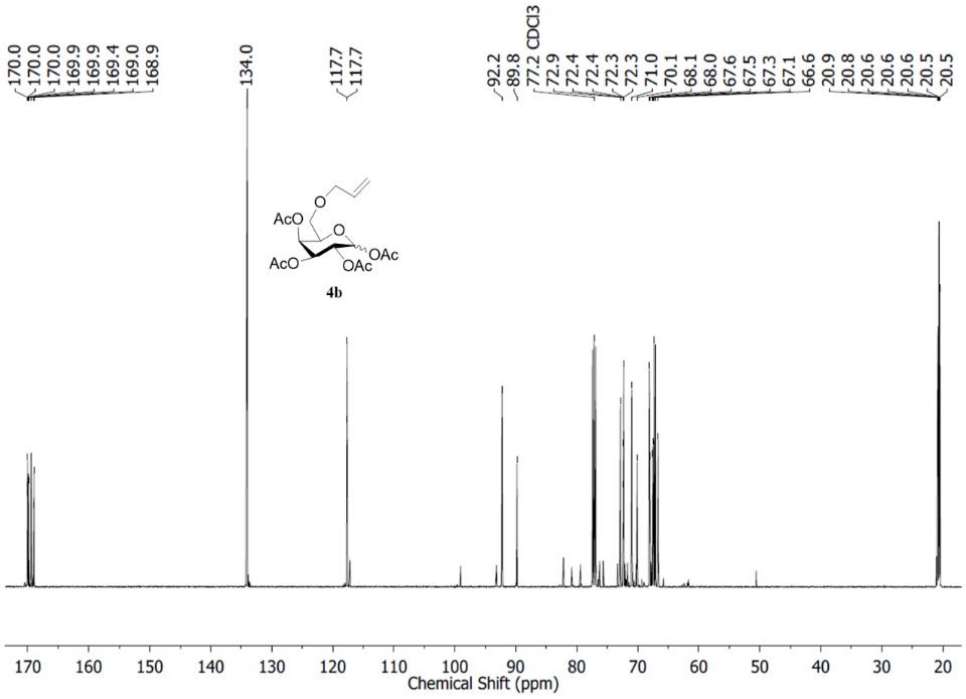

Figure 8.10 ^{13}C-NMR spectrum (125.8 MHz) of **4b** measured in $CDCl_3$.

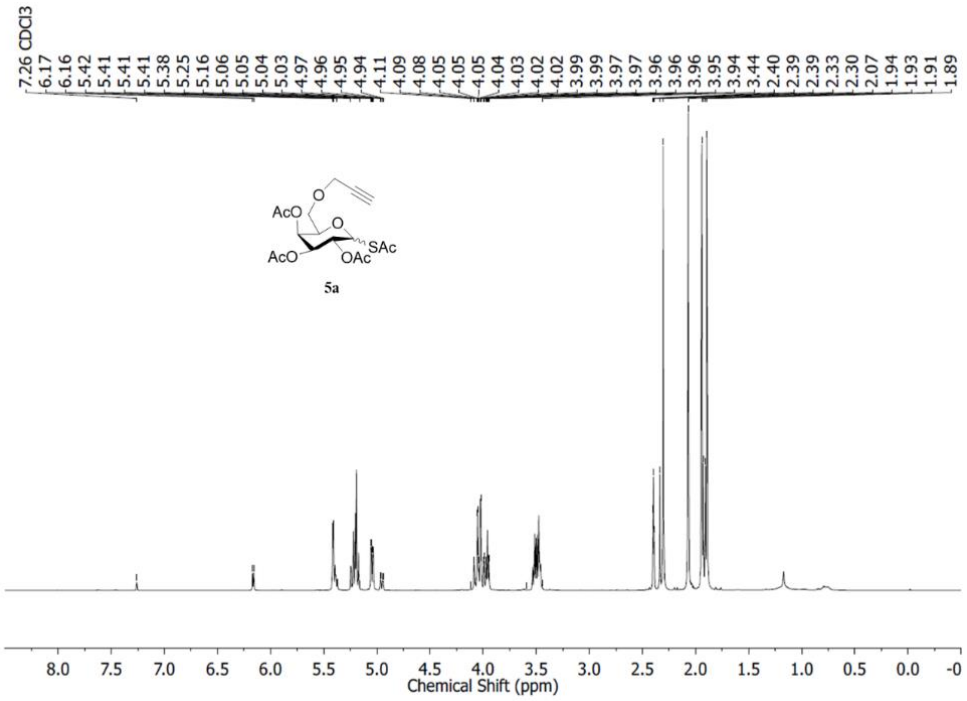

Figure 8.11 ^{1}H-NMR spectrum (500.2 MHz) of **5a** measured in $CDCl_3$.

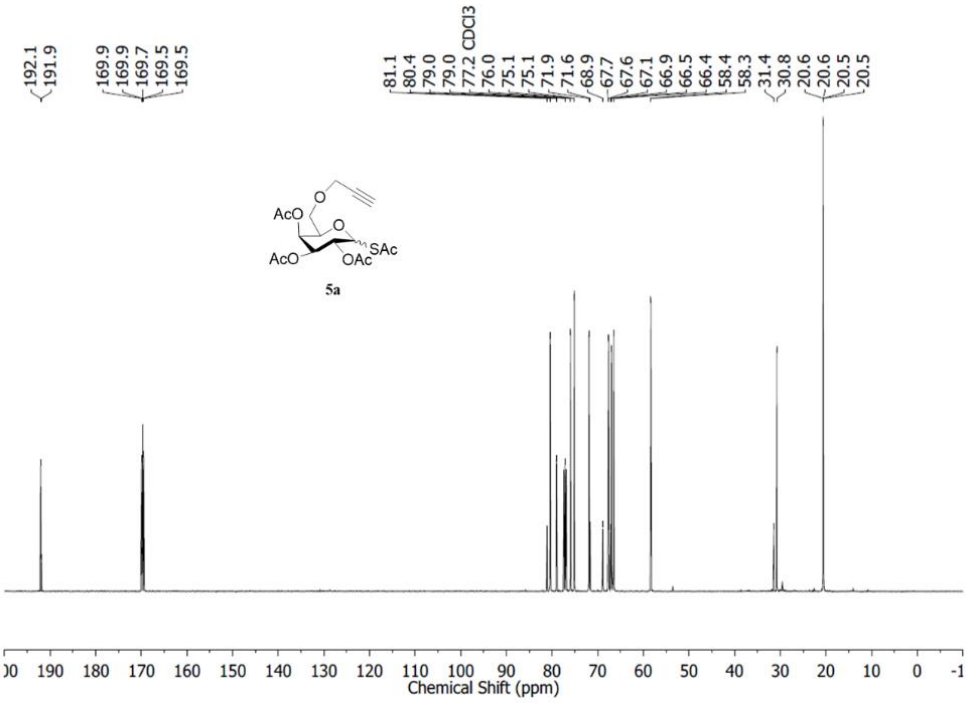

Figure 8.12 ^{13}C-NMR spectrum (125.8 MHz) of **5a** measured in $CDCl_3$.

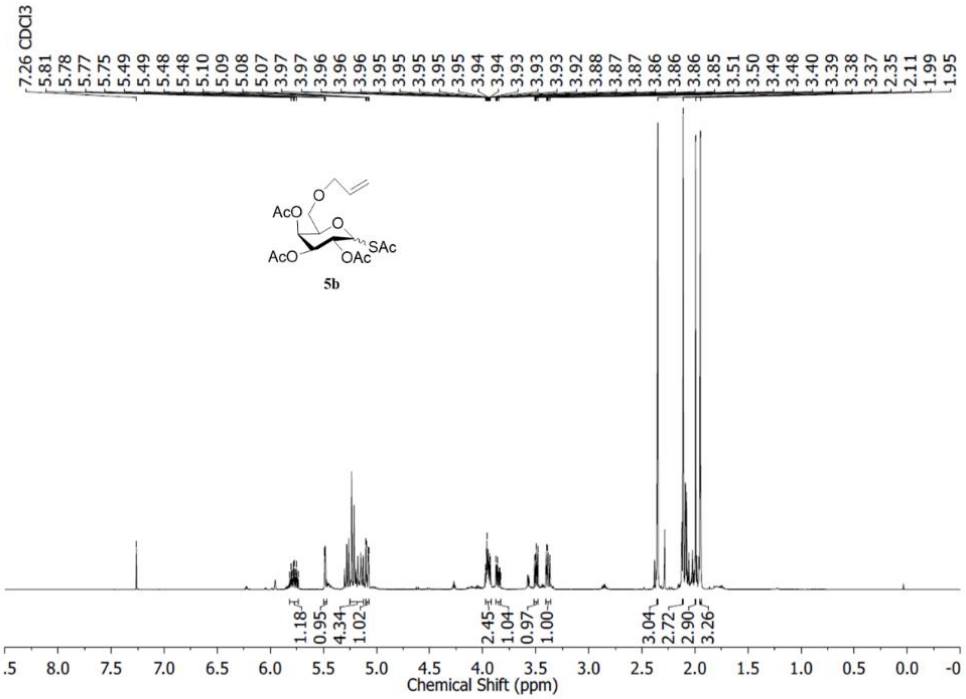

Figure 8.13 ^{1}H-NMR spectrum (500.2 MHz) of **5b** measured in $CDCl_3$.

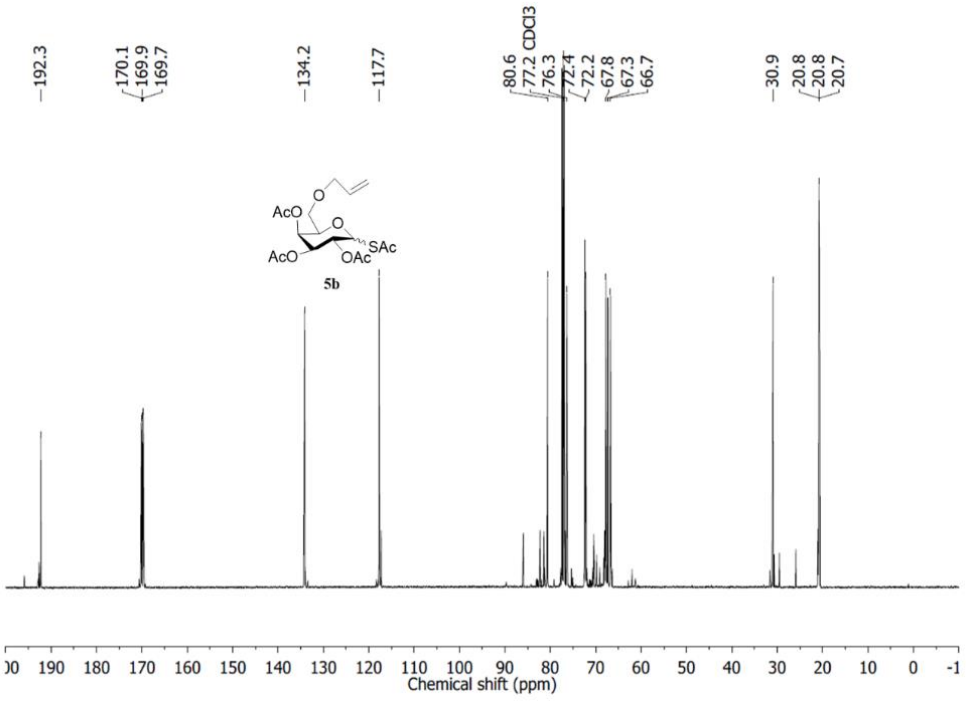

Figure 8.14 ^{13}C-NMR spectrum (125.8 MHz) of **5b** measured in $CDCl_3$.

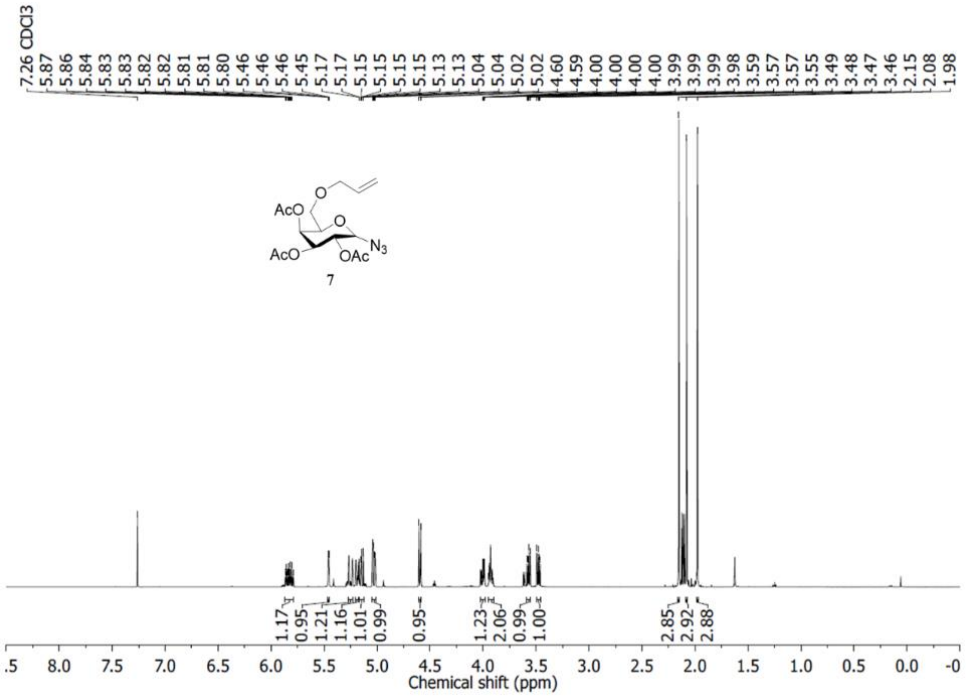

Figure 8.15 ^{1}H-NMR spectrum (500.2 MHz) of **7** measured in $CDCl_3$.

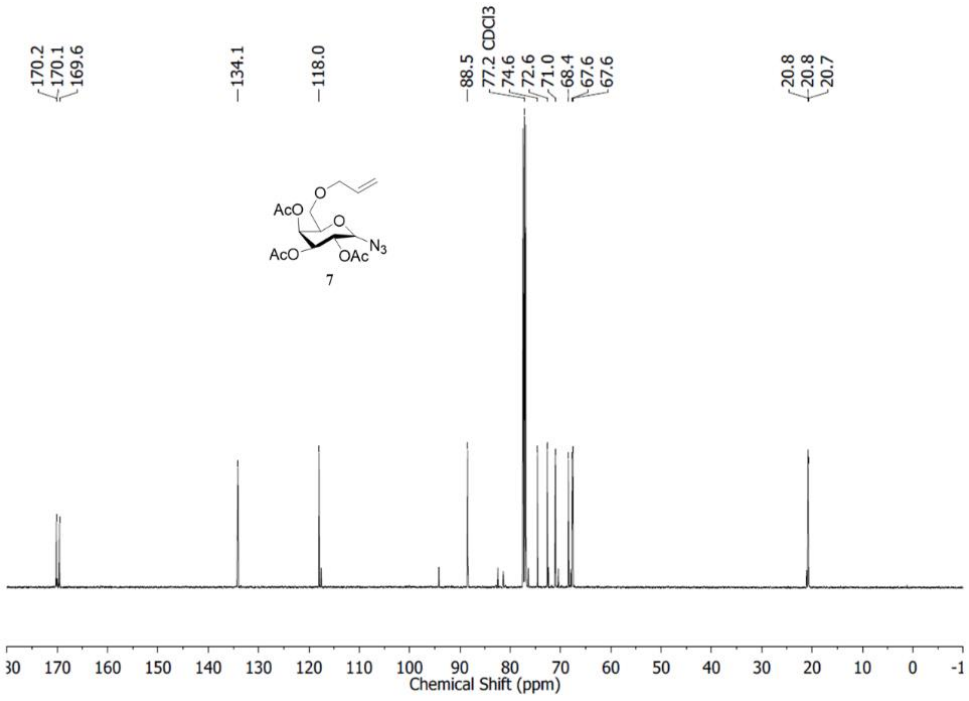

Figure 8.16 ^{13}C-NMR spectrum (125.8 MHz) of **7** measured in $CDCl_3$.

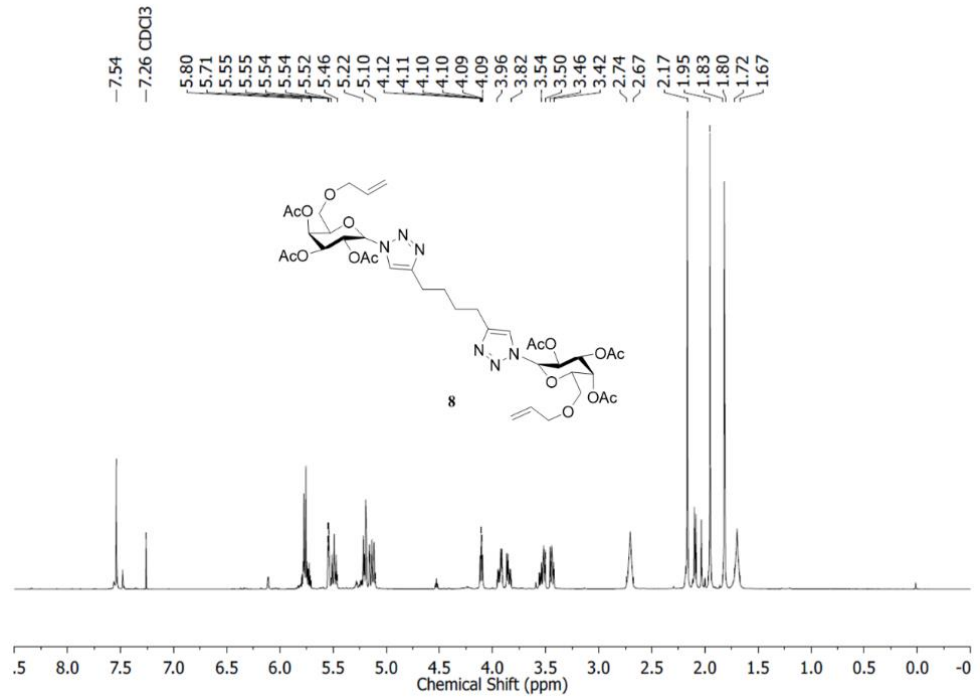

Figure 8.17 ^{1}H-NMR spectrum (500.2 MHz) of **8** measured in $CDCl_3$.

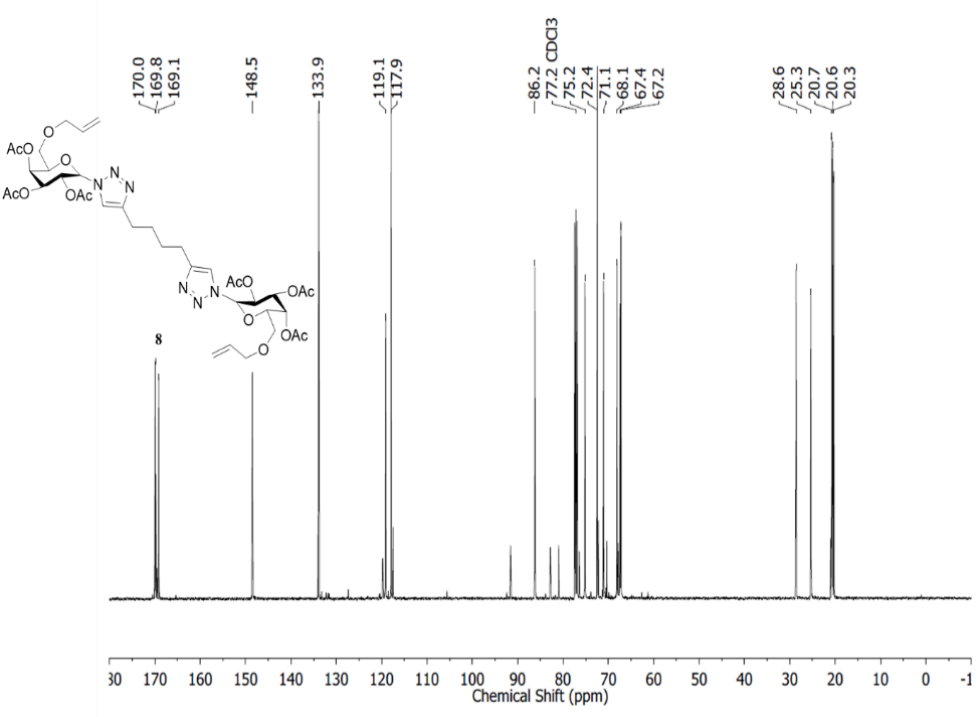

Figure 8.18 ^{13}C-NMR spectrum (125.8 MHz) of **8** measured in $CDCl_3$.

9 Literature

[1] A. Behr, T. Seidensticker, *Einführung in die Chemie nachwachsender Rohstoffe. Vorkommen, Konversion, Verwendung*, Springer Spektrum, Berlin, **2018**.

[2] E. Breitmaier, G. Jung, *Organische Chemie. Grundlagen, Verbindungsklassen, Reaktionen, Konzepte, Molekülstruktur, Naturstoffe, Syntheseplanung, Nachhaltigkeit*, Georg Thieme Verlag, Stuttgart, New York, **2012**.

[3] D. Klemm, F. Kramer, S. Moritz, T. Lindström, M. Ankerfors, D. Gray, A. Dorris, *Angew. Chem.* **2011**, *123*, 5550.

[4] D. Klemm, F. Kramer, S. Moritz, T. Lindström, M. Ankerfors, D. Gray, A. Dorris, *Angew. Chem. Int. Ed.* **2011**, *50*, 5438.

[5] L. P. Datta, S. Manchineella, T. Govindaraju, *Biomaterials* **2020**, *230*, 119633.

[6] B. Franck, *Angew. Chem. Int. Ed.* **1979**, *18*, 429.

[7] B. Franck, *Angew. Chem.* **1979**, *91*, 453.

[8] Y. Xiao, Q. Chen, C. Guang, W. Zhang, W. Mu, *Applied microbiology and biotechnology* **2019**, *103*, 3683.

[9] S. Patel, A. Goyal, *World J Microbiol Biotechnol* **2011**, *27*, 1119.

[10] E. K. McCranie, B. O. Bachmann, *Nat. Prod. Rep.* **2014**, *31*, 1026.

[11] O. O. Ibrahim, *J Food Chem Nanotechol* **2018**, *04*.

[12] D. Klemm, B. Heublein, H.-P. Fink, A. Bohn, *Angew. Chem. Int. Ed.* **2005**, *44*, 3358.

[13] D. Klemm, B. Heublein, H.-P. Fink, A. Bohn, *Angew. Chem.* **2005**, *117*, 3422.

[14] Y. Meng, F. Lyu, X. Xu, L. Zhang, *Biomacromolecules* **2020**, *21*, 1653.

[15] Y. Wang, J. Nie, W. Fang, L. Yang, Q. Hu, Z. Wang, J. Z. Sun, B. Z. Tang, *Chemical reviews* **2020**, *120*, 4534.

[16] a) V. Mukwaya, C. Wang, H. Dou, *Polym. Int.* **2019**, *68*, 306; b) R. R. R. Sardari, E. Nordberg Karlsson, *Journal of agricultural and food chemistry* **2018**, *66*, 11544.

[17] C. Colombo, O. Pitirollo, L. Lay, *Molecules* **2018**, *23*.

[18] A. Nešić, G. Cabrera-Barjas, S. Dimitrijević-Branković, S. Davidović, N. Radovanović, C. Delattre, *Molecules* **2019**, *25*.

[19] A. K. Qaroush, H. S. Alshamaly, S. S. Alazzeh, R. H. Abeskhron, K. I. Assaf, A.'a. F. Eftaiha, *Chem. Sci.* **2018**, *9*, 1088.

[20] S. Mitura, A. Sionkowska, A. Jaiswal, *Journal of materials science. Materials in medicine* **2020**, *31*, 50.

[21] M. V. Khvostov, T. G. Tolstikova, S. A. Borisov, A. V. Dushkin, *Russ J Bioorg Chem* **2019**, *45*, 438.

[22] D. Zhao, Y. Zhu, W. Cheng, W. Chen, Y. Wu, H. Yu, *Advanced materials* **2020**, e2000619.

[23] M. Alavi, *e-Polymers* **2019**, *19*, 103.

[24] R. Prathapan, R. F. Tabor, G. Garnier, J. Hu, *ACS Appl. Bio Mater.* **2020**, *3*, 1828.

[25] a) Z. J. Gallagher, S. Fleetwood, T. L. Kirley, M. A. Shaw, E. S. Mullins, N. Ayres, E. J. Foster, *Biomacromolecules* **2020**, *21*, 1103; b) A. Nishiguchi, T. Taguchi, *Biomacromolecules* **2019**, *20*, 1385; c) C. Xu, R. Feng, F. Song, X.-L. Wang, Y.-Z. Wang, *ACS Sustainable Chem. Eng.* **2018**, *6*, 14679.

[26] S. H. Kyne, J. E. Camp, *ACS Sustainable Chem. Eng.* **2017**, *5*, 41.

[27] P. Sosicka, B. G. Ng, H. H. Freeze, *Biochemistry* **2019**.

[28] A. I. Coelho, G. T. Berry, M. E. Rubio-Gozalbo, *Current opinion in clinical nutrition and metabolic care* **2015**, *18*, 422.

[29] M. T. Ngo, J. W. Han, S. Yoon, S. Bae, S.-Y. Kim, H. Kim, G. J. Choi, *Journal of agricultural and food chemistry* **2019**, *67*, 7706.

[30] B. Kim, J. W. Han, M. Thi Ngo, Q. Le Dang, J.-C. Kim, H. Kim, G. J. Choi, *Scientific reports* **2018**, *8*, 14522.

[31] S. S. Yuan, M. L. Li, J. S. Chen, L. Zhou, W. Zhou, *ChemMedChem* **2018**, *13*, 764.

[32] P. Sharma, B. C. Sharma, *Metabolic brain disease* **2013**, *28*, 313.

[33] M. Manwar Hussain, M. Hassan, N. Shaik, Z. Iqbal, *Open Medicine* **2012**, *7*, 409.

[34] D. P.M. Torres, M. d. P. F. Gonçalves, J. A. Teixeira, L. R. Rodrigues, *Comprehensive Reviews in Food Science and Food Safety* **2010**, *9*, 438.

[35] a) D. S. Newburg, G. Grave, *Pediatric research* **2014**, *75*, 675; b) C. Vera, A. Córdova, C. Aburto, C. Guerrero, S. Suárez, A. Illanes, *World J Microbiol Biotechnol* **2016**, *32*, 197.

[36] M. Intanon, S. L. Arreola, N. H. Pham, W. Kneifel, D. Haltrich, T.-H. Nguyen, *FEMS microbiology letters* **2014**, *353*, 89.

[37] M. Ebrahimi, L. Placido, L. Engel, K. S. Ashaghi, P. Czermak, *Desalination* **2010**, *250*, 1105.

[38] K. M. Craft, S. D. Townsend, *Accounts of chemical research* **2019**, *52*, 760.

[39] a) S. S. Kulkarni, C.-C. Wang, N. M. Sabbavarapu, A. R. Podilapu, P.-H. Liao, S.-C. Hung, *Chemical reviews* **2018**, *118*, 8025; b) A. Tamburrini, C. Colombo, A. Bernardi, *Medicinal research reviews* **2020**, *40*, 495.

[40] H. C. Kolb, M. G. Finn, K. B. Sharpless, *Angew. Chem. Int. Ed.* **2001**, *40*, 2004.

[41] H. C. Kolb, M. G. Finn, K. B. Sharpless, *Angew. Chem.* **2001**, *113*, 2056.

[42] A. Brinkø, C. Risinger, A. Lambert, O. Blixt, C. Grandjean, H. H. Jensen, *Organic letters* **2019**, *21*, 7544.

[43] A. Borbás, *Chem. Eur. J.* **2020**, *26*, 6090.

[44] A. Jakas, A. Višnjevac, I. Jerić, *J. Org. Chem.* **2020**, *85*, 3766.

[45] a) F. Fan, P. Zhang, L. Wang, T. Sun, C. Cai, G. Yu, *Biomacromolecules* **2019**, *20*, 3798; b) J. Madeira do O, F. Mastrotto, N. Francini, S. Allen, C. F. van der Walle, S. Stolnik, G. Mantovani, *Journal of materials chemistry. B* **2018**, *6*, 1044.

[46] S. Rühlicke, K. Zhang, *Materials Today Communications* **2020**, *24*, 101015.

[47] L. Ionov, *Langmuir : the ACS journal of surfaces and colloids* **2015**, *31*, 5015.

[48] A. Lendlein, S. Kelch, *Angew. Chem. Int. Ed.* **2002**, *41*, 2034.

[49] L. T. de Haan, C. Sánchez-Somolinos, C. M. W. Bastiaansen, A. P. H. J. Schenning, D. J. Broer, *Angew. Chem. Int. Ed.* **2012**, *51*, 12469.

[50] G. Stoychev, N. Puretskiy, L. Ionov, *Soft Matter* **2011**, *7*, 3277.

[51] A. Azam, K. E. Laflin, M. Jamal, R. Fernandes, D. H. Gracias, *Biomedical microdevices* **2011**, *13*, 51.

[52] J. S. Randhawa, K. E. Laflin, N. Seelam, D. H. Gracias, *Adv. Funct. Mater.* **2011**, *21*, 2395.

[53] a) T. Hwang, Z. Frank, J. Neubauer, K. J. Kim, *Scientific reports* **2019**, *9*, 9658; b) J. Shang, X. Le, J. Zhang, T. Chen, P. Theato, *Polym. Chem.* **2019**, *10*, 1036; c) A. J. R. Amaral, G. Pasparakis, *Polym. Chem.* **2017**, *8*, 6464; d) Q. M. Zhang, M. J. Serpe, *Chemphyschem : a European journal of chemical physics and physical chemistry* **2017**, *18*, 1451; e) Q. Zhao, J. W. C. Dunlop, X. Qiu, F. Huang, Z. Zhang, J. Heyda, J. Dzubiella, M. Antonietti, J. Yuan, *Nature communications* **2014**, *5*, 4293.

[54] a) M. Wei, Y. Gao, X. Li, M. J. Serpe, *Polym. Chem.* **2017**, *8*, 127; b) H. Lin, S. Zhang, Y. Xiao, C. Zhang, J. Zhu, J. W. C. Dunlop, J. Yuan, *Macromolecular rapid communications* **2019**, *40*, e1800896.

[55] G. M. Whitesides, *Angew. Chem. Int. Ed.* **2018**, *57*, 4258.

[56] T. Someya, *Stretchable Electronics*, Wiley-VCH Verlag, Weinheim, **2012**, 305-324.

[57] a) G. Stoychev, S. Zakharchenko, S. Turcaud, J. W. C. Dunlop, L. Ionov, *ACS nano* **2012**, *6*, 3925; b) V. Stroganov, S. Zakharchenko, E. Sperling, A. K. Meyer, O. G. Schmidt, L. Ionov, *Adv. Funct. Mater.* **2014**, *24*, 4357.

[58] a) K.-U. Jeong, J.-H. Jang, D.-Y. Kim, C. Nah, J. H. Lee, M.-H. Lee, H.-J. Sun, C.-L. Wang, S. Z. D. Cheng, E. L. Thomas, *J. Mater. Chem.* **2011**, *21*, 6824; b) J. Wei, X. Qiu, L. Zhang, *ACS applied materials & interfaces* **2019**, *11*, 16252.

[59] G. Zhao, Z. Z. Sun, Y. Ge, L. L. Li, *JBBBE* **2015**, *25*, 19.

[60] S. R. MacEwan, A. Chilkoti, *Biopolymers* **2010**, *94*, 60.

[61] Leeladhar, J. P. Singh, *ACS applied materials & interfaces* **2018**, *10*, 33956.

[62] M. Amjadi, M. Sitti, *Advanced science* **2018**, *5*, 1800239.

[63] A. Rath, P. M. Geethu, S. Mathesan, D. K. Satapathy, P. Ghosh, *Soft Matter* **2018**, *14*, 1672.

[64] J. K. Pandey, S. H. Ahn, C. S. Lee, A. K. Mohanty, M. Misra, *Macromol. Mater. Eng.* **2010**, *295*, 975.

[65] D. Chen, Q. Pei, *Chemical reviews* **2017**, *117*, 11239.

[66] Q. Zhu, Y. Jin, W. Wang, G. Sun, D. Wang, *ACS applied materials & interfaces* **2019**, *11*, 1440.

[67] a) H. C. Kim, S. Mun, H.-U. Ko, L. Zhai, A. Kafy, J. Kim, *Smart Mater. Struct.* **2016**, *25*, 73001; b) J. K. Pandey, H. Takagi, A. N. Nakagaito, D. R. Saini, S.-H. Ahn, *Composites Part B: Engineering* **2012**, *43*, 2822.

[68] C. Wang, R. A. Venditti, K. Zhang, *Applied microbiology and biotechnology* **2015**, *99*, 5791.

[69] a) S. H. Hassan, L. H. Voon, T. S. Velayutham, L. Zhai, H. C. Kim, J. Kim, *j renew mater* **2018**, *6*, 1; b) A. Khan, F. R. Khan, H. S. Kim, *Sensors* **2018**, *18*; c) J.-H. Jeon, I.-K. Oh, C.-D. Kee, S.-J. Kim, *Sensors and Actuators B: Chemical* **2010**, *146*, 307; d) Z. Sun, S. Du, F. Li, L. Yang, D. Zhang, W. Song, *Cellulose* **2018**, *25*, 5807; e) J. Li, S. Vadahanambi, C.-D. Kee, I.-K. Oh, *Biomacromolecules* **2011**, *12*, 2048.

[70] K. Zhang, S. Fischer, A. Geissler, E. Brendler, *Carbohydrate Polymers* **2012**, *87*, 894.

[71] A. Geissler, E. Bonaccurso, L.-O. Heim, T. Heinze, K. Zhang, *J. Phys. Chem. C* **2014**, *118*, 2408.

[72] Y. Wang, L.-O. Heim, Y. Xu, G. Buntkowsky, K. Zhang, *Adv. Funct. Mater.* **2015**, *25*, 1434.

[73] Y. Wang, C. Zhang, J. Tian, Y. Xie, K. Zhang, *Macromol. Chem. Phys.* **2018**, *219*, 1800229.

[74] S. D.M. Atkinson, M. J. Almond, P. Hollins, S. L. Jenkins, *Spectrochimica Acta Part A: Molecular and Biomolecular Spectroscopy* **2003**, *59*, 629.

[75] H. I. Bernstein, W. C. Quimby, *J. Am. Chem. Soc.* **1943**, *65*, 1845.

[76] G. Kaupp, *Angew. Chem. Int. Ed.* **1992**, *31*, 592.

[77] S. M. Hein, *J. Chem. Educ.* **2006**, *83*, 940.

[78] G. P. Moss, P. A. S. Smith, D. Tavernier, *Pure and Applied Chemistry* **1995**, *67*, 1307.

[79] V. Morozov, G. Hansman, F.-G. Hanisch, H. Schroten, C. Kunz, *Molecular nutrition & food research* **2018**, *62*, e1700679.

[80] W. Cheng, J. Lu, B. Li, W. Lin, Z. Zhang, X. Wei, C. Sun, M. Chi, W. Bi, B. Yang et al., *Frontiers in microbiology* **2017**, *8*, 1750.

[81] a) P.-A. Faugeras, B. Boëns, P.-H. Elchinger, F. Brouillette, D. Montplaisir, R. Zerrouki, R. Lucas, *Eur. J. Org. Chem.* **2012**, *2012*, 4087; b) Y. Cui, S. Xu, J. Mao, *J Incl Phenom Macrocycl Chem* **2015**, *83*, 187.

[82] a) P. Wang, C.-x. Huo, S. Lang, K. Caution, S. T. Nick, P. Dubey, R. Deora, X. Huang, *Angew. Chem.* **2020**, *74*, 108; b) P. Wang, C.-X. Huo, S. Lang, K. Caution, S. T. Nick, P. Dubey, R. Deora, X. Huang, *Angew. Chem. Int. Ed.* **2020**.

[83] M. D. Bandara, K. J. Stine, A. V. Demchenko, *Organic & biomolecular chemistry* **2020**, *18*, 1747.

[84] C. Marino, A. Rinflerch, R. M. de Lederkremer, *Future science OA* **2017**, *3*, FSO199.

[85] V. Dimakos, M. S. Taylor, *Chemical reviews* **2018**, *118*, 11457.

[86] J. Neumann, S. Weingarten, J. Thiem, *Eur. J. Org. Chem.* **2007**, *2007*, 1130.

[87] V. L. Campo, I. Carvalho, C. H. T. P. Da Silva, S. Schenkman, L. Hill, S. A. Nepogodiev, R. A. Field, *Chem. Sci.* **2010**, *1*, 507.

[88] S. Hotha, S. Kashyap, *J. Org. Chem.* **2006**, *71*, 852.

[89] S. Hotha, S. Kashyap, *The Journal of organic chemistry* **2006**, *71*, 364.

[90] P. Fuchs, P. Vana, K. Zhang, *Journal of Polymer Science* **2020**, *58*, 1535.

[91] M. L. Uhrig, J. Kovensky, *Click Chemistry in Glycoscience: New Developments and Strategies*, Wiley-VCH Verlag, Weinheim, **2013**, 107-142.

[92] C. E. Hoyle, C. N. Bowman, *Angew. Chem. Int. Ed.* **2010**, *49*, 1540.

[93] C. E. Hoyle, A. B. Lowe, C. N. Bowman, *Chemical Society reviews* **2010**, *39*, 1355.

[94] D. Witt, R. Klajn, P. Barski, B. Grzybowski, *COC* **2004**, *8*, 1763.

[95] D. C. Kennedy, C. S. McKay, M. C. B. Legault, D. C. Danielson, J. A. Blake, A. F. Pegoraro, A. Stolow, Z. Mester, J. P. Pezacki, *J. Am. Chem. Soc.* **2011**, *133*, 17993.

[96] a) D. P. Nair, M. Podgórski, S. Chatani, T. Gong, W. Xi, C. R. Fenoli, C. N. Bowman, *Chem. Mater.* **2014**, *26*, 724; b) A. B. Lowe, C. E. Hoyle, C. N. Bowman, *J. Mater. Chem.* **2010**, *20*, 4745; c) A. B. Lowe, *Polymer* **2014**, *55*, 5517.

[97] A. Dondoni, A. Marra, *Chemical Society reviews* **2012**, *41*, 573.

[98] M. Fiore, A. Marra, A. Dondoni, *J. Org. Chem.* **2009**, *74*, 4422.

[99] R. Zelli, P. Dumy, A. Marra, *Organic & biomolecular chemistry* **2020**.

[100] L. Lázár, M. Csávás, M. Herczeg, P. Herczegh, A. Borbás, *Organic letters* **2012**, *14*, 4650.

[101] J. R. Kramer, T. J. Deming, *J. Am. Chem. Soc.* **2012**, *134*, 4112.

[102] D. A. Fulton, J. F. Stoddart, *J. Org. Chem.* **2001**, *66*, 8309.

[103] N. Floyd, B. Vijayakrishnan, J. R. Koeppe, B. G. Davis, *Angew. Chem. Int. Ed.* **2009**, *48*, 7798.

[104] J. L. García Ruano, A. Parra, J. Alemán, *Green Chem.* **2008**, *10*, 706.

[105] N. Bagi, J. Kaizer, G. Speier, *RSC Adv.* **2015**, *5*, 45983.

[106] N. Taniguchi, K. Kitayama, *Synlett* **2018**, *29*, 2712.

[107] W. W. CLELAND, *Biochemistry* **1964**, *3*, 480.

[108] H. Schott (Ed.) *Die Chronik der Medizin*, Chronik, Dortmund, **1993**.

[109] F. von Nussbaum, M. Brands, B. Hinzen, S. Weigand, D. Häbich, *Angew. Chem. Int. Ed.* **2006**, *45*, 5072.

[110] F. von Nussbaum, M. Brands, B. Hinzen, S. Weigand, D. Häbich, *Angew. Chem.* **2006**, *118*, 5194.

[111] a) J. Liu, S. Lu, J. Feng, C. Li, W. Wang, Y. Pei, S. Ding, M. Zhang, H. Li, R. Na et al., *Journal of agricultural and food chemistry* **2020**, *68*, 2116; b) D. J. Newman, G. M. Cragg, *Journal of natural products* **2016**, *79*, 629.

[112] R. Yang, Y. Y. Hu, S. Huang, Z. F. Fang, M. Ma, B. Chen, *J. Chem. Educ.* **2020**, *97*, 778.

[113] a) J.-M. Lü, Q. Yao, C. Chen, *Current vascular pharmacology* **2009**, *7*, 293; b) T. K. Yun, *Nutrition reviews* **1996**, *54*, S71-81; c) A. S. Attele, Y.-P. Zhou, J.-T. Xie, J. A. Wu, L. Zhang, L. Dey, W. Pugh, P. A. Rue, K. S. Polonsky, C.-S. Yuan, *Diabetes* **2002**, *51*, 1851.

[114] a) L. R. L. Diniz, M. T. d. S. Souza, J. N. Barboza, R. N. d. Almeida, D. P. d. Sousa, *Molecules* **2019**, *24*; b) S. Choo, V. K. Chin, E. H. Wong, P. Madhavan, S. T. Tay, P. V. C. Yong, P. P. Chong, *Folia microbiologica* **2020**.

[115] C. Huang, Z. Zhang, W. Cui, *Marine drugs* **2019**, *17*.

[116] a) W. Wang, S. Gopal, R. Pocock, Z. Xiao, *Molecules* **2019**, *24*; b) S. Andrade, M. J. Ramalho, J. A. Loureiro, M. d. C. Pereira, *International journal of molecular sciences* **2019**, *20*.

[117] M. Gehan I Kh, A. Samir A M, *Plant Protect. Sci.* **2017**, *54*, 9.

[118] E. Hedenström, A. Fagerlund Edfeldt, M. Edman, B.-G. Jonsson, *Wood Sci Technol* **2016**, *50*, 617.

[119] J. Chen, Y. Shen, C. Chen, C. Wan, *Plants* **2019**, *8*.

[120] Y. Huang, J. Zhao, L. Zhou, J. Wang, Y. Gong, X. Chen, Z. Guo, Q. Wang, W. Jiang, *Molecules* **2010**, *15*, 7558.

[121] T. Esposito, R. Celano, C. Pane, A. L. Piccinelli, F. Sansone, P. Picerno, M. Zaccardelli, R. P. Aquino, T. Mencherini, *Molecules* **2019**, *24*.

[122] A. Evidente, L. Maddau, B. Scanu, A. Andolfi, M. Masi, A. Motta, A. Tuzi, *Journal of natural products* **2011**, *74*, 757.

[123] A. Costa, L. Moreira, R. Pinto, T. Alves, V. Schwan, V. de Queiroz, M. Praça-Fontes, R. R. Teixeira, P. Morais, W. de Jesus, *J. Braz. Chem. Soc.* **2020**.

[124] K. Bozorov, J. Zhao, H. A. Aisa, *Bioorganic & medicinal chemistry* **2019**, *27*, 3511.

[125] L. T. M. van der Ven, E. Rorije, R. C. Sprong, D. Zink, R. Derr, G. Hendriks, L.-H. Loo, M. Luijten, *Chemical research in toxicology* **2020**, *33*, 834.

[126] R. Jalaja, S. G. Leela, P. K. Valmiki, C. T. F. Salfeena, K. T. Ashitha, V. R. D. Krishna Rao, M. S. Nair, R. K. Gopalan, S. B. Somappa, *ACS medicinal chemistry letters* **2018**, *9*, 662.

[127] R. S. Keri, S. A. Patil, S. Budagumpi, B. M. Nagaraja, *Chemical biology & drug design* **2015**, *86*, 410.

[128] B. Hu, H. Zhao, Z. Chen, C. Xu, J. Zhao, W. Zhao, *Molecules* **2018**, *23*.

[129] H. Militz, W. J. Homan, *Holz als Roh-und Werkstoff* **1994**, *52*, 28.

[130] C. Vaca-Garcia, M. E. Borredon, A. Gaseta, *Cellulose* **2001**, *8*, 225.

[131] G. R. Fulmer, A. J. M. Miller, N. H. Sherden, H. E. Gottlieb, A. Nudelman, B. M. Stoltz, J. E. Bercaw, K. I. Goldberg, *Organometallics* **2010**, *29*, 2176.

[132] F. S. Ekholm, H. Pynnönen, A. Vilkman, V. Pitkänen, J. Helin, J. Saarinen, T. Satomaa, *ChemMedChem* **2016**, *11*, 2501.

[133] H. Ito, T. Kamachi, E. Yashima, *Chemical communications* **2012**, *48*, 5650.

[134] S.-J. Zhu, H.-Z. Ying, Y. Wu, N. Qiu, T. Liu, B. Yang, X.-W. Dong, Y.-Z. Hu, *RSC Adv.* **2015**, *5*, 103172.

[135] H. Murakami, T. Minami, F. Ozawa, *J. Org. Chem.* **2004**, *69*, 4482.

[136] D. Bhunia, P. M. C. Pallavi, S. R. Bonam, S. A. Reddy, Y. Verma, M. S. K. Halmuthur, *Archiv der Pharmazie* **2015**, *348*, 689.